Climate dynamics across scales in a mountain landscape:

Macro- and microclimatic modelling in the Río Puelo basin, northern Patagonia

Dissertation

for the award of the degree

“Doctor rerum naturalium” (Dr. rer. nat.)

of the Georg-August-Universität Göttingen

within the doctoral program Geography

of the Georg-August University School of Science (GAUSS)

submitted by

Jonas Fierke

from Stuttgart, Germany

Göttingen, 2025

Thesis Advisory Committee

Prof. Dr. Martin Kappas
Institute of Geography, Department of Cartography, GIS and Remote Sensing, Georg-August Universität Göttingen

Prof. Dr. Helge Walentowski
Faculty of Resource Management, University of Applied Science and Art (HAWK) Hildesheim/Holzminden/Göttingen

Dr. Daniel Wyss
Institute of Geography, Department of Cartography, GIS and Remote Sensing, Georg-August Universität Göttingen

Members of the Examination Board

Reviewer
Prof. Dr. Martin Kappas
Institute of Geography, Department of Cartography, GIS and Remote Sensing, Georg-August Universität Göttingen

Second Reviewer
Prof. Dr. Helge Walentowski
Faculty of Resource Management, University of Applied Science and Art (HAWK) Hildesheim/Holzminden/Göttingen

Further members of the Examination Board

Prof. Dr. Heiko Faust
Department of Human Geography, Georg-August Universität Göttingen

Dr. Daniel Wyss
Institute of Geography, Department of Cartography, GIS and Remote Sensing, Georg-August Universität Göttingen

Dr. Birgitta Putzenlechner
Competence Center Landscape Resilience, Georg-August Universität Göttingen

Dr. Stephen Boahen Asabere
Department of Physical Geography, Georg-August Universität Göttingen

Date of the oral examination: November 20, 2025

Articles included in the dissertation

(1) Fierke, J., Joelson, N. Z., Loguercio, G. A., Putzenlechner, B., Simon, A., Wyss, D., Kappas, M., & Walentowski, H. (2024). Assessing uncertainty in bioclimatic modelling: a comparison of two high-resolution climate datasets in northern Patagonia. *Regional Environmental Change*, *24*(3). https://doi.org/10.1007/s10113-024-02278-5

(2) Fierke, J., Putzenlechner, B., Simon, A., Gowda, J. H., Reiter, E. J., Walentowski, H., & Kappas, M. (2025). Modelling microclimatic variability in Andean forests of northern Patagonia. *International Journal of Biometeorology, 69(6), 1279–1295.* https://doi.org/10.1007/s00484-025-02891-x

(3) Fierke, J., Gowda, J. H., Díaz, G. M., Koal, P., Walentowski, H., Kappas, M., & Putzenlechner, B. (submitted-a). Vegetation structure and elevation provide stronger thermal buffering than slope orientation during summer heat in northern Patagonia. *Manuscript submitted for publication to Scientific Reports.*

Book chapter partially included in the dissertation

(1) Fierke, J., Simon, A., Putzenlechner, B., Winter, A., Gowda, J. H., & Kappas, M. (submitted-b). Climate variations across landscape gradients of northern Patagonian Andean forests: Lessons from high-resolution climate datasets and microclimatic records. In H. Walentowski, T. Kitzberger, M. Kappas, S. Zerbe, & G. A. Loguercio (Eds.), *Ecology, structure and dynamics of North Patagonian Andean forests and derivations for ecosystem management*. Springer Nature.

Acknowledgements

I would like to express my deepest gratitude to my supervisors Martin Kappas, Helge Walentowski, and Daniel Wyss for their invaluable guidance, encouragement, and constant support throughout this journey. Their advice and mentorship have been crucial at every stage.

I am sincerely thankful to Birgitta Putzenlechner and Alois Simon, whose expertise and support greatly enriched both my publications and my fieldwork.

I am grateful to the members of my examination board, Martin Kappas, Helge Walentowski, Heiko Faust, Daniel Wyss, Birgitta Putzenlechner, and Stephen Boahen Asabere, for their willingness to serve on my committee and for the time and attention they dedicate to this dissertation.

My warmest thanks go to Natalia Joelson, Ernesto Reiter, and Ariel Neri Winter, who were not only companions through challenges and triumphs, but also made the journey lighter with countless rounds of mate, laughter, and survival strategies.

I gratefully acknowledge the support of the BMEL, which funded the KLIMNEM project, and the whole KLIMNEM team, whose collaboration shaped many aspects of this thesis. I also want to thank the student assistants who contributed with dedication in the field and beyond, as well as Sören Merkle for his technical advice and Martina Beckmann for her always reliable support.

Special thanks go to Timo Lehmann, not only for his help but also for providing a place for countless fruitful coffee breaks.

I also acknowledge the support of CIEFAP, which was essential for the completion of this thesis and the success of the field campaigns. My appreciation extends to José Daniel Lencinas, Marina Caselli, José Bava, Gabriel Loguercio, Melisa Rago, Diego Mohr Bell, Facundo Heinzle, Clara Pissolito, Héctor Gonda, Gastón Díaz, María Florencia Urretavizcaya, Thais Efron, Horacio Ivancich, and everyone else involved. My appreciation also extends to the landowners who generously provided access to their land for research.

I am profoundly grateful to my family in Germany and South Africa, whose love and encouragement have accompanied me throughout this journey. Their enduring support gave me strength and perspective in moments of difficulty.

A very special thanks goes to my wife, Uhuru, for her trust, love, and endless support. She has been my anchor, my partner, and my greatest source of motivation throughout this journey. Her patience, encouragement, and confidence in me have carried me through moments of doubt, and her presence has made every success even more meaningful.

Finally, I wish to thank all others who, in one way or another, were part of this path.

Abstract

Mountain forests in northern Patagonia are exposed to rapid climatic changes, with increasing temperatures, changing precipitation regimes, and more frequent and severe extreme events threatening their current structure and resilience. Understanding these short- and long-term dynamics requires integrating climate information across scales: from macroclimatic datasets that inform broad biogeographic analyses to microclimatic measurements that capture the conditions organisms directly experience. This dissertation addresses how macroclimatic and microclimatic modelling can be combined to improve ecological assessments in mountainous forest landscapes, focusing on the Río Puelo watershed of northern Patagonia.

Three empirical studies form the core of this work. The first compares two widely used high-resolution climate datasets (CHELSA v2.1 and WorldClim v2.1), showing substantial differences in precipitation estimates and associated bioclimatic classifications, with direct implications for how forest distribution may be projected under future climate scenarios. The second develops spatial models of microclimatic variability based on a dense network of in-situ sensors combined with remote sensing, as well as weather station and reanalysis data. Results highlight the strong and dynamic influence of vegetation structure and topographic position on forest microclimates, affecting both near-ground and sub-canopy (2 m) temperature and moisture conditions, and demonstrate the feasibility of modelling these patterns at 30 m resolution. The third study examines microclimatic buffering during summer heat extremes, revealing that forest structure and elevation consistently reduce maximum temperatures and moderate diurnal warming and cooling rates, while slope orientation exerts weaker and more variable effects. Importantly, buffering strength increases under extreme heat, underscoring the temperature-sensitive character of microclimatic regulation.

Taken together, the findings show that the regions of highest ecological sensitivity are also those where climate representation is most uncertain, and where fine scale vegetation and topographic features exert the greatest influence on local conditions. By integrating macroclimatic uncertainty with microclimatic evidence, this dissertation advances conceptual and methodological links between climate and ecosystem research across scales. The results have direct implications for modelling species distributions, understanding forest regeneration dynamics, and informing ecosystem-based management strategies in the fire prone temperate forests of northern Patagonia. Beyond the case study region, the work shows how combining climate data across scales supports more robust evaluations of climate–ecosystem relationships in mountainous terrain. It also provides a framework that can be applied to other forested landscapes where microclimatic processes are critical for resilience. Finally, it highlights the need to account for both uncertainty in global climate products and the buffering capacity of local ecosystems when assessing biodiversity responses to climate change.

Table of Contents

Acknowledgements vii

Abstract ix

Table of Contents xi

List of Figures xiii

List of Tables xvi

List of Abbreviations xviii

1. Introduction 22

2. Conceptual background 26

2.1 Landscape and ecosystem ecology 26

2.2 Microclimatology 29

3. Environmental setting and data collection 32

3.1 Study region 32

3.2 Regional climate 33

3.3 Data acquisition 35

4. Study I - Assessing uncertainty in bioclimatic modelling: a comparison of two high-resolution climate datasets in northern Patagonia 37

4.1 Introduction 38

4.2 Data and methods 39

4.3 Results 45

4.4 Discussion 51

4.5 Conclusion 55

4.6 Data availability 55

4.7 Funding 55

4.8 Supplementary information 55

4.9 Rights and permissions 56

5. Study II - Modelling microclimatic variability in Andean forests of northern Patagonia 57

5.1 Introduction 58

5.2 Data and methods 60
5.3 Results 66
5.4 Discussion 71
5.5 CRediT authorship contribution statement 76
5.6 Data availability 76
5.7 Acknowledgements 76
5.8 Funding 76
5.9 Supplementary information 77
5.10 Rights and permissions 77
6. Study III - Vegetation structure and elevation provide stronger thermal buffering than slope orientation during summer heat in northern Patagonia 78
6.1 Introduction 79
6.2 Material and methods 81
6.3 Results 85
6.4 Discussion 88
6.5 CRediT authorship contribution statement 91
6.6 Data availability 91
6.7 Funding 91
6.8 Competing interest 92
6.9 Acknowledgement 92
6.10 Supplementary information 92
7. Synthesis and outlook 96
7.1 Synthesis of main findings 96
7.2 From macroclimatic uncertainty to microclimatic evidence: Implications for forest dynamics and management in northern Patagonia 98
7.3 Conceptual and methodological contributions 101
7.4 Methodological reflections, limitations, and outlook 103
References 105
Annex 141

List of Figures

Figure 3.1 Dominant native tree species within the Río Puelo watershed. Photos by Jonas Fierke (all except upper right) and Birgitta Putzenlechner (upper right). 32

Figure 3.2 Río Puelo watershed including the study areas of the studies included in this dissertation. Figure adapted from Fierke et al. (submitted-b). 33

Figure 3.3 Microclimatic sensors used in Studies 2 and 3. Shown are (from upper left to bottom right): a TOMST TMS-4 Standard logger (overview), a TMS-4 Standard logger installed in the field, an iButton DS1923 Hygrochron logger (overview), and an iButton logger installed in the field. Photos by Jonas Fierke. 36

Figure 4.1 Map of eastern Río Puelo watershed (showing Río Puelo and Lago Puelo exclusively), located at the Argentina-Chile border in north-west Patagonia. Topography of the study area is illustrated on basis of the digital elevation model SRTM (Farr et al. 2007). 40

Figure 4.2 Comparative framework for assessing bioclimatic modelling uncertainty using historical and future climate data, as well as species, elevation, and meteorological station data. Where grey boxes represent the data input as well as the bioclimatic pre-analysis and coloured boxes represent the two validation phases. 41

Figure 4.3 The bioclimatic zones of the eastern Río Puelo watershed, analysed using two key datasets: CHELSA, with data averaged from 1981 to 2010 (Karger et al. 2021), and WorldClim, with averages from 1970 to 2000 (Fick and Hijmans 2017a). Each dataset categorizes the region's ombric and thermotypic horizons, ranging from arid to humid and from lower supramediterranean to lower crioromediterranean, respectively. Visual differentiation is achieved through varying colour intensities, indicating moisture variations. Additionally, the figure marks bioclimatic zones A through D, representing species and showing their bioclimates and relative cover percentages across these environmental gradients. 46

Figure 4.4 Current and future densities of the annual ombrothermic index (Io) and the positive annual temperature (Tp) with marked quantiles (0.1, 0.5, and 0.9) for CHELSA (a-j) and WorldClim (k-t) under different shared socioeconomic pathways (blue for SSP1-2.6 and red for SSP3-7.0) and on basis of different global climate models..... 48

Figure 4.5 Spatial intersection between a) thermotypic horizons, b) ombric horizons, and c) bioclimates based on reference periods of CHELSA and WorldClim. Where red pixels are without and blue pixels are with intersection between both datasets. Marks of c) represent points of reference for specific areas with (transparent) and without (hatched) intersection of the overall bioclimatic classification..... 49

Figure 4.6 Potential development of bioclimatic zones under different scenarios with reference to main tree species based on CHELSA and WorldClim climate data. Where CHELSA is marked by solid lines and WorldClim by dashed lines. 50

Figure 4.7 Comparative analysis of monthly relative precipitation and temperature estimates by gridded climate data across five locations. Panels (a to e) show the monthly relative precipitation measured by station data (black line) and estimated by CHELSA (blue) and WorldClim (red), highlighting the variability and patterns of over- or underestimation of the datasets across a west-to-east precipitation gradient (a to c) as well as two stations located in the centre of the investigation area (d and e). Panel (f) presents a comparison of monthly temperature records of the station with estimates of the gridded datasets, demonstrating seasonal alignment and deviations. 51

Figure 5.1 Study area. Where (a) is showing the section of iButton data loggers, (b) the section of TMS-4 data loggers, and (c) the intersection of both. Photos (d) and (e) show exemplary sites of TMS and iButton loggers respectively. Mean Annual Air Temperature (MAAT) of the region is based on climate data of (Karger et al. 2017). 61

Figure 5.2 Relative importance of 13 selected biophysical variables for predicting microclimatic observations. Predictors are categorized as related to vegetation (v), topography (t), or macroclimate. The vertical lines in the bar indicate the range (maximum and minimum), while the bars represent the mean R^2 values across 100 ensembles. Each monthly bar corresponds to a specific set of biophysical variables identified after a recursive variable elimination process. 65

Figure 5.3 Selected examples of microclimatic maps in Valle del Río Manso Inferior (Figure 5.1c). Depicted variables at a soil depth of 6 cm, as well as at heights of 15 cm and 2 m above ground level, for the period from 1981 to 2010. February represents the warm and dry extreme, July the cold extreme, and June the wet extreme. The section covers an area of 12 by 19 km and spans an elevational gradient from 433 to 2239 m. Grey areas indicate regions not covered by forest. 68

Figure 5.4 Microclimatic variables across periods and heights. Plots illustrating the distribution of microclimatic variables over historical and observed periods at 2 m and 15 cm heights, as well as 6 cm depth, highlighting the median, quartiles, and the frequency of values at different points. The observation period is 2022-2023 for the iButton loggers and 2022-2024 for the TMS loggers, while the historical reference period spans from 1981 to 2010. Temperature (red) at 6 cm depth and 15 cm height, as well as VWC (blue) at 6 cm depth, represent data from TMS loggers. Temperature (red) and relative humidity (blue) at 2 m height represent data from iButton loggers. 70

Figure 5.5 Vertical temperature variations. Where the left panel shows the mean monthly minimum and the right panel the mean monthly maximum temperatures for different vertical horizons at 2 m and 15 cm height, as well as 6 cm depth for the period from 1981 to 2010. Variations are related to a section of our study area where both spatial interpolations of iButton and TMS data overlap (Figure 5.1c). 71

Figure 6.1 Overview of the study area in the Río Manso Valley showing the locations of microclimate loggers across three environmental gradients: vegetation structure, elevation, and slope orientation. Site numbers correspond to contrasting conditions used in the paired-sampling design (see Table 6.1). 82

Figure 6.2 Daily differences in (a, d) warming rate (K/h), (b, e) maximum temperature (K), and (c, f) cooling rate (K/h) between buffered and exposed sites across six environmental gradients: vegetation structure (low-height [V-L], medium-height [V-M]), elevation (north-facing [E-N], south-facing [E-S]), and slope orientation (high elevation [A-H], low elevation [A-L]). Panels (a–c) show marginal means (±95% confidence intervals) estimated from linear mixed-effects models fitted with an autoregressive correlation structure. Solid lines indicate statistically significant differences ($p < 0.05$); dashed lines indicate non-significant results. Panels (d–f) display conditional R^2 values for each model, reflecting the proportion of variance explained by both fixed and random effects. 86

Figure 6.3 Temperature-dependent amplification of microclimatic differences in (a, d) warming rate (K/h), (b, e) maximum temperature (K), and (c, f) cooling rate (K/h) across six environmental gradients: vegetation structure (low-height [V-L], medium-height [V-M]), elevation (north-facing [E-N], south-facing [E-S]), and slope orientation (high elevation [A-H], low elevation [A-L]). Panels (a–c) show model-estimated slopes (±95% confidence intervals) from linear mixed-effects models with maximum temperature at the exposed site as a covariate. These slopes quantify how thermal differences between buffered and exposed sites scale with increasing heat load. Solid lines indicate statistically significant relationships ($p < 0.05$); dashed lines indicate non-significant trends. Panels (d–f) display marginal (left) and conditional (right) R^2 values for each model. 87

Figure 6.4 Predicted differences in microclimatic buffering across six environmental contrasts at fixed exposed-site temperatures of 15 °C and 30 °C. Arrows indicate the shift in predicted differences in warming rate, cooling rate, and maximum temperature between buffered and exposed sites as heat load increases. Each point represents model-derived differences at 15 °C (arrow base) and 30 °C (arrow tip) for a given contrast. Results illustrate the temperature-dependent and multidimensional nature of microclimatic buffering (compare Fig. 6.3). 88

List of Tables

Table 4.1 Ranges of the annual ombrothermic index (IO) and the annual positive temperature in tenth degrees (Tp) that determine ombric and thermotypic horizons within the study area (in reference to Fig. 4.2). 47

Table 5.1 Predictor variables for statistical downscaling of ERA5 data. Using even years from 2004 to 2014 for the Valle del Río Manso Inferior station and even years from 1991 to 2014 for the El Bolsón station, predictor variables were selected from the 26 available options (Table S1) based on their partial correlation coefficients (r) and p-values. Where hPa is the atmospheric pressure level in hectopascals. 63

Table 5.2 Summary of top predictor variables for microclimatic response variables. Predictor variables are listed according to their relevance, expressed as percentages, across all months. 67

Table 6.1 Overview of environmental gradients used in the study, including definitions of buffered and exposed conditions and the corresponding site pairs. Each gradient represents a paired comparison between two sites differing in a single variable (elevation, slope orientation, or vegetation structure) while keeping other factors constant. Site numbers refer to locations shown in Fig. 6.1. 82

Supplementary Table 6.1 Summary statistics of temperature and diurnal metrics recorded at eight study sites in the Río Manso Valley during the austral summer. Variables include daily maximum temperature (TMAX), minimum temperature (TMIN), and their respective times of occurrence (TMAX Time, TMIN Time), as well as warming and cooling rates. For each variable and site, sample size (n), median, interquartile range (IQR), minimum (Min), and maximum (Max) are reported. Time values are presented in HH:MM format. 92

Supplementary Table 6.2 Number of summer frost nights (nights with at least one 15-minute interval below 0 °C) recorded at each study site during the period from 15 February 2024 to 13 February 2025, based on site-averaged temperature data. Frost nights were identified using nighttime temperature data (20:00–10:00), and sites are grouped by vegetation structure, elevation, and slope orientation as described in Figure 1. 93

Supplementary Table 6.3 Results of linear mixed-effects models quantifying absolute differences in warming rate (K/h), maximum temperature (K), and cooling rate (K/h) between buffered and exposed microclimates across six environmental gradients: vegetation structure (low-height [V-L], medium-height [V-M]), elevation (north-facing [E-N], south-facing [E-S]), and slope orientation (high elevation [A-H], low elevation [A-L]). For each variable and gradient, model estimates (intercept), standard error (SE), t-value, and p-value are shown. Marginal (R^2

m) and conditional (R^2 c) R^2 values indicate the variance explained by fixed effects alone and by the full model including random effects, respectively. 94

Supplementary Table 6.4 Results of linear mixed-effects models including maximum temperature at the exposed site as a covariate. Models quantify absolute differences in warming rate (K/h), maximum temperature (K), and cooling rate (K/h) between buffered and exposed microclimates across six environmental gradients: vegetation structure (low-height [V-L], medium-height [V-M]), elevation (north-facing [E-N], south-facing [E-S]), and slope orientation (high elevation [A-H], low elevation [A-L]). For each variable and gradient, model estimates (intercept and slope), standard error (SE), t-value, and p-value are shown. Marginal (R^2 m) and conditional (R^2 c) R^2 values indicate the variance explained by fixed effects alone and by the full model including random effects, respectively. 95

Tables in Appendix

Table A.1 List of all TMS-4 Standard loggers used in Studies 2 and 3 of this thesis, with their respective locality IDs, serial numbers, aspects, elevations, and coordinates. 141

Table A.2 List of all iButton loggers used in Study 2 of this thesis, with their respective serial numbers, aspects, elevations, and coordinates. 142

List of Abbreviations

A-H	Gradient comparing north- vs. south-facing slopes at high elevation
A-L	Gradient comparing north- vs. south-facing slopes at low elevations
AAO	Antarctic Oscillation, also known as Southern Annular Mode (SAM)
CHELSA	Climatologies at High Resolution for the Earth's Land Surface Areas (v2.1)
CMIP6	Coupled Model Intercomparison Project Phase 6
DEM	Digital Elevation Model
ECMWF	European Centre for Medium-Range Weather Forecasts
EM-Earth	Ensemble Meteorological Dataset for Planet Earth
ENSO	El Niño-Southern Oscillation
E-N	Gradient comparing low vs. high elevation on north-facing slopes
E-S	Gradient comparing low vs. high elevation on south-facing slopes
ERA5	Fifth generation reanalysis for the global climate and weather for the past 8 decades
EPSG:22181	European Petroleum Survey Group POSGAR 98 / Argentina Zone 2
EPSG:32719	European Petroleum Survey Group WGS 84 / UTM Zone 19S
EVI	Enhanced Vegetation Index
FAPAR	Fraction of Absorbed Photosynthetically Active Radiation
FWI	Canadian Forest Fire Weather Index
GBIF	Global Biodiversity Information Facility
GCM	Global Climate Model
GFDL-ESM4	Geophysical Fluid Dynamics Laboratory Earth System Model (version 4)
GMTED2010	Global Multi-resolution Terrain Elevation Data
Io	Annual ombrothermic index
IPSL-CM6A-LR	Institut Pierre-Simon Laplace Coupled Model (version 6A, low resolution)
IQR	Interquartile range
LAI	Leaf Area Index
LiDAR	Light Detection and Ranging
MAyDS	Ministry of the Environment and Sustainable Development of Argentina (Spanish: Ministerio de Ambiente y Desarrollo Sostenible)
m a.s.l.	Meters above sea level
MODIS	Moderate-Resolution Imaging Spectroradiometer
MPI-ESM1-2-HR	Max Planck Institute Earth System Model (version 1.2, high resolution)

MRI-ESM2	Meteorological Research Institute Earth System Model (version 2)
NDMI	Normalized Difference Moisture Index
POSGAR	Posiciones Geodésicas Argentinas
R^2	Coefficient of determination
RCP	Representative Concentration Pathway
RH	Relative humidity
RMSE	Root Mean Square Error
SAM	Southern Annular Mode (see AAO)
SD	Standard deviation
SDSM	Statistical DownScaling Model
Sentinel-3/OLCI	Copernicus Sentinel-3 Ocean and Land Colour Instrument
SMN	Servicio Meteorológico Nacional
SRTM	Shuttle Radar Topography Mission
SSP	Shared Socioeconomic Pathways
TMAX	Maximum daily temperature
TMIN	Minimum daily temperature
TMS	Temperature-Moisture-Sensor
Tp	Positive annual temperature
TPI	Topographic Position Index
TWI	Topographic Wetness Index
UKESM1-0-LL	United Kingdom Earth System Model (version 1.0, low-resolution atmosphere and low-resolution ocean configuration)
UAV	Unmanned Aerial Vehicle
UTM	Universal Transverse Mercator
V-L	Gradient comparing low-height vegetation vs. forest
V-M	Gradient comparing medium-height vegetation vs. forest
VWC	Volumetric water content
WBCS	World Wide Bioclimatic Classification System
WGS	World Geodetic System
WorldClim	WorldClim database of high spatial resolution global weather and climate data (v2.1)

1. Introduction

Climate change is reshaping forest ecosystems across the globe. Rising temperatures, altered precipitation patterns, and an increasing frequency and severity of extreme events such as droughts, storms, and wildfires are transforming the structure, composition, and functioning of forests (Allen et al. 2010; Seidl et al. 2014; Millar and Stephenson 2015; Seidl et al. 2017; Sommerfeld et al. 2018; Forzieri et al. 2022; Seidl and Turner 2022). These changes are particularly consequential in mountainous regions, where steep topographic gradients and high climatic variability create ecologically complex and diverse landscapes (Rangwala and Miller 2012; Albrich et al. 2020; Adler et al. 2022). While topographic complexity can buffer climate change impacts through a moderation of local conditions and a delay of vegetation shifts, this buffering capacity has limits, and even moderate warming may push mountain forests past critical thresholds, leading to irreversible changes and alternative states, especially under reduced precipitation scenarios (Albrich et al. 2020).

The temperate forests of northern Patagonia, composed largely of *Austrocedrus chilensis* and *Nothofagus* species, are arranged along steep elevation and climate gradients shaped by Andean topography (Veblen et al. 1996). Although this forest belt remains broadly continuous across north-western Patagonia, it is increasingly affected by rising temperatures, drought, and shifts in disturbance regimes (Rodríguez-Catón et al. 2016; Kitzberger et al. 2022; Tovar et al. 2022). Fire activity has intensified over recent decades and is projected to increase under continued warming (Kitzberger et al. 2022). As composition and structure shift under these pressures, local climate also changes, which in turn shapes ecological processes and long-term forest resilience (Paritsis et al. 2015; Tepley et al. 2018; Tiribelli et al. 2024).

In this context, understanding climatic responses in mountain forests, including those of northern Patagonia, requires examining how topography and terrain shape local climatic variability. Temperature and moisture conditions in mountain landscapes often vary markedly over short distances due to differences in elevation and slope orientation that influence incoming solar radiation (Barry 2008b). This variability, in turn, impacts species distributions, the extent to which they approach physiological thresholds, and their capacity to regenerate after disturbance events (Körner 2004; Graae et al. 2018; Rahbek et al. 2019; Marsh et al. 2022b). Recent findings highlight that such fine-scale heterogeneity modulates forest resilience, leading to spatially heterogeneous responses to climate change even within the same population or forest stand (Carnicer et al. 2021). Besides topographically associated variation, forests also have substantial interior climatic heterogeneity due to structural attributes. Canopy cover, canopy density, and composition of the understory affect temperature and humidity, generally creating cooler, more humid, and more stable conditions within the forest (De Frenne et al. 2019; Zellweger et al. 2020). Likewise, these interior

conditions shape species-level responses to climate change, such as physiological performance (Zweifel et al. 2007; Sanczuk et al. 2021), and also mediate ecological processes including regeneration dynamics (Marsh et al. 2022a; Espinosa del Alba et al. 2024), and species turnover (De Frenne et al. 2013; Iseli et al. 2025). Thus, the interior climate within forests has emerged as a key attribute in defining ecological resilience and biodiversity patterns under the pressure of climate change (De Frenne et al. 2019; Zellweger et al. 2020; De Frenne et al. 2021).

Recognizing the ecological importance of climatic variability at small scales raises important questions about how climate is represented in ecological research. Climate data are central to most analyses of biodiversity patterns and ecosystem functioning, yet there is often a mismatch between the scales at which such data are represented and the scales at which organisms experience climate (Franklin et al. 2013; Potter et al. 2013; Slavich et al. 2014; Suggitt et al. 2017). This mismatch underscores the need to distinguish between macroclimate and microclimate. While macroclimate describes regional climate regimes at large spatial scales, microclimate refers to the local conditions as they are perceived by many organisms (Barry and Blanken 2016). Whereas macroclimate provides a foundation for broad biogeographic patterns, microclimate captures the fine-scale variability shaped by topography and vegetation structure. In this context, identifying where and when microclimate provides explanatory value is a significant step toward more accurate measures of ecological response to climate change (Senf and Seidl 2018; Stark and Fridley 2022; Klinges et al. 2024). This, however, depends above all on the availability of datasets that can serve as a foundation for such identification.

Macroclimatic datasets such as CHELSA (Karger et al. 2017) or WorldClim (Fick and Hijmans 2017b) provide the fine spatial resolution needed for many regional assessments and are often the only available source of such climate grids. However, these products are built by interpolating weather-station observations. Where station networks are sparse or unevenly distributed in complex terrain, the interpolation struggles to capture local conditions (Bobrowski and Schickhoff 2017; Abdulwahab et al. 2022; Hemp and Hemp 2024). This is particularly true for precipitation estimates and for capturing the intensity and frequency of extreme events. In mountainous regions such as northern Patagonia, these datasets may fail to represent steep environmental gradients or localized processes such as cold-air pooling or orographic rainfall effects on a small scale, leading to systematic biases in temperature or moisture estimates. These inaccuracies can ultimately propagate into ecological models, potentially compromising assessments of habitat suitability, species vulnerability, and conservation priorities (Bobrowski and Schickhoff 2017; Datta et al. 2020; Bobrowski et al. 2021).

At the same time, modelling microclimates faces several challenges. These are especially relevant when scaling up measurements to estimate temperature and moisture across heterogeneous landscapes (Bramer et al. 2018). From a methodological perspective, there is

still a need for greater temporal flexibility in microclimatic information. Although spatial resolution has advanced, long term interpolations that are crucial for many analyses are still often missing (Kemppinen et al. 2024). A further issue concerns proximity, meaning how closely the climate variables represent the conditions experienced by the organism or ecological process of interest (Klinges et al. 2024). Downscaled topoclimatic products may provide fine spatial grids, yet they frequently still reflect free air conditions derived from weather stations (Bramer et al. 2018). This mismatch is critical in forests, where temperature and humidity can be decoupled or buffered relative to the free atmosphere, and where vertical structure adds further complexity (De Frenne et al. 2021). Mapping microclimates across space and time is therefore essential for understanding how local dynamics scale up to influence broader processes (Zellweger et al. 2019a). Beyond these methodological issues, geographic coverage in microclimate research remains uneven (Kemppinen et al. 2024). Northern Patagonia, including the Río Puelo basin, lacks extensive microclimate monitoring. As a result, many studies in the region rely on high resolution global products rather than datasets collected inside forests with explicit vertical coverage.

Against this background, this thesis examines how climate data across spatial scales can both improve and, if uncertain, impair our understanding of forest ecosystems in mountainous regions under climate change.

The overarching goal is to assess the strengths and limitations of both macro- and microclimatic approaches, and to identify how fine-scale variability can be integrated into landscape-scale modelling.

The thesis itself is embedded in the research project *Sustainable forest management of temperate deciduous forests – Northern hemisphere beech and southern hemisphere beech forests (KLIMNEM)*, a collaboration between the University of Göttingen (Germany), the Free University of Bozen-Bolzano (Italy), the University of Applied Sciences and Arts (HAWK, Germany), and the Andean Patagonian Forest Research and Extension Centre (CIEFAP, Argentina). The project is funded by the German Federal Ministry of Food and Agriculture (BMEL) through the Federal Office for Agriculture and Food (BLE, grant No. 28I-042–01). Within KLIMNEM, this dissertation contributes to project module 2, which focuses on the assessment of risks and opportunities using GIS-based, multifactorial modelling and multi-sensor remote sensing. In this context, my research addresses the climate modelling of the Río Puelo basin, raising the central questions of what climatic information is currently available, how reliable these data are, and how climate assessments can be improved to support ecological applications in the region. Therefore, the thesis is structured around three empirical studies, each addressing a distinct set of research questions:

The **first study** examines the representation of climate in global datasets and its influence on bioclimatic assessments in forested mountain landscapes. It addresses:

> *Q1: How do CHELSA v2.1 and WorldClim v2.1 differ in their spatial representation of temperature and precipitation patterns within the Río Puelo watershed?*
>
> *Q2: Does the choice of CHELSA v2.1 versus WorldClim v2.1 affect projections of the spatial extent and distribution of forest bioclimatic zones within the Río Puelo watershed under future climate scenarios?*

The **second study** focuses on spatial modelling of microclimatic variability, using in-situ measurements and remote sensing to identify drivers of fine-scale conditions in Andean forests. It addresses:

> *Q3: Which macroclimatic, vegetation, and terrain predictors account for the largest share of variation in monthly microclimatic conditions across multiple vertical levels in Andean forests of northern Patagonia?*
>
> *Q4: How consistent is the influence of key vegetation and terrain predictors across months and seasons, and do these effects vary across vertical levels and between temperature- and moisture-related microclimatic variables?*

The **third study** investigates near-surface thermal buffering during summer heat, examining how vegetation structure, topography, and heat stress interact to shape diurnal temperature dynamics. It addresses:

> *Q5: Does microclimatic buffering, measured as temperature differences between buffered and exposed sites, vary with higher maximum temperatures at exposed sites, and which environmental gradients are associated with the greatest increases?*

Following this framing, the thesis begins with a review of relevant theoretical and conceptual frameworks, establishing the broader context for the research questions. The subsequent chapter describes the study area, its regional climate, and the tools applied for data acquisition. The core chapters present the three empirical studies, each addressing different components of the overarching research aim and corresponding to the research questions outlined above. The final chapter integrates findings from all studies, emphasizing their collective contribution to understanding forest ecosystem responses to climate change, and discusses methodological limitations, practical implications, and directions for future research.

2. Conceptual background

2.1 Landscape and ecosystem ecology

Landscape ecology developed at the intersection of ecology, geography, and spatial planning, seeking to explain how spatial heterogeneity influences ecological processes and vice versa (Forman and Godron 1986; Turner 1989). The term *landscape* is not merely descriptive of scenery but analytical, capturing the spatial mosaics where ecological processes and human influences interact and transform over time (Forman 1995). In this sense, the discipline provides a bridge between local ecological dynamics and broader geographic patterns. A core principle of landscape ecology is therefore its focus on heterogeneity as both driver and outcome, which inherently requires examining the relationships among pattern, process, and scale (Turner 1989; Wu 2013). Variation in vegetation cover, soil properties, hydrology, or microclimate creates distinct habitat conditions. These variations, in turn, regulate species distributions, energy and material fluxes, and dynamics of disturbances (Billings et al. 1987; Pickett and Cadenasso 1995; Stein et al. 2014; Premke et al. 2016; Seidl et al. 2018). Conversely, ecological processes such as dispersal, succession, or fire actively shape the structure of the landscape, producing feedback loops between pattern and process (Suding et al. 2004; Tepley et al. 2018). Over time, landscape ecology has expanded from a primarily descriptive discipline into a more predictive and analytical science. Early focus on visual interpretation of landscapes has been complemented by quantitative models, spatial statistics, and large-scale datasets, with geospatial technologies now forming mainstream tools for analysing spatial patterns and processes (Wiens 1992; Bastian and Steinhardt 2002; Wang et al. 2025). Parallel to these methodological advances, the field has increasingly positioned itself as a problem-oriented science, engaging directly with ecological and social challenges (Opdam et al. 2001; Wang et al. 2025; Wu et al. 2025).

Among the central concepts of landscape ecology, scale is widely recognized as one of the most fundamental (Delcourt and Delcourt 1988; Wiens 1989; Turner 1990). Ecological processes unfold across multiple spatial and temporal scales, from localized biogeochemical cycling (Ladau and Eloe-Fadrosh 2019) to the global carbon cycle (Falkowski et al. 2000). Observed patterns often shift depending on whether analysis is conducted at fine-grained resolutions or broader extents. This phenomenon, sometimes referred to as *the problem of scale*, means that ecological inference depends on matching the scale of observation with the scale of the underlying process (Levin 1992). Another critical concept is hierarchy theory, which emphasizes that processes are nested: local conditions are constrained by broader regional dynamics, while simultaneously influencing them (Allen and Starr 1988). For example, a patch-level disturbance such as treefall may influence microhabitat conditions, yet its longer-term impact depends on regional climate and land-use legacies. This layered understanding

prevents simplistic conclusions and instead encourages analyses that recognize interactions across scales (Peters et al. 2007). Landscape structure is also frequently formalized through models such as the patch-corridor-matrix framework, which views landscapes as mosaics of habitat units embedded in a broader matrix. Within this framework, each location in the landscape is interpreted as belonging to one of three elements: patch, corridor, or matrix (Forman 1995). While this representation is a simplification, it provides a useful conceptual tool for thinking about connectivity, fragmentation, and flow across landscapes (Blois et al. 2002). Later perspectives have extended this to gradient-based approaches, recognizing that many ecological variables vary continuously rather than discretely across space (McGarigal et al. 2009). Together, these concepts build the core of the discipline, highlighting that landscapes are structured, scale-dependent systems where ecological outcomes arise from the interaction of local conditions with broader configurations.

These concerns with scale and structure also reveal the close intellectual and methodological ties between landscape ecology and geographic science. Geographers have long emphasized the importance of space, place, and spatial relationships, concerns that resonate deeply with landscape ecological approaches and have informed perspectives across the social and life sciences (Hunziker et al. 2007; Agnew 2011). The development of geospatial technologies has revolutionized the field, providing new levels of capacity to observe and analyse landscapes at multiple resolutions (Newton et al. 2009; Yu et al. 2019). Recent developments in geospatial data and computational capacity have steadily expanded the ability to analyse landscapes, enabling researchers to connect ecological patterns with processes in greater detail, over finer scales, and through more dynamic perspectives than was previously possible. For instance, integrating high-resolution vegetation and topographic data into spatial models makes it possible to capture microclimatic variability and reveal ecological dynamics that remain hidden in coarser-scale species distribution models (Frey et al. 2016a; Meineri and Hylander 2017). Beyond technical advances, the geographic tradition contributes a conceptual orientation: the idea that spatial context matters. Ecological patterns cannot be fully understood without considering proximity, neighbourhood effects, and connectivity (Legendre and Fortin 1989; Tilman and Kareiva 1997; Dale 2009). Whether examining species distributions, disturbance spread, or climate gradients, geographic thinking ensures that analysis is not limited to isolated patches but instead considers their embeddedness in wider landscapes.

Climate change further underscores the importance of these geographic and technological perspectives, as its impacts are rarely uniform across space. Global averages mask substantial spatial heterogeneity in exposure and vulnerability (Rangwala and Miller 2012; Garcia et al. 2014; Xie et al. 2015). Next to regional patterns of change, local factors such as topography, vegetation, and land use can amplify or buffer climatic signals, producing diverse outcomes even within small geographical units (Barry 2008b; Pielke et al. 2011; De Frenne et

al. 2021). Landscape ecology's focus on heterogeneity, therefore, makes it uniquely suited to investigate these fine-scale variations. Homogenous landscapes may exacerbate vulnerability by limiting species' movement to more suitable habitats, while heterogeneous landscapes may provide refugia where species persist under otherwise unfavourable conditions (Ackerly et al. 2010; Lenoir et al. 2017). Such insights highlight, once again, the importance of considering spatial context when evaluating resilience and adaptation potential to climate change (Allen et al. 2016). Thus, landscape ecology offers conceptual and analytical tools to disentangle the interplay between climate and spatial patterns. By emphasizing scale-dependent processes, it facilitates understanding of how global drivers translate into local impacts, and conversely, how local buffering may scale up to influence broader ecosystem stability. The field thus contributes not only to ecological theory but also to applied efforts in conservation and land management under climate change (Nowakowski et al. 2018; Keppel et al. 2024).

Climate change rarely operates in isolation but interacts with disturbances that are central to landscape dynamics (Turner 2010). These disturbances, including abiotic drivers such as fire, wind, and drought, as well as biotic agents like insects and pathogens, are closely linked to climatic conditions and influence the structure and composition of landscapes (Seidl et al. 2017). Landscape ecology frames disturbances not as anomalies but as integral processes that create and maintain mosaics of different successional stages (Turner et al. 1993; Turner et al. 1998). The ecological consequences of disturbance depend strongly on landscape context: topographic complexity modulates the size, shape, and distribution of disturbance patches, thereby influencing whether disturbances lead to landscape homogenization or increased heterogeneity (Senf and Seidl 2018). Fire in continuous forests often spreads differently than in fragmented mosaics, where edges, altered connectivity, and human activities can obstruct, redirect, or intensify fire progression (Driscoll et al. 2021); regeneration is likewise shaped by landscape context, with establishment success varying across burn edges, elevations, and interior patches (Coop et al. 2010). Moreover, disturbances frequently interact with one another and with broader climatic processes. Such interactions are often complex and can lead to counterintuitive dynamics, highlighting the need to consider multiple drivers simultaneously rather than in isolation (Burton et al. 2020). Recognizing these interactions highlights the importance of feedbacks: disturbances alter vegetation and ecosystem processes in ways that, when coupled with climatic extremes, not only shape future disturbance regimes but also feed back into the climate system (Thom et al. 2017). This dynamic perspective shifts focus away from paradigms of stability toward resilience, sensitivity, and regime shifts (Seidl et al. 2014; Anderegg et al. 2020; Forzieri et al. 2022; Seidl and Turner 2022). For landscape ecology, this means viewing disturbance not only as a driver of change but also as a process tightly interwoven with spatial pattern and ecological response.

The ecological consequences of such disturbances cannot be understood without considering the organisms that inhabit these landscapes, since species perceive and interact with spatial patterns in different ways. In fragmented landscapes, connectivity and corridors are not only critical for species movement but also for maintaining ecological processes such as pollination and seed dispersal (Tewksbury et al. 2002). For plants and less mobile organisms, the fine-scale availability of microhabitats and refugia becomes critical, especially under changing climates or disturbance regimes (Ashcroft 2010; Denney et al. 2020; De Frenne et al. 2021). From a landscape perspective, ecological responses cannot be explained by macro-level drivers alone; instead, they arise from the interplay of organismal traits, landscape structure, the climate as it is locally experienced, and competition under changing conditions (Alexander et al. 2015; Pacifici et al. 2015; Fei et al. 2017). To understand these dynamics, it is crucial to capture the fine-scale climatic conditions organisms experience and the structural features that shape them. These factors strongly influence survival, reproduction, and disturbance processes, which in turn affect the distribution of plant species across landscapes (D'Odorico et al. 2013; Just et al. 2016; Zellweger et al. 2019b).

2.2 Microclimatology

Microclimates describe the local climatic conditions that are actually experienced at the scale of organisms, and these often differ substantially from regional climate averages (Bramer et al. 2018). These deviations arise because climate is filtered through local biotic and abiotic features such as topography, vegetation, and soils, which regulate radiation, wind, humidity, and energy fluxes (Geiger et al. 2009; Barry and Blanken 2016). Topographic variation, including elevational gradients, slope orientation, and terrain roughness, can generate pronounced temperature contrasts across very short distances (Barry 2008b; Dobrowski 2011; Rita et al. 2021). Vegetation and soils add further complexity: dense canopies reduce incoming radiation and wind speed, buffering organisms from extremes, whereas open or patchy vegetation exposes ground surfaces to greater heating and drying (Renaud and Rebetez 2009; von Arx et al. 2013; De Frenne et al. 2019). The ability of vegetation to buffer local climates is further influenced by water availability, meaning that shifts in canopy cover or soil moisture can alter how effectively ecosystems moderate temperature extremes (Davis et al. 2019; Greiser et al. 2024).

These fine-scale conditions are ecologically important because they directly influence the physiological limits of organisms, governing survival and reproduction (Körner 2004; Graae et al. 2018; Rahbek et al. 2019; Crockett and Hurteau 2022; Marsh et al. 2022a). Their effects scale up from individuals to populations, communities, and ecosystems, shaping demographic rates, competitive dynamics, and ultimately species distributions (Kemppinen et al. 2024). Microclimates can buffer organisms from broader climatic extremes by providing microrefugia,

or conversely, amplify stress through locally intensified droughts or heat events. In this way, they may mediate the ecological consequences of climate change (Suggitt et al. 2018; De Frenne et al. 2019). However, such local modifications are not captured by macroclimatic datasets, which are typically based on standardized weather stations in open, wind-exposed sites (Fick and Hijmans 2017b; Karger et al. 2017) and therefore miss the terrain, vegetation, and soil effects that shape the actual conditions experienced by organisms (Lembrechts and Lenoir 2020).

Microclimates also provide a critical link between landscape ecology and climate change biology. Local heterogeneity in vegetation and topography generates mosaics of thermal and moisture niches that reinforce the pattern–process feedbacks central to landscape ecology. Disturbances such as fire, wind, or drought both shape and are shaped by microclimatic conditions, influencing regeneration pathways and the resilience of ecosystems (Just et al. 2016; Kopáček et al. 2020; Thom et al. 2020; Atkins et al. 2023). Thus, understanding landscape dynamics under climate change requires explicit consideration of microclimatic variation. Furthermore, acknowledging the ecological significance of microclimatic variation has created new possibilities in applied disciplines like biodiversity conservation and forestry, where managing microclimatic heterogeneity is increasingly viewed as a strategy to strengthen resilience in the face of climate change (Hylander et al. 2022; Kemppinen et al. 2024). Recent advances in methods have accelerated this development. In-situ loggers and wireless sensor networks provide high-resolution microclimatic data (Wild et al. 2019; Rebaudo et al. 2023), while remote sensing technologies such as LiDAR, UAV-based thermal imaging, and satellite-derived products enable mapping microclimate drivers across landscapes (Zellweger et al. 2019a).

Approaches to modelling microclimates span a continuum from mechanistic to statistical (Kemppinen et al. 2024).

Mechanistic or process-based models, rooted in energy-balance equations, offer a detailed representation of the physical processes that govern near-ground climate (Porter et al. 1973; Kearney and Porter 2009). Despite advances in computational power and theoretical understanding, mechanistic models remain difficult to apply at large scales, as they require detailed input data and face persistent challenges of scaling, calibration, and validation (Cabral et al. 2017). Nonetheless, they play a crucial role in advancing our understanding of how biotic and abiotic drivers shape microclimates and will be increasingly important for developing reliable projections of ecosystem responses to climate change (Maclean et al. 2019; Briscoe et al. 2023).

Statistical models, by contrast, establish empirical relationships between microclimates and their drivers such as terrain or canopy cover. While they cannot establish causation, they can

describe functional relationships between organisms and their environment (Box 1966; Sokal 2009). These approaches are computationally efficient and scalable, but their transferability across regions or time periods is limited. This is partly because the geospatial predictors they rely on, such as topographic indices or vegetation cover, act only as proxies for the underlying physical processes, and their statistical relationships with microclimates can shift across landscapes and seasons (Aalto et al. 2022). In applied contexts, statistical frameworks are often used for spatial interpolation or downscaling, for example converting point-based logger data into continuous climate surfaces or refining coarse-grained macroclimate datasets into fine-scale predictors for species distribution models (Ashcroft and Gollan 2012; Meineri and Hylander 2017). While such techniques improve the spatial resolution of climate information, they remain constrained by the quality and representativeness of predictor variables and by assumptions about the stability of their relationships with microclimate. In addition, the effectiveness of statistical models depends on how well ecological theory is incorporated into the modelling framework, since purely correlative approaches risk overlooking key processes or interactions (Austin 2002). Nevertheless, statistical models remain valuable tools for predicting microclimatic patterns across large spatial and temporal extents, especially when combined with ecological insights that improve their explanatory power (Zellweger et al. 2019b; Zellweger et al. 2020).

3. Environmental setting and data collection

3.1 Study region

This dissertation focuses on the temperate mountain landscapes of northern Patagonia, Argentina, situated in the Andean foothills around the Río Puelo and Río Manso watersheds (between 41-42° S, 71-72° W). The region is characterized by steep topographic gradients, complex valley systems, and a pronounced west-east precipitation decline caused by the Andean rain shadow. Annual precipitation, based on 1991–2020 climate normals, exceeds 1,400 mm in the western ranges (Río Manso Inferior; 41.6° S, 71.8° W; 439 m a.s.l.) but falls below 500 mm in the east (El Maitén; 42.1° S, 71.2° W; 652 m a.s.l.), while elevations span from below 500 m to over 3000 m a.s.l. (Sistema Nacional de Información Hídrica 2023). These climatic and topographic gradients interact to generate high environmental heterogeneity over short spatial scales.

Figure 3.1 *Dominant native tree species within the Río Puelo watershed. Photos by Jonas Fierke (all except upper right) and Birgitta Putzenlechner (upper right).*

Vegetation is dominated by temperate forests of *Nothofagus* species (*N. pumilio, N. dombeyi, N. antarctica*) and *Austrocedrus chilensis*, forming a continuous but compositionally diverse belt across the landscape (Figure 3.1). Dense *N. dombeyi* and mixed forests occur at lower and mid-elevations, whereas *N. pumilio* dominates at upper montane and subalpine

elevations. In drier and more disturbed settings, forests give way to shrublands or open stands of *N. antarctica* and *A. chilensis* (Eskuche 1973; Veblen and Lorenz 1987; Veblen et al. 1996). Historical land use and recurrent natural disturbances, especially wildfires, have further shaped vegetation mosaics and structural diversity of the Río Puelo watershed (Gowda et al. 2012; Kitzberger 2012).

An overview of the Río Puelo watershed and the study sites included in this dissertation is provided in Figure 3.2. More detailed site descriptions, including transect designs and measurement setups, are available in the respective case study chapters.

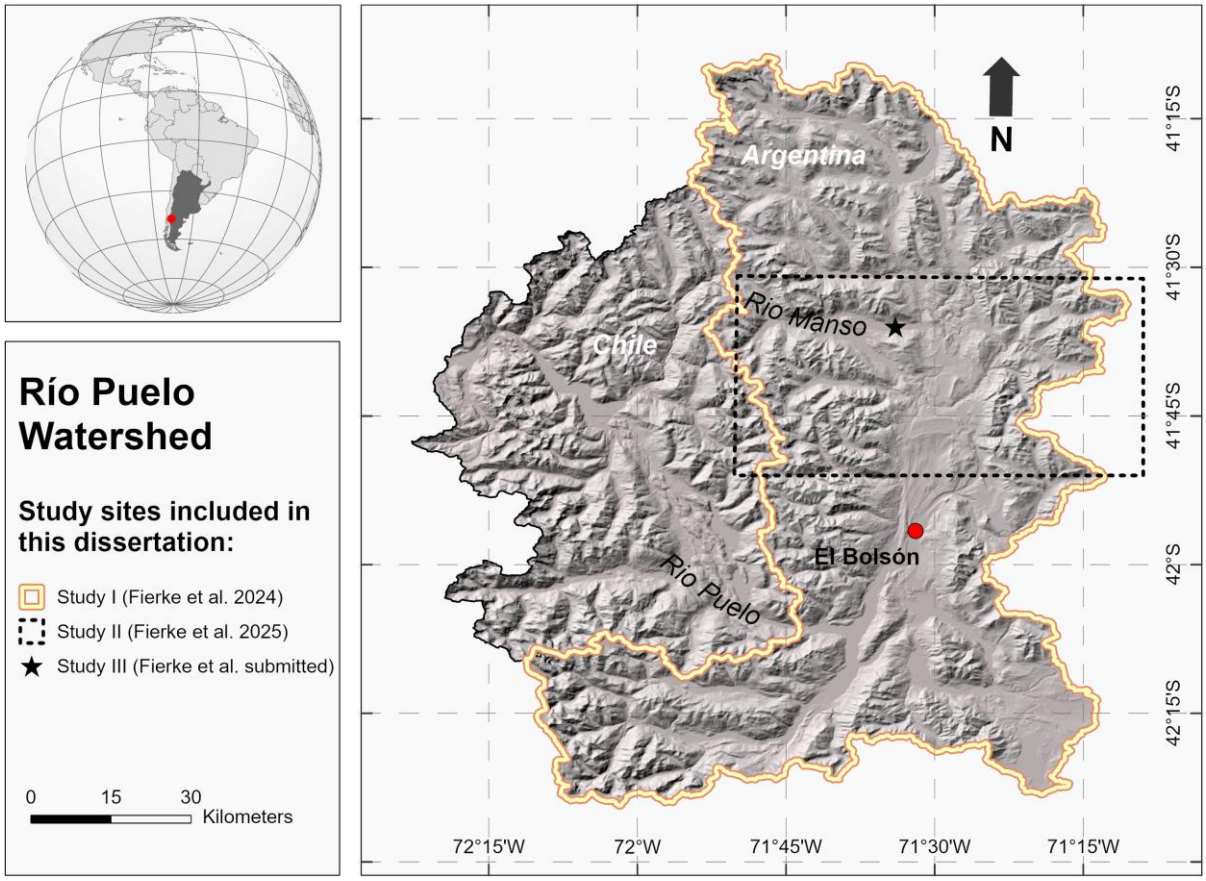

Figure 3.2 *Río Puelo watershed including the study areas of the studies included in this dissertation. Figure adapted from Fierke et al. (submitted-b).*

3.2 Regional climate

The climate of the Patagonian Andes is shaped by atmospheric circulation and orographic effects, further modulated by large-scale variability and anthropogenic climate change. At its foundation, regional climate is governed by the interaction of major circulation systems around the Andes: the Southeast Pacific Subtropical Anticyclone (SPSA), which regulates tropical rainfall and coastal aridity; the South American Low-Level Jet (SALLJ), which channels Amazonian moisture southward; the South Atlantic Subtropical Anticyclone (SASA), influencing cloud formation and sea surface temperatures; and the midlatitude westerlies, whose storm track delivers the bulk of precipitation to Patagonia (Garreaud et al. 2009;

Garreaud et al. 2013). Orographic forcing by the Andes amplifies these processes, producing strong east-west climate gradients between the humid slopes of Chile and the dry Argentine steppe (Paruelo et al. 1998).

Climate variability arises through interactions across multiple timescales. At the base are the diurnal and seasonal cycles, both driven by solar forcing, which establish the fundamental rhythm of temperature and precipitation in the region. The diurnal cycle interacts with intra-seasonal variability (weeks) primarily through synoptic weather systems (days), as passing storms influence daily heating and cooling. The seasonal cycle likewise shapes intra-seasonal variability, since the background state of the atmosphere (such as the position and intensity of the westerlies) determines how sub-seasonal oscillations unfold. At a broader scale, variability on interannual and longer timescales is driven by the El Niño-Southern Oscillation (ENSO), the Indian Ocean Dipole (IOD), and the Southern Annular Mode (SAM), which together shape year-to-year and decadal climate anomalies (Garreaud et al. 2009; Silvestri and Vera 2009; Andrian et al. 2024). These processes are, again, further modulated by orographic forcing from the Andes and by land-atmosphere-ocean interactions, which influence how anomalies develop, intensify, or persist. Finally, anthropogenic forcing overlays all these natural cycles, shifting the baseline around which variability occurs and influencing the frequency of these modes (Cai et al. 2020; Mindlin et al. 2020; Mindlin et al. 2021).

Among the large-scale climate modes, ENSO exerts a strong influence. During El Niño events, tropical Pacific warming alters atmospheric circulation via Rossby wave trains, shifting the trajectory of the westerlies and storm systems. While this signal is relatively strong further north of the study region, its influence weakens toward southern Patagonia, where variability in the westerlies and the Southern Annular Mode play a more dominant role (Silvestri and Vera 2009; Penalba and Rivera 2016). Still, in parts of northern Patagonia such as Esquel, summer precipitation shows a negative relationship with ENSO, with El Niño years tending to be drier and La Niña years wetter (Agosta et al. 2020). The IOD, though centered far away, frequently co-occurs with ENSO and reinforces its teleconnections (Andrian et al. 2024). The Southern Annular Mode (SAM), reflecting shifts in the Southern Hemisphere westerlies, is another key driver. During its positive phase, weakened westerlies reduce precipitation over Patagonia, whereas during its negative phase, stronger westerlies bring more storms and wetter conditions (Silvestri and Vera 2009; Holz et al. 2017; Fogt and Marshall 2020). Importantly, the impacts of ENSO and SAM are not stationary but vary over decades, reflecting shifts in teleconnection pathways and background climate conditions (Silvestri and Vera 2009). Although ENSO's influence may appear straightforward, its regional impacts are highly complex, shaped by event diversity, interactions with other climate modes, and inter-basin linkages (Cai et al. 2020). Moreover, ENSO and SAM may also interfere with one another, sometimes reinforcing and sometimes offsetting their impacts. For instance, the 2015–2016 El

Niño coincided with a positive SAM phase, modifying the expected circulation anomalies and weakening the usual precipitation response (Vera and Osman 2018).

These atmospheric modes translate directly into hydrological impacts. In northern Patagonia, variability in ENSO, SAM, and related modes strongly modulates precipitation and snow accumulation, which govern streamflow seasonality. Changes in the timing and intensity of winter precipitation affect snowpack development, while warming trends accelerate snowmelt and reduce summer flows. As a result, river discharge shows pronounced interannual fluctuations, with droughts and low-flow periods often amplified beyond the precipitation deficits that trigger them (Aguayo et al. 2019). This sensitivity underscores how large-scale climate variability and long-term warming combine to shape water availability and ecosystem responses within the region (Holz et al. 2017; León-Muñoz et al. 2018).

Future climate projections highlight both risks and uncertainties. Model simulations consistently suggest a poleward shift of the westerlies under greenhouse gas forcing, which is associated with a reduction of precipitation in the northern Patagonian Andes. Yet the magnitude of this shift depends on remote drivers, particularly tropical Pacific warming and polar vortex dynamics (Mindlin et al. 2020; Mindlin et al. 2021). By framing projections in terms of these drivers, uncertainties can be narrowed, offering more confidence in anticipating regional hazards. Importantly, across different scenarios the signal of drying is robust, with most models indicating declining precipitation (Mindlin et al. 2020). These dynamics underscore the sensitivity of Patagonia's hydroclimate to both natural oscillations and future global warming, with profound implications for ecosystems, water resources, and human activity in the region.

3.3 Data acquisition

Studies 2 and 3 were based on empirical microclimatic measurements obtained with autonomous sensors (Figure 3.3). Two types of devices were deployed: TOMST TMS-4 Standard dataloggers for Study 2 and 3 as well as Analog Devices iButton DS1923 Hygrochron loggers for Study 2. The TMS-4 Standard is a multi-sensor device designed for ecological field applications, equipped with three temperature sensors (MAXIM/DALLAS Semiconductor DS7505U+) with a resolution of 0.0625 °C and an accuracy of ±0.5 °C (Wild et al. 2019). It records air temperature at 15 cm above the ground, surface temperature at 2 cm above the ground, and soil temperature at a depth of 6 cm. In addition, the logger includes a belowground soil moisture sensor based on the time-domain transmission principle. Measurements were taken every 15 minutes, producing continuous high-resolution time series suitable for analysing both seasonal dynamics and short-term extreme events. To minimize bias from direct solar radiation, all TMS-4 loggers are equipped with an integrated radiation shield and were installed at representative microhabitats across environmental gradients.

Additionally, iButton DS1923 Hygrochron loggers (Maxim Integrated) were installed at 2 m above the ground. These devices measure humidity with either 8-bit (0.6 % RH) or 12-bit (0.04 % RH) resolution, and temperature with 8-bit (0.5 °C) or 11-bit (0.0625 °C) resolution, achieving an accuracy of ±0.5 °C from -10 °C to +65 °C with software correction (Analog Devices, Inc., USA). These sensors were sheltered from sunlight and weather exposure using inverted white plastic cups (250 cm³), which served as simple radiation shields. The iButtons recorded both air temperature and relative humidity, enabling the analysis of vertical variation in thermal and moisture conditions. iButtons are widely used in ecological monitoring because of their compact size and low energy consumption.

Figure 3.3 *Microclimatic sensors used in Studies 2 and 3. Shown are (from upper left to bottom right): a TOMST TMS-4 Standard logger (overview), a TMS-4 Standard logger installed in the field, an iButton DS1923 Hygrochron logger (overview), and an iButton logger installed in the field. Photos by Jonas Fierke.*

Together, the two systems enabled the simultaneous characterization of near-ground, soil, and above-ground microclimatic conditions. The geographic locations of all sensors are provided in Annex Tables A.1 and A.2, while the detailed sampling designs are described in the respective publications.

4. Study I - Assessing uncertainty in bioclimatic modelling: a comparison of two high-resolution climate datasets in northern Patagonia

Original Article (open access)

Published on 16. July 2024 in *Regional Environmental Change* (Springer Nature) Volume 24, article number 110

Jonas Fierke, Natalia Zoe Joelson, Gabriel Angel Loguercio, Birgitta Putzenlechner, Alois Simon, Daniel Wyss, Martin Kappas & Helge Walentowski

Abstract

Climate change is reshaping forest ecosystems, presenting urgent and complex challenges that demand attention. In this context, research that quantifies interactions between climate and forests is substantial. However, modelling at a spatial resolution relevant for ecological processes presents a significant challenge, especially given the diverse geographical contexts in which it is applied. In our study, we aimed to assess the effects of applying CHELSA v.2.1 and WorldClim v2.1 data on bioclimatic analysis within the Río Puelo catchment area in northern Patagonia. To achieve this, we inter-compared and evaluated present and future bioclimates, drawing on data from both climate datasets. Our findings underscore substantial consistency between both datasets for temperature variables, confirming the reliability of both for temperature analysis. However, a strong contrast emerges in precipitation predictions, with significant discrepancies highlighted by minimal overlap in bioclimatic classes, particularly in steep and elevated terrains. Thus, while CHELSA and WorldClim provide valuable temperature data for northern Patagonia, their use for precipitation analysis requires careful consideration of their limitations and potential inaccuracies. Nevertheless, our bioclimatic analyses of both datasets under different scenarios reveal a uniform decline in mountain climates currently occupied by *N. pumilio*, with projections suggesting a sharp decrease in their coverage under future climate scenarios.

Keywords: Climate change, Regional climate models, Terrain, WorldClim, CHELSA

4.1 Introduction

Climate change poses significant challenges to forest ecosystems, affecting their composition, structure, and function. Rising temperatures, shifting precipitation patterns, extreme weather events, and hazards such as droughts and wildfires are altering their ecological dynamics. These changes can lead to shifts in species distribution and disruptions due to transformed ecological processes such as tree establishment and tree mortality (Rodríguez-Catón et al. 2016; Srur et al. 2016, 2018; Tovar et al. 2022) along with changing patterns of invasive species (Iglesias et al. 2022). Additionally, the loss of glacier-fed rivers and decreased snowpack levels impact hydrological regimes, further intensifying stress on ecosystems (Aguayo et al. 2019; Rivera et al. 2023).

Studying the nexus of climate and ecosystems, bioclimatology emerges as a comprehensive framework. It explores in depth the intricate relationship between climate variables and biological processes, with a particular emphasis on their impact on species and ecosystems. This analytical approach integrates climatology, ecology, and biology to understand species distribution and interactions in space and time (Saslis-Lagoudakis et al. 2014). Thus, bioclimatic analysis can be a basis for biodiversity conservation (Ferrier et al. 2020), future-oriented forestry management (MacKenzie and Mahony 2021), and enhancing ecosystem resilience (Piraino et al. 2022). To effectively address these challenges and capture the nuances of small-scale ecological processes, research must be conducted at a relevant spatial scale, ensuring the precision needed for detailed bioclimatic insights.

Nevertheless, modelling at high-resolution presents a significant challenge, especially given the diverse geographical contexts in which it is applied. Peripheral mountainous regions, in particular, face hurdles due to limited coverage of in-situ observations (Condom et al. 2020; Thornton et al. 2022) and their inherent topographic complexity. Access to reliable climate information at high resolution for these regions is often challenging. The scarcity of precise and localized data restricts the ability to capture the intricate interactions and dynamics of the systems under study, thereby introducing significant uncertainties into model outputs. Further, limited availability of data complicates the validation and calibration of models, reducing their reliability in decision-making processes (Littell et al. 2011; Otto et al. 2016).

Climatologies at high resolution for the Earth's land surface areas (CHELSA) (Karger et al. 2017) and WorldClim (Fick and Hijmans 2017a) stand out as proven climate datasets for bioclimatic analysis, valued for their high spatial resolution, global coverage, and user-friendly accessibility. Both datasets provide researchers with a range of climatic variables crucial for understanding ecological processes and environmental changes within bioclimatic analysis (Körner et al. 2011; Pesaresi et al. 2017; Pham et al. 2023). Nevertheless, studies in different geographical settings have shown that particularly precipitation-related variables may lack

reliability and should be examined carefully (Bobrowski and Schickhoff 2017; Bobrowski et al. 2021; Abdulwahab et al. 2022). Applying and comparing both datasets can thus shed light on the specific needs and challenges in accurately modelling a region's ecological and climatic dynamics.

Within the Andes of northern Patagonia, a pronounced precipitation gradient stretches from west to east over a relatively short distance, leading to a distinct vegetation productivity gradient across the region (Kitzberger et al. 2022). This underscores the importance of precipitation-related bioclimatic variables at high resolution for accurately understanding the region's complex ecosystem dynamics. However, despite the area's unique terrain and the critical role of input data in bioclimatic analysis (Morales-Barbero and Vega-Álvarez 2019), there is a notable research gap in comparing different datasets for bioclimatic analysis within northern Patagonia. The study by Derguy et al. (2022), which compares bioclimatic changes based on two local climate models in southern South America, stands as a rare but vital exception. However, similar studies are needed to uncover the strengths, limitations, and potential biases of various datasets, thereby improving the accuracy and reliability of bioclimatic models (Bobrowski and Schickhoff 2017; Abdulwahab et al. 2022).

In our study, we hypothesized that within the Río Puelo catchment area in northern Patagonia, precipitation-related variables would demonstrate greater uncertainty compared to temperature-related variables, as observed in other geographical settings. Guided by this hypothesis, our primary objective was to assess the impact of using CHELSA and WorldClim data on bioclimatic analysis in this region. To do this, we first compared current and future bioclimates based on these two distinct climate datasets, conducting an inter-comparison to identify any inherent patterns, trends, or discrepancies. Subsequently, we performed a comparison against available reference data to contextualize our findings further. This approach was designed to provide a comprehensive understanding of the potential implications of employing CHELSA and WorldClim data for bioclimatic studies within the Río Puelo catchment.

4.2 Data and methods

4.2.1 Study area

The Río Puelo watershed in northern Patagonia, spanning from 41.2° to 42.5° South and 72.2° to 71.5° West, crosses the Río Negro and Chubut provinces in the Andes and features diverse topography and notable climatic gradients. Precipitation decreases from west to east due to the rain shadow of western mountains (Villalba et al. 2003), while an elevation range from 190 to 3,157 meters affects temperature and precipitation patterns, including snowfall. The area's macroclimate is influenced by the Antarctic Oscillation (AAO) and the El Niño-Southern Oscillation (ENSO). Dominant vegetation includes *Austrocedrus chilensis* and *N. antarctica,*

N. dombeyi, and *N. pumilio*, with certain *Nothofagus* species at their climatic limit in the east (Amigo and Rodríguez-Guitián 2011; Kitzberger et al. 2022).

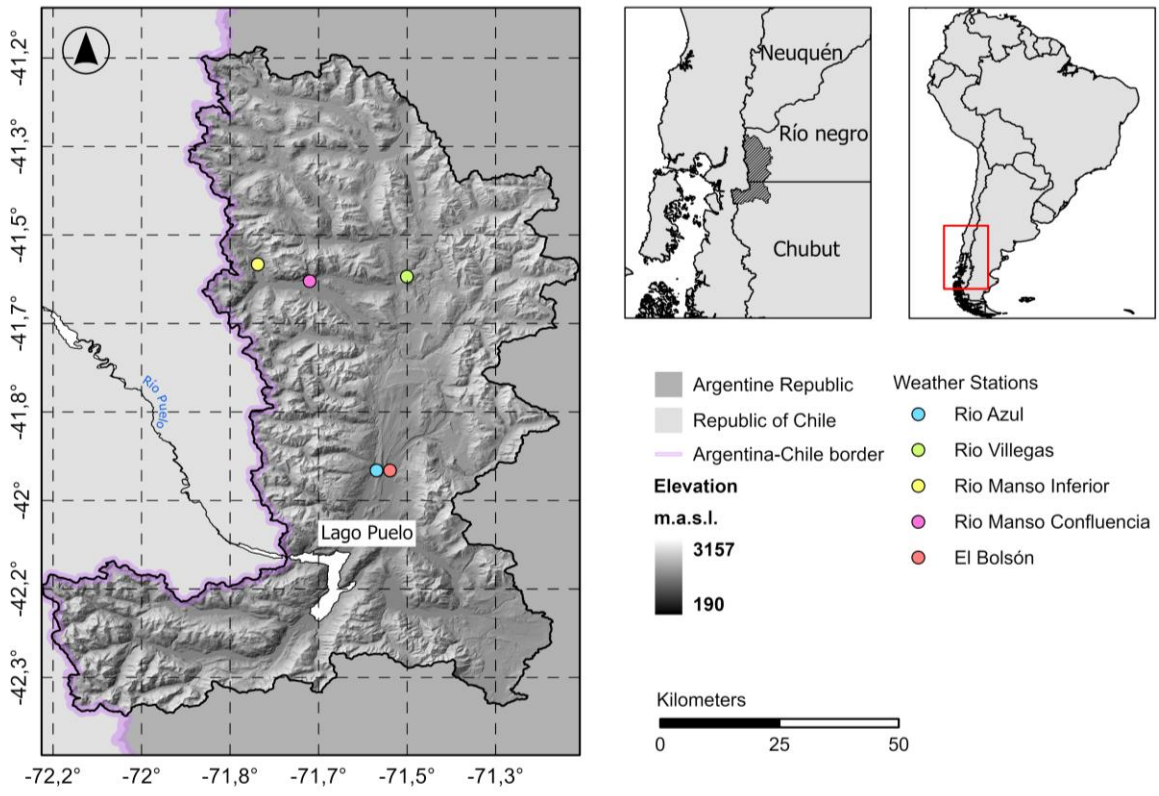

Figure 4.1 *Map of eastern Río Puelo watershed (showing Río Puelo and Lago Puelo exclusively), located at the Argentina-Chile border in north-west Patagonia. Topography of the study area is illustrated on basis of the digital elevation model SRTM (Farr et al. 2007).*

4.2.2 Study design

The experimental design of the study (Fig. 4.2) comprises two principal comparative analyses based on CHELSA and WorldClim. The first phase involves deriving current and future bioclimatic zones for a comparison between both data sources, which aims to identify intrinsic patterns, trends, or discrepancies between both datasets that are then framed as different types of uncertainty. In the initial phase of our study, we leverage climate, species, and elevation data to delineate bioclimatic zones. This process is critical for identifying areas with distinct climate characteristics that influence local vegetation patterns. In the second phase, historical data from CHELSA and WorldClim, alongside meteorological station data, are applied in a validation to contextualize and the findings of the first phase. Collectively, these comparative phases constitute a comparative framework for examining the applied climate datasets.

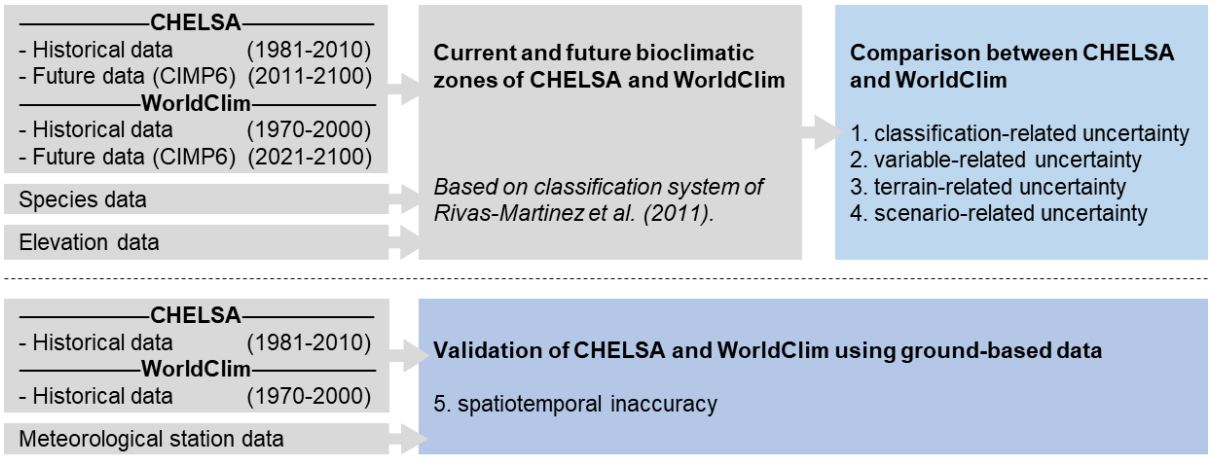

Figure 4.2 *Comparative framework for assessing bioclimatic modelling uncertainty using historical and future climate data, as well as species, elevation, and meteorological station data. Where grey boxes represent the data input as well as the bioclimatic pre-analysis and coloured boxes represent the two validation phases.*

4.2.3 Elevation data

We used the digital elevation model of the Shuttle Radar Topography Mission (SRTM) at a spatial resolution of 1 arc second which corresponds to approximately 28 meters within the study area (Farr et al. 2007).

4.2.4 Historical climate data

For both evaluation processes (Fig. 4.2), we investigated the climate datasets of WorldClim v2.1 and CHELSA v2.1. These are publicly available, easily accessible, and of high spatial resolution (required to capture altitudinal layers of vegetation). Due to these advantageous properties, both datasets are widely used - highly cited within Clarivate Web of Science - and applied in ecological research (e.g., Fuentes-Castillo et al. 2020), hydrological modelling (e.g., Oliveira-Júnior et al. 2021), as well as studies related to agriculture and forestry (e.g., Barrueto et al. 2018; Fadrique et al. 2018). This widespread use underscores the significance and the comprehensive nature of the datasets in ecological modelling. Nevertheless, it should be mentioned that other high-resolution datasets and attempts to correct the datasets exist (Beck et al. 2020). However, within the scope of our study, we specifically concentrate on two datasets that have extensively been applied within our area of investigation.

CHELSA V.2.1 is a gridded climate dataset with a 30 arc-second resolution (~0.8 km for the study area), covering monthly temperature and precipitation from 1979 to 2013. It uses ERA-Interim climatic reanalysis, with a temperature algorithm based on statistical downscaling and a precipitation algorithm considering orographic factors, corrected using Global Precipitation Climatology Centre (GPCC) and Global Historical Climatology Network (GHCN) data. Topo-climatic effects are covered through integration of Global Multi-resolution Terrain Elevation Data (GMTED2010) (Karger et al. 2017, 2021). WorldClim 2, similarly at 30 arc-second resolution, provides a 30-year average of temperature and precipitation from 1970 to 2000,

based on weather station data interpolated with elevation (SRTM), coastline proximity, and satellite parameters, including land surface temperatures and cloud cover from MODIS (Fick and Hijmans 2017a).

Next to gridded climate data, and as an integral part of the validation (Fig. 4.2), meteorological station data (Fig. 4.1) for El Bolsón (41.9°S; 71.5°W at 343 m.a.s.l.), Río Villegas (41.6°S; 71.5°W at 526 m.a.s.l.), a location west of El Bolsón (hereafter referred to as Río Azul [41.9°S; 71.6°W at 347 m.a.s.l.]), as well as two locations in the valley of Río Manso (hereafter referred to as Río Manso Inferior [41.6°S; 71.8°W at 439 m.a.s.l.] and Río Manso Confluencia [41.6°S; 71.7°W at 455 m.a.s.l.]) was retrieved from Servicio Meteorológico Nacional (2023) and Sistema Nacional de Información Hídrica (2023). In order to function as a source of validation for high-resolution climate datasets, only station data with available timeseries from 1990 until 2018 was chosen. With the exception of El Bolsón, only data concerning precipitation was accessible for the remaining stations.

4.2.5 Future climate data

Building on the pre-selection by Karger et al. (2017), grounded in the Intersectoral Impact Model Intercomparison Project (ISIMIP) (Lange 2021), and considering the constrained overlap between CHELSA and WorldClim, our analysis was narrowed to a suite of five readily available climate models and two Shared Socioeconomic Pathways (SSP). Specifically, we utilized the pathways SSP1-2.6 and SSP3-7.0 as well as the climate models GFDL-ESM4, MRI-ESM2-0, UKESM1-0-LL, IPSL-CM6A-LR, and MPI-ESM1-2-HR, all of which are based on CMIP6. The scenario SSP1-2.6 with 2.6 Wm^{-2} by the year 2100 is comparable to the optimistic scenario RCP2.6 and was designed with the aim of simulating a development that is comparable to the 2 °C target, according to the Paris Agreement (UNFCCC 2015). This scenario, too, assumes climate protection measures being taken. The Scenario SSP3-7.0 with 7 Wm^{-2} by the year 2100 is located in the upper-middle part of the full range of scenarios. It was newly introduced after the RCP scenarios, closing the gap between RCP6.0 and RCP8.5 (O'Neill et al. 2016). CHELSA and WorldClim data differ in timescales, with CHELSA using 30-year intervals (2011-2040, 2041-2070, 2071-2100) and WorldClim using 20-year intervals (2021-2040, 2041-2060, 2061-2080, and 2081-2100).

4.2.6 Species data

To identify the best data source for establishing vegetation-relevant bioclimatic zones, we extracted occurrence data from the Global Biodiversity Information Facility (GBIF.org 2021) based on the key natural tree species in northern Patagonia: *A. chilensis*, *N. antarctica*, *N. dombeyi*, and *N. pumilio*. Within the process, only species occurrences within the Patagonia region were selected. Thus, anthropogenic distributions (e.g., from botanical gardens) were excluded. Simultaneously, we analysed the updated Forest Type Classification of Andean

Patagonia of the year 2016 which is based on field and remote sensing data (CIEFAP-MAyDS 2016). Out of three available classification levels, level two, which classifies the main forest types within the study area, was used within the present study (Supplementary Fig. 1). According to the authors, the second classification level comes with an overall accuracy of 87%.

4.2.7 Bioclimatic analysis

Bioclimates of both high-resolution climate datasets were calculated based on the World Wide Bioclimatic Classification System (WBCS) of Rivas-Martínez et al. (2011). The classification system integrates both moisture levels and temperature conditions to define distinct bioclimatic classes, essential for understanding various ecosystems and climatic impacts (Torregrosa et al. 2013; Rodríguez-Catón et al. 2016; Pesaresi et al. 2017; Del Arco Aguilar and Rodríguez Delgado 2018; Andrade and Contente 2020; Cutini et al. 2021; Szabó et al. 2021). On one side, it categorizes climates into ombric types based on the ombrothermic index (Io), indicating moisture availability with classifications such as Arid, Semiarid, and Dry, each specified further into 'lower' and 'upper' horizons based on Io value ranges (Table 4.1). On the other side, it details thermotypic classifications through the thermotypic index (Tp), delineating temperature-based categories like Supramediterranean, Oromediterranean, and Crioromediterranean, again divided into 'lower' and 'upper' horizons based on Tp value ranges (Table 4.1):

Where *Tp* is $\sum Ti_{1-12} > 0°C$ in tenths of degrees;

Pp is the positive annual precipitation of the months with an average monthly temperature (*Ti*) higher than 0°C;

and *Io* is $\left(\frac{Pp}{Tp}\right)\ 10$.

This dual approach allows for a comprehensive understanding of climatic conditions, offering insights into the suitability of regions for different types of vegetation, agriculture, and habitat sustainability. All bioclimates were calculated using “raster” in RStudio (Hijmans 2023). Since mountains represent altitudinal thermic variations, classification of macro-bioclimate (submediterranean) was elaborated through temperature and precipitation values of the valley floors considering the macro-climate of the nearest listed station (Esquel; 42.9°S; 71.2°W at 815 m.a.s.l.) according to Rivas-Martínez et al. (2011). As such, the site is located at the border to a temperate macro-bioclimate (west) and thus classified as “extremely strong submediterranean” climate (submediterraneity index of El Bolsón = 539) of a balanced oceanic type (simple continentality index of El Bolsón = 14.21) (Rivas-Martínez et al. 2011; Servicio Meteorológico Nacional 2023).

Based on the bioclimatic classification, we derived four bioclimatic zones (A, B, C, and D) in relation to the four primary tree species (*A. chilensis*, *N. antarctica*, *N. dombeyi*, and *N. pumilio*)

for both climate datasets (Fig. 4.3). Each zone encompasses the primary bioclimates (more than 5% of occurrence) associated with a dominant tree species. Hence, in order to determine a bioclimatic zone, occurrence data of a species was layered with our previously created bioclimatic classification and then filtered by all encompassed bioclimatic classes that have a share greater than 5%. Due to the very low amount of available species data within the investigation area (cf. GBIF.org 2021), base data for tree species distribution was adopted from the available forest classification product of CIEFAP-MAyDS (2016).

In order to model bioclimatic projections, different scenarios and timescales were calculated based on the above mentioned SSPs and CMIP6 models. For this purpose, an altitudinal level of 1,800 m.a.s.l. was set to restrict potential upshifting of habitat-specific species pools above bare rock terrain without natural soil, where the establishment of natural subalpine *N. pumilio* forest can be excluded. Within this study, relative cover is defined as factor of change and can be explained as the proportion (in percent) of a bioclimatic zone in reference to the total area of the eastern Río Puelo watershed. For each projection, points of origin are the reference periods of CHELSA (1981-2010) and WorldClim (1970-2000). Projections were individually calculated for each GCM and SSP.

4.2.8 Comparison between data sources

In the first step of the comparison between data sources, we used linear regression analysis (Lumley 2020) to explore *uncertainties linked to our bioclimatic classification*, focusing on the impact of various predictor variables, including 19 bioclimatic factors (Supplementary Table 1) from Brun et al. (2022) and Fick and Hijmans (2017a), on forest distribution. This aimed to test our zonation's explanatory power to variations arising from different species datasets. The analysis, utilizing data from CIEFAP-MAyDS (2016) and GBIF.org (2021), sought to pinpoint the most suitable input data for bioclimatic zonation and evaluate the explanatory power and associated uncertainties of the WBCS in our study area.

In the second step of the comparison between data sources, a descriptive analysis of distribution patterns, using “ggridges” (Wilke 2022), served as support to identify *variable-related uncertainties* in regard to ombric and thermotypic horizons. This visualization tool offers good capabilities for visualizing changes in distribution over time and space. To better understand variability of means and extremes of both variables, the 0.1, 0.5 as well as the 0.9 quantile were retrieved for each period, SSP, GCM and high-resolution climate dataset. Since a considerable amount of ground-based data for validation and prioritisation of climate datasets was missing, we considered the disagreement between CHELSA and WorldClim as a way to quantify spatial consistency regarding the precipitation and temperature related variables (annual ombrothermic index and positive annual temperature).

In the third step, we assessed *terrain-related uncertainty* by measuring the percentage of non-intersecting pixels between CHELSA and WorldClim datasets regarding ombric horizons, thermotypic horizons, and bioclimates. We evaluated each cell for overlaps across these data sets and criteria. Non-intersecting pixels indicated higher uncertainty. To analyze topographical characteristics of cells without intersection, we utilized SRTM-DEM for slope and elevation data. Spatial analyses were conducted in RStudio using “rgdal” (Bivand et al. 2023), “raster” (Hijmans 2023), and “sf” (Pebesma 2018; Pebesma and Bivand 2023) tools, based on EPSG:22181.

In the last step of the comparison between data sources, we compared future scenarios of both climate datasets as they were calculated by the bioclimatic analysis in the first place (section 2.6). This step unveiled the *scenario-related uncertainty* due to the application of different GCMs and SSPs. The subject of the comparison are the bioclimatic zones A, B, C, and D, as well as their relative coverage degree.

4.2.9 Validation of data sources

In a second step of our framework (Fig. 4.2), we identified spatiotemporal inaccuracy in climate data as deviations over time (months) or across locations (from west to east) through a validation of both datasets. This inaccuracy is measured by the relative precipitation or absolute temperature differences between high-resolution climate datasets and meteorological station data. Since station data was limited to a common reference period starting from 1980, a validation period from 1980 to 2010 was used to validate CHELSA and WorldClim datasets, which cover the periods 1981-2010 and 1970-2000, respectively. Spatiotemporal inaccuracy assessments focused on temperature and precipitation for El Bolsón, and precipitation only for Río Azul, Río Villegas, Río Manso Confluencia, and Río Manso Inferior due to data limitations.

4.3 Results

4.3.1 Bioclimatic analysis

Our bioclimatic analysis revealed differing categories between CHELSA and WorldClim datasets (Fig. 4.3 a and b). CHELSA spans from lower arid and lower-supramediterranean to upper humid and lower crioromediterranean, whereas WorldClim covers a narrower range, from lower arid and lower-supramediterranean to lower dry and lower crioromediterranean. Variations in thermotypic horizons are represented by different colors, and ombric horizons by color intensity. WorldClim data, indicated by lower overall color intensity, shows fewer wet end scale bioclimates (compare Table 1). Despite these differences, there is substantial overlap in the supramediterranean zone, highlighted by red and yellow categories.

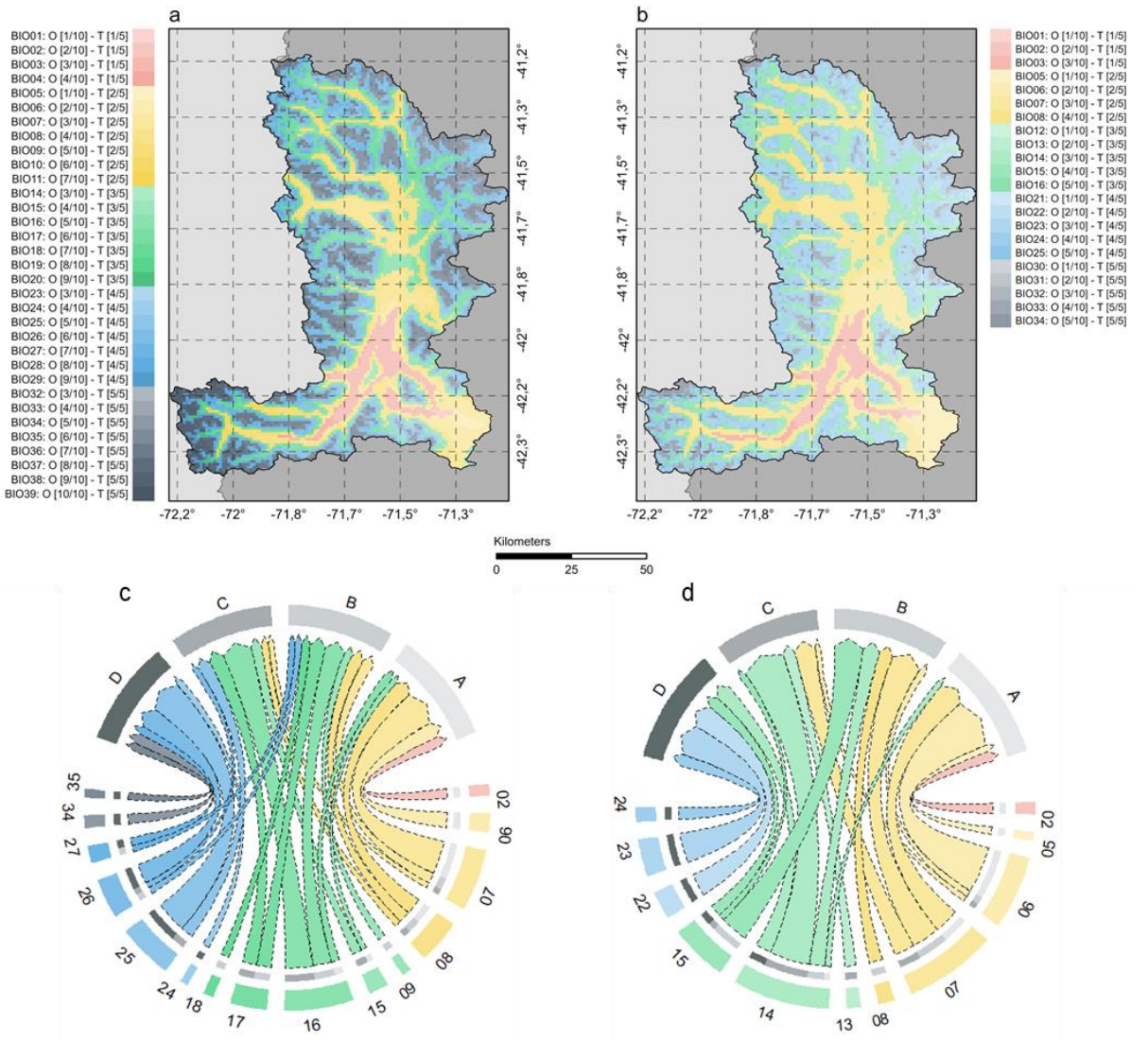

Figure 4.3 *The bioclimatic zones of the eastern Río Puelo watershed, analysed using two key datasets: CHELSA, with data averaged from 1981 to 2010 (Karger et al. 2021), and WorldClim, with averages from 1970 to 2000 (Fick and Hijmans 2017a). Each dataset categorizes the region's ombric and thermotypic horizons, ranging from arid to humid and from lower supramediterranean to lower crioromediterranean, respectively. Visual differentiation is achieved through varying colour intensities, indicating moisture variations. Additionally, the figure marks bioclimatic zones A through D, representing species and showing their bioclimates and relative cover percentages across these environmental gradients.*

Further clarification of these patterns is provided by examining the bioclimatic zones, as illustrated in Fig. 4.4 c (1981-2010 average of CHELSA) and Fig. 4.4 d (1970-2000 average of WorldClim). As previously stated, the bioclimatic classification based on CHELSA data is more diversified compared to that derived from WorldClim data, leading to similarly diverse bioclimatic zones. In either case, all, or most of the upper oromediterranean as well as the lower crioromediterranean bioclimates are dedicated to zone D, where *N. pumilio* is predominant. Due to a low cover of natural forests in the low-lying areas south of El Bolsón, bioclimates of a supramediterranean character are almost non-existent within the present zonation. Finally, yet importantly, a large overlap of bioclimates between zone B and C (CHELSA) and zone A, B, and C (WorldClim) can be noticed.

Table 4.1 *Ranges of the annual ombrothermic index (IO) and the annual positive temperature in tenth degrees (Tp) that determine ombric and thermotypic horizons within the study area (in reference to Fig. 4.2).*

Ombric types	**ID**	**Horizon**	**Io**
Arid	1	lower	0.41-0.70
	2	upper	0.71-1.00
Semiarid	3	lower	1.01-1.50
	4	upper	1.51-2.00
Dry	5	lower	2.01-2.80
	6	upper	2.81-3.60
Subhumid	7	lower	3.61-4.80
	8	upper	4.81-6.00
Humid	9	lower	6.01-9.00
	10	upper	9.01-12.00
Thermotypes	**ID**	**Horizon**	**Tp**
Supramediterranean	1	lower	1,201-1,500
	2	upper	901-1,200
Oromediterranean	3	lower	676-900
	4	upper	451-675
Crioromediterranean	5	lower	101-450
	-	-	-

4.3.2 Classification-related uncertainty

Analysing classification-related uncertainty, we found varying determination coefficients across datasets and bioclimatic indices, underlining how species and climate data choices affect bioclimatic zoning. Coefficients ranged from low (0.10 with GBIF and WorldClim) to moderate (0.50 with CIEFAP-MAyDS and WorldClim) across species datasets (GBIF, CIEFAP-MAyDS), climate datasets (CHELSA, WorldClim), and classification indices (annual ombrothermic index, annual positive temperature). Significant correlations with species distribution were found for both indices using CIEFAP-MAyDS data, but only for the annual ombrothermic index with GBIF data. Linear model fitting indicated improved results with more predictor variables (Supplementary Fig. 2 and 3), highlighting the significant impact of input data on bioclimatic zones.

4.3.3 Future bioclimates and variable-related uncertainty

Analysing variable-related uncertainty reveals distinct patterns in current and future precipitation and temperature distributions (Fig. 4.4), highlighting pronounced contrasts between CHELSA and WorldClim data (Supplementary Table 2 and 3). The most conspicuous appearance is the contrast of the precipitation related variable between CHELSA (Fig. 4.4 a, c, e) and WorldClim (Fig. 4.4 g, i, k). Whereas a value of 2.5 (Io) is at the 0.5 quantile of CHELSA data, a value of 2.5 (Io) is beyond the 0.9 quantile of WorldClim data. This explains the substantial differences between both datasets regarding the determination of ombric horizons. Instead, distributions of temperature-related variables are more similar to each other. In regard to future conditions, lower (0.1) and upper (0.9) quantiles for all scenarios show a shift to warmer and dryer bioclimates. Within the WorldClim dataset, strong variations regarding the precipitation related variable can be seen between UKESM1-00-LL (Fig 4.4. i) and the other two GCMs (Fig 4.4. g and k). Especially for the SSP3-7.0 scenario at the end of

the century, range between the 0.1 and the 0.9 quantile is relatively small in case of the UKESM1-00-LL GCM (i, SSP3-7.0 2081-2100).

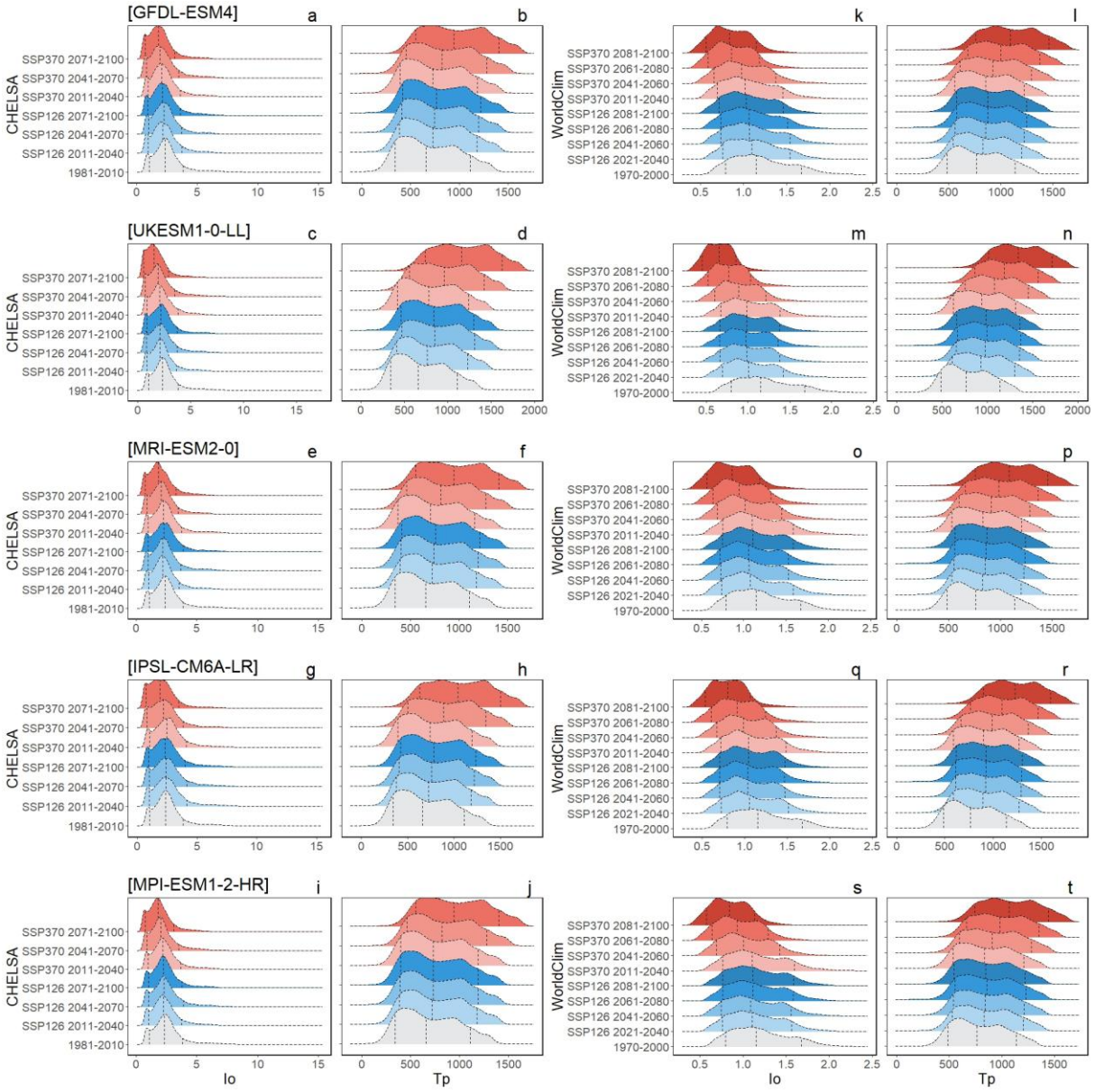

Figure 4.4 *Current and future densities of the annual ombrothermic index (Io) and the positive annual temperature (Tp) with marked quantiles (0.1, 0.5, and 0.9) for CHELSA (a-j) and WorldClim (k-t) under different shared socioeconomic pathways (blue for SSP1-2.6 and red for SSP3-7.0) and on basis of different global climate models.*

4.3.4 Terrain-related uncertainty

Terrain-related uncertainty analysis showed varying intersection levels between ombric and thermotypic horizons across datasets for reference periods, influenced by elevation and slope. Ombric horizons had a low 11% intersection, while thermotypic horizons showed a 62% intersection (Fig. 4.5 and Supplementary Fig. 4). Higher intersections for ombric horizons were generally below 600 meters above sea level (m.a.s.l.) with slopes under 10°, despite some outliers. Thermotypic horizon intersections were mainly below 800 m.a.s.l., with exceptions. Regarding the overall bioclimatic classification (Fig. 4.5 c), higher intersections were noted

along Río Azul (label 1), Río Foyel (label 2), Río Manso (label 3), and the areas around Lago Puelo and Lago Epuyén (label 4), while lower intersections were found in the Río Turbio catchment area (label 5), in narrow valleys of tributary streams (label 6), as well as around Lago Marscardi, Lago Giullelmo, and Lago Fonck (label 7).

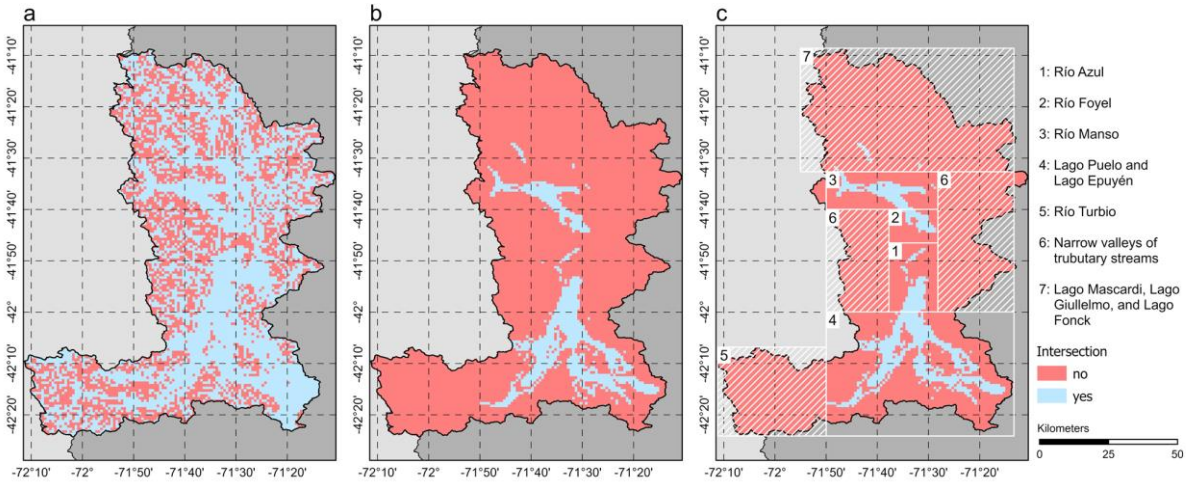

Figure 4.5 *Spatial intersection between a) thermotypic horizons, b) ombric horizons, and c) bioclimates based on reference periods of CHELSA and WorldClim. Where red pixels are without and blue pixels are with intersection between both datasets. Marks of c) represent points of reference for specific areas with (transparent) and without (hatched) intersection of the overall bioclimatic classification.*

4.3.5 Future bioclimates and scenario-related uncertainty

In examining the scenario-related uncertainty inherent in the projected impacts on bioclimates, our analysis demonstrates the multifaceted declines and shifts in the near and distant future. Overall, the datasets from both CHELSA and WorldClim demonstrate a notable variability in the reference periods as well as projected future bioclimatic cover, revealing trends where certain bioclimatic zones are expected to experience increases, while others may face declines (Fig. 4.6). These trends are not uniform but rather vary significantly across different models and scenarios (e.g., SSP3-7.0 for UKESM1-0-LL and all other models), highlighting the nuanced responses of bioclimates to changing climatic conditions. The evident discrepancies between the projections of CHELSA and WorldClim underscore the inherent uncertainties within climate impact models based on input data, thus warranting a careful and cautious interpretation of future bioclimatic trends. However, despite the variability, results from all projections consistently indicate a pronounced decline in the bioclimates of zone D. This zone is associated with the upper orobiome, where *N. pumilio* predominates (see Fig. 4.3). Zone D inhabits oro- and to some extent crioromediterranean bioclimates and can thus be classified as a bioclimatic segment of a typical mountain biome (Rivas-Martínez et al. 2011). Hence, a strong areal decrease can be attributed to an upward shift of the limit of Tp and an expansion limit at the upper orographic or rather edaphic tree line, where rocky habitats and lacking soil prevent the establishment of native subalpine *N. pumilio* ecosystems. This trend is particularly strong for scenarios based on the global climate model UKESM1-0-LL, where zone D shrinks

to 28.5% (WorldClim) and 25.1% (CHELSA) under SSP1-2.6 respectively 1.3% (WorldClim) and 0.8% (CHELSA) under SSP3-7.0.

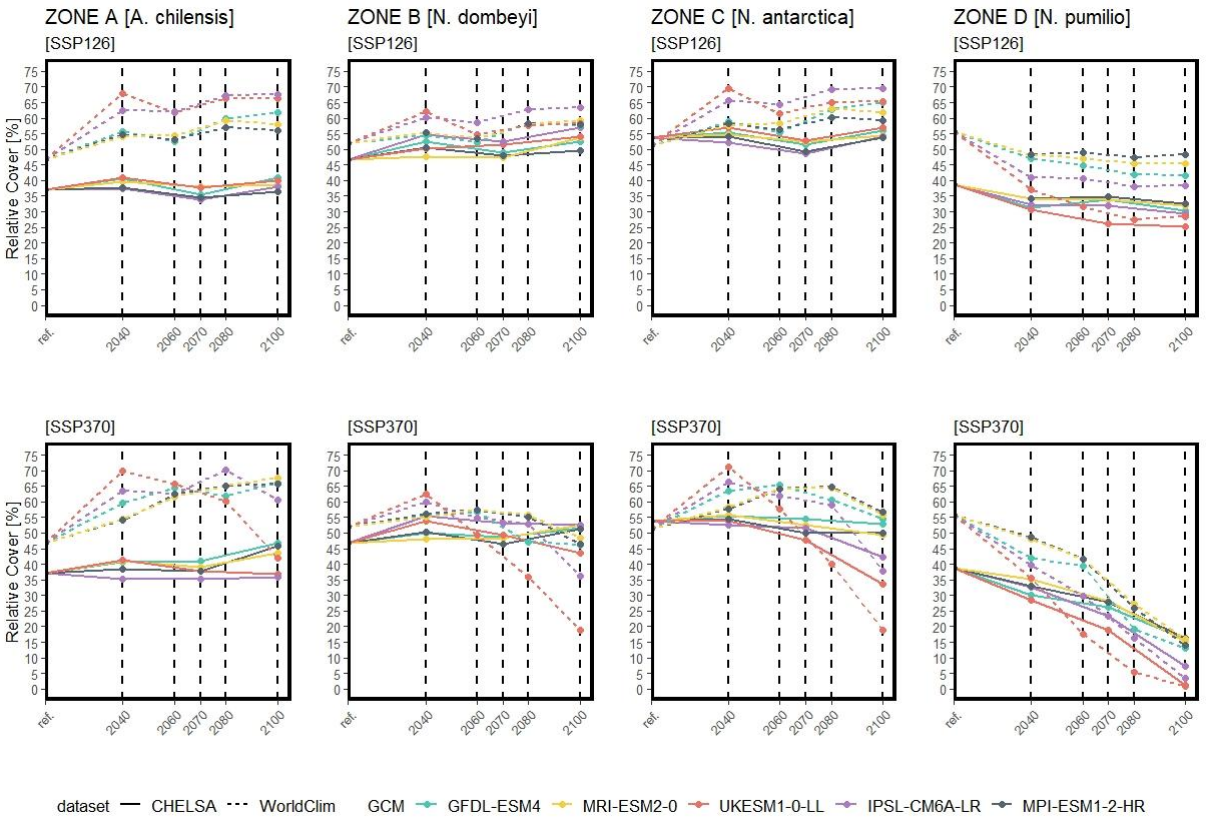

Figure 4.6 *Potential development of bioclimatic zones under different scenarios with reference to main tree species based on CHELSA and WorldClim climate data. Where CHELSA is marked by solid lines and WorldClim by dashed lines.*

4.3.6 Spatiotemporal inaccuracy

Figure 4.7 shows the analysis of spatiotemporal inaccuracies showing differences between gridded climate datasets and meteorological station observations, particularly for precipitation. The analysis expands along a west-to-east gradient (Fig. 4.7, a to c) and includes two stations in the central area (Fig. 4.7, d to f). Across this gradient, gridded datasets often overestimate monthly precipitation compared to stations, with varying degrees of accuracy. Specifically, Río Manso Inferior and Río Villegas data consistently show higher precipitation in gridded datasets year-round with a mean Mean Absolute Error (MAE) of 24.28% for CHELSA and 37.29% for WorldClim at the first and mean MAE of 47.44% for CHELSA and 19.85% for WorldClim at the latter. At Río Manso Confluencia, station data typically exceeds gridded estimates except in March, July, and September with a mean MAE of 14.32% for CHELSA and 21.09% for Worldclim. At Río Azul, underestimations are common, except in specific months like March and July. Here, mean MAE is only 6.80% for CHELSA and 17.81% for WorldClim. El Bolsón Airport's data shows no consistent trend, with notable overestimation by WorldClim in July and a mean MAE of only 4.78 for CHELSA and 15.56% for WorldClim. Temperature analysis for

El Bolsón reveals closer alignment in late autumn and winter, though gridded datasets tend to underestimate, with some exceptions. Overall, variability and inconsistencies across months and years prevent a definitive judgment on the datasets relative reliability.

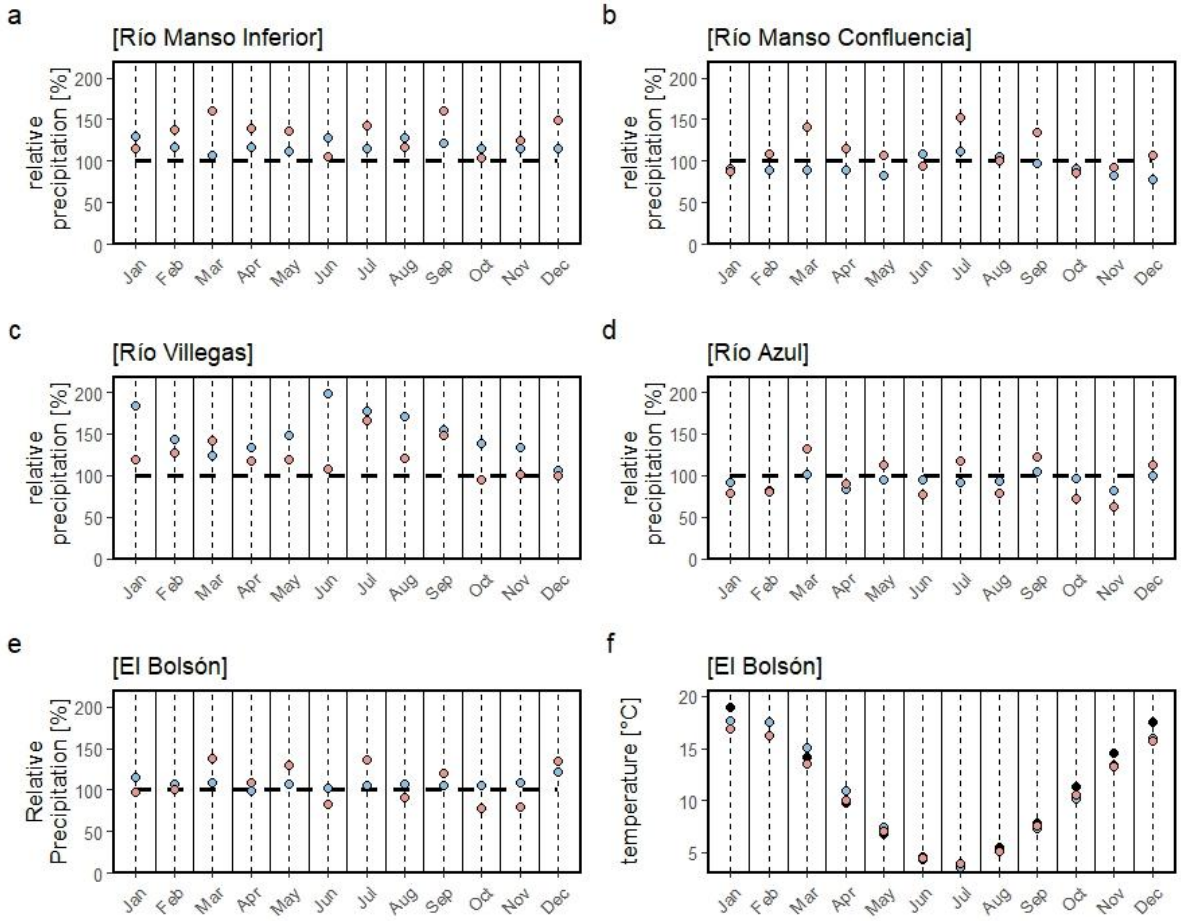

Figure 4.7 *Comparative analysis of monthly relative precipitation and temperature estimates by gridded climate data across five locations. Panels (a to e) show the monthly relative precipitation measured by station data (black line) and estimated by CHELSA (blue) and WorldClim (red), highlighting the variability and patterns of over- or underestimation of the datasets across a west-to-east precipitation gradient (a to c) as well as two stations located in the centre of the investigation area (d and e). Panel (f) presents a comparison of monthly temperature records of the station with estimates of the gridded datasets, demonstrating seasonal alignment and deviations.*

4.4 Discussion

In this study, we combined bioclimatic modelling with a comparison of two widely used high-resolution climate datasets. Our aim was to study the current and future bioclimatological conditions of an area that is characterized by complex topography, diverse structure of mountain climates, and limited data availability. Due to climatic data limitations, we focused on evaluating several types of uncertainty and inaccuracy that come along with the application of WorldClim and CHELSA.

4.4.1 Comparison of CHELSA and WorldClim

As expected, the comparison between CHELSA and WorldClim, in regard to temperature-related variables, reveals broad consistency. Both bioclimatic classifications show substantial

overlaps, especially in the low-lying sections of the investigation area, below 800 m.a.s.l. Current and future temperature densities are similar for the reference periods, as well as for all scenarios. Therefore, our findings are consistent with those of Bobrowski and Schickhoff (2017), that found high consistency between temperature-related variables of CHELSA and WorldClim in the Himalayas. Furthermore, the results of the validation show that discrepancies between both gridded climate datasets and station data are rather marginal. However, there are some qualitative differences between seasons, and accuracy for both datasets is higher from May to September.

The perspective changes markedly with respect to precipitation-related variables. In this case, only 11% of the classes overlap when both climate datasets are compared independently of external reference data. Moreover, this overlap approaches zero in areas characterized by steep slopes (approximately above 10°) and higher elevations (approximately above 600 m.a.s.l.). The densities of current and future precipitation show wide variations for the reference periods and individual scenarios, with CHELSA's estimates in precipitation significantly exceeding those of WorldClim. The selection of a wide range of GCMs is crucial, as demonstrated by the significant differences observed between the models used in this study (e.g., UKESM1-0-LL in comparison with all other models). This discrepancy is further confirmed by validating the estimates against station data, which reveals marked monthly fluctuations in both over- and underestimation, along with significant interannual variability. It is crucial, however, to approach these results with caution, as the rain gauges at the stations (mostly tipping buckets) are known to underestimate precipitation during snowfall (Kochendorfer et al. 2020). Despite these limitations, the findings are consistent with those reported in the study by Morales-Barbero and Vega-Álvarez (2019), which identified large discrepancies between climate datasets in mountainous regions on a global scale. Similarly, Bobrowski et al. (2021) highlight the potential drawbacks of using CHELSA and WorldClim data for ecological modelling in remote areas of the Himalayas, primarily due to major differences in precipitation-related variables. As stated previously, within the eastern Río Puelo watershed, the notable inconsistency between the datasets can be attributed to CHELSA data indicating higher precipitation levels, in contrast to WorldClim data, which shows lower levels. This observation is in line with the findings of Bobrowski et al. (2021). The appearance of precipitation related over- and underestimation was also perceived by Newell et al. (2022) for complex topography with low density of meteorological stations in northern Peru. In this respect, our study confirms the findings of lower accuracy of precipitation-related variables compared to temperature-related variables derived from high-resolution climate data as stated by Fick and Hijmans (2017a), Karger et al. (2017), and Beck et al. (2020). This is warranted by local terrain conditions and wind patterns that significantly influence small-scale atmospheric processes, making them largely independent of latitude or altitude (Bobrowski

and Schickhoff 2017). Hence, estimating precipitation in remote and complex terrains, as given by the Río Puelo watershed, remains a significant challenge. Moreover, the underlying CMIP6 models generally struggle with accurately representing the spatial patterns of precipitation in Patagonia, as indicated by Gateño et al. (2024) and Salazar et al. (2024). However, the models pre-selected by Karger et al. (2017) perform relatively well in northern Patagonia, according to a comparative study by Salazar et al. (2024).

In summary, while CHELSA and WorldClim provide valuable temperature data for northern Patagonia, their use for precipitation analysis requires careful consideration of their limitations and potential inaccuracies. Practitioners and researchers should prioritize dataset validation with local observations and remain cautious of seasonal and topographical factors that may influence data reliability. Furthermore, future studies could benefit from utilizing probabilistic meteorological datasets, such as EM-Earth. These datasets typically outperform deterministic ones in regions with complex topography and significant uncertainties due to sparse measurements. They may not only offer a better understanding of uncertainty but also provide a more accurate representation of extremes (Tang et al. 2022).

4.4.2 Bioclimatic analysis

Concerning bioclimatic analysis, we found a strong decline in mountain climates that are currently occupied by *N. pumilio*. This decline is particularly strong for SSP3-7.0 scenarios, where projections show a decrease to 15% and less of relative cover by end of the century. Our study is thus in line with Tovar et al. (2022), indicating a decrease of Temperate deciduous forests in the Andes. A decline in unique bioclimates of mountainous areas can be explained by the interaction of changing climate and an upper altitudinal limit. This has been observed in other geographies (Zomer et al. 2014) and is closely linked to complex topographies. There is robust evidence that global warming will lead to an upward shift of bioclimatic zones, consequently posing a risk of range contraction and extinction for species inhabiting mountainous regions (Adler et al. 2023). Overall, the future climate of northern Patagonia is expected to be warmer and drier (Gateño et al. 2024; Salazar et al. 2024), with critical impacts on water resources (Aguayo et al. 2019; Pessacg et al. 2020) and corresponding impacts on regional ecosystems.

4.4.3 Implications for regional ecosystems

Despite assessed uncertainties, our study reveals consistent bioclimatic trends across both climate data sets and different scenarios. These are especially evident regarding exposures of oro- and crioromediterranean climates and shed light on the future of *N. pumilio* forests (Supplementary Fig. 5) under a changing climate in northern Patagonia.

Northern Patagonian forests with a predominance of evergreen species such as *N. dombeyi* and *A. chilensis*, change to *N. pumilio*-dominated Subantarctic-Andean deciduous forests

(Adenocaulo-Nothofagetalia pumilionis Oberd. 1960 em. Hildebrand-Vogel, Godoy & Vogel 1990 [Nothofagetea pumilionis-antarcticae Oberd. 1960]) above certain altitudes. This vegetation shift indicates a division into different altitudinal zones, each characterised by specific plant communities whose life forms and species composition differ significantly (Cagnacci et al. 2020; Aschero et al. 2022). Biotic exchange by the invasion of non-native species such as *Pinus contorta* (Supplementary Fig. 6 and 7) poses a significant ecological threat to ecosystems of oro- and crioromediterranean climates (cf. Sala et al. 2000), particularly above the treeline of *N. pumilio*, altering fire dynamics and threatening native ecosystems (Raffaele et al. 2016). Since fire is a current and most likely amplified future threat (Kitzberger et al. 2022), “new forests”, “higher timberline”, “timber production at higher altitudes”, etc. cannot be considered strong “restoration” arguments.

Longitudinally, vegetation types below the subalpine level change less discriminatory and more ecotonal, with deciduous forests (Myrceugenio-Nothofagetum dombeyi Eskuche 1999), mixed forests (Austrocedro-Nothofagetum dombeyi Eskuche 1968) and coniferous forests (Gavileo-Austrocedretum Eskuche 1968) showing overlapping species compositions. This is in line with our study indicating a large overlap between bioclimates of zone B *(N. dombeyi)* and C *(N. antarctica)* but a relative distinction between zone A (*A. chilensis*) and B (*N. dombeyi*) as well as D (*N. pumilio*) from zone A (*A. chilensis*), B (*N. dombeyi*), and C (*N. antarctica*). However, even though our classification results show a minimal overlap between zone A (*A. chilensis*) and C (*N. antarctica*), a combination of both species can usually be observed in the succession process of the lower slopes or valley bottoms. This continuum suggests a complex interaction amongst forest types, potentially offering resilience against disturbances like wildfires. However, future climate change may challenge this balance, with *N. dombeyi* and *A. chilensis* showing differing moisture preferences (Veblen 2007) and the potential for range contractions under changing climatic conditions.

4.4.4 Limitations and further research

While our study did not focus on future species coverage projections, it signals potential risks to species like *N. pumilio*. In this respect, future studies should explore how species respond to climate change, including the impact of climate extremes on ecosystem disturbances. Understanding the bioclimatology of Wintero-Nothofagetea species and climate change effects on their viability is crucial for informed forest management. We advocate for maintaining and expanding meteorological monitoring to enhance climatology data accuracy, and the improvement of gridded climate datasets, as seen in Beck et al. (2020). Our findings also suggest that bioclimatic projections could lead to divergent adaptation strategies. Following Gregor et al. (2022), it's important to tailor climate-smart forestry to specific scenarios. For these reasons, we recommend using our data to foster local dialogue and workshops, improving regional decision-making with expert insights into adaptation strategies and

embracing a transdisciplinary approach to unite various knowledge systems for better climate understanding and decision-making, as discussed by Bremer et al. (2019) and Moure et al. (2023).

4.5 Conclusion

Our study investigates the bioclimatological conditions of northern Patagonia, facing complex topography and sparse data, through a comparative analysis of high-resolution climate datasets CHELSA v2.1 and WorldClim v.2.1. Our findings underscore substantial consistency between these datasets for temperature variables, confirming the reliability of both for temperature analysis. However, a strong contrast emerges in precipitation estimates, with significant discrepancies highlighted by minimal overlap in bioclimatic classes, particularly in steep and elevated terrains. Such variations underscore the challenges of accurately modelling precipitation in mountainous regions, where local topography and wind patterns play crucial roles. Thus, the study highlights the importance of a comparison between different data sources and validations against ground-based data and the careful consideration of precipitation-related variables in bioclimatic modelling within the Río Puelo watershed.

However, despite the differences of the applied climate datasets, our bioclimatic analysis reveals a concerning decline in mountain climates suitable for *N. pumilio*, with projections suggesting a sharp decrease in their coverage under future climate scenarios. This demonstrates that, despite the detected uncertainties, it is possible to identify vulnerable bioclimatic zones within the Río Puelo watershed based on CHELSA and WorldClim data.

4.6 Data availability

Derived data supporting the findings of this study are available upon request from the corresponding author.

4.7 Funding

This study is part of the research project *Sustainable forest management of temperate deciduous forests – Northern hemisphere beech and southern hemisphere beech forests (KLIMNEM)*, a cooperation between the universities of Göttingen (Germany), Free University of Bozen-Bolzano (Italy), the University of Applied Sciences and Arts, and the Andean Patagonian Forest Research and Extension Centre (CIEFAP, Argentina). The project is supported by funds of the Federal Ministry of Food and Agriculture (BMEL) based on a decision of the Parliament of the Federal Republic of Germany via the Federal Office for Agriculture and Food (BLE, grant No. 28I-042-01).

4.8 Supplementary information

Below is the link to the electronic supplementary material.

Supplementary file: https://static-content.springer.com/esm/art%3A10.1007%2Fs10113-024-02278-5/MediaObjects/10113_2024_2278_MOESM1_ESM.docx

4.9 Rights and permissions

5. Study II - Modelling microclimatic variability in Andean forests of northern Patagonia

Original Article (open access)

Published on 25 March 2025 in *International Journal of Biometeorology* (Springer Nature) Volume 69, pages 1279-1295

Jonas Fierke, Birgitta Putzenlechner, Alois Simon, Juan Haridas Gowda, Ernesto Juan Reiter, Helge Walentowski & Martin Kappas

Abstract

Information on microclimatic conditions beneath canopies is key to understanding small-scale ecological processes, especially concerning the response of biodiversity to climate change. In north-western Patagonia, where data on climate-driven species distribution are scarce, our study provides valuable insights by providing microclimatic models covering spatiotemporal dynamics at 30 × 30 m resolution. Applying in-situ data from 2022 to 2024, we employed a random forest-based regression to assess the impact of several biophysical predictor variables describing terrain and vegetation properties on four microclimatic response variables at three vertical levels within forests. We also interpolated this data spatiotemporally, using statistical downscaling of ERA5 data. Our analysis reveals that the influence of the predictor variables varies strongly by month and response variable. Moreover, significant variability was observed between the models and months regarding their explanatory power and error range. For instance, the model predicting maximum air temperature at 2 m height achieved an R^2 of 0.88 and an RMSE of 1.5 °C, while the model for minimum air temperature resulted in an R^2 of 0.73 and an RMSE of 1.8 °C. Our model approach provides a benchmark for spatiotemporal projections in this data-scarce region, aligned with the climate normal from 1981 to 2010. Future refinement could benefit from data on snow cover, land use and land cover, soil, as well as structural information on vegetation over an extended period, to enhance the dynamical aspects of microclimatic modelling. We are confident that our present model will substantially enhance possibilities to analyse species distribution across vegetation types and terrain-related features within the area.

Keywords: Random forest-based regression, Remote sensing, Microclimate, Forests, Statistical downscaling

5.1 Introduction

Small-scale variations in temperature, humidity, and soil moisture significantly influence forest ecosystems, affecting biological and biochemical functions. These microclimatic conditions impact the distribution and persistence of understory species by influencing their physiological traits and adaptation strategies (Geiger et al. 2009). Additionally, microclimate drives nutrient cycling, notably through its effects on litter decomposition (Coûteaux et al. 1995) and soil organic matter turnover (Conant et al. 2011). The microclimate within a forest, such as the thermal environment, affects various aspects of understory plant dynamics, including growth rates, photosynthetic activity, and interspecific competition (Geiger et al. 2009; Vinod et al. 2023).

Forest microclimate results from interactions between terrain, vegetation, and macroclimate. Terrain affects factors like sunlight exposure and drainage, causing temperature and moisture variations in small areas (Barry 2008a; Aalto et al. 2017). Vegetation, through canopy density and type, regulates solar radiation and transpiration, creating diverse conditions below (Hardwick et al. 2015; Barry and Blanken 2016). Macroclimate establishes broader environmental conditions that influence these microclimates at both regional and local scales (De Frenne et al. 2021). The resulting mosaic of microclimates shapes ecological processes and species distributions. Climate change will likely alter microclimatic buffering, highlighting the need for research to understand its effects on ecosystem resilience (Maclean et al. 2015; Lenoir et al. 2017; Zellweger et al. 2020; De Frenne et al. 2021; Lombaerde et al. 2022). Understanding these interactions is essential for managing habitats and refugia, thereby conserving biodiversity (Hylander et al. 2022; Kemppinen et al. 2024).

The landscape of microclimatic research is characterized by a variety of methods that, among others, include the development of microclimatic models (Zellweger et al. 2019a; Lembrechts et al. 2022; Zignol et al. 2023). As a review on the discipline shows, future microclimatic research should aim to achieve greater flexibility in spatial and temporal scaling (Kemppinen et al. 2024). This flexibility, in turn, can further help to represent abiotic conditions at scales that define the distribution and performance of species as well as ecosystem functions and services (Potter et al. 2013; Lembrechts et al. 2019; Lembrechts et al. 2022). So far, an increasing number of studies are addressing this issue. For instance, Haesen et al. (2021) and Zignol et al. (2023) have implemented spatiotemporal interpolation techniques, utilizing ground-based measurements and geospatial data, to predict long-term microclimatic patterns in forests at continental and local scales. Lembrechts et al. (2020) are constantly improving their global database on soil and near-surface temperatures that has already demonstrated its function as valuable input data for spatiotemporal modelling, all the way up to a global scale (Lembrechts et al. 2022). Previous research has shown that microclimatic models substantially

improve our understanding of spatial interactions between species and their environments at local levels (Zellweger et al. 2019a). Other research has also demonstrated that microclimate modelling benefits from remote sensing data integration, especially in landscapes where ground-based measurements are challenging (Zignol et al. 2023). However, as Klinges et al. (2024) point out, it is not always higher spatial or temporal resolution that improves the prediction accuracy of ecological responses. Rather, it requires datasets with high climate proximity, i.e., datasets that represent the climatic conditions that organisms under consideration are exposed to. Collectively, these arguments underscore the critical role of advanced microclimatic mapping and modelling techniques in enhancing our predictive capabilities for diverse ecosystems under different climatic conditions.

Despite progress in microclimatic modelling, some regions remain underrepresented, including northern Patagonia, where gridded microclimatic data is still lacking. This is further reinforced by the considerable uncertainties within the region's available high-resolution gridded climate datasets, which are crucial for ecological studies (Fierke et al. 2024). Moreover, these datasets have the disadvantage of not accurately representing the climatic conditions experienced by organisms under the canopy and underneath the surface, focusing instead on open-air temperatures (Fick and Hijmans 2017b; Karger et al. 2017). As a result, critical processes, such as how species reliant on stable microclimates respond to climate change, remain poorly understood. Understanding these processes is essential, as climate change poses a significant threat to suitable habitats for many plant species in northern Patagonia, potentially jeopardizing biodiversity hotspots and disrupting ecosystem stability (Soliani et al. 2024). While existing studies on microclimate in the region focus on the important issue of understanding microclimatic processes (Barberá et al. 2023; Simon et al. 2024), they do not aim to comprehensively create microclimatic models over a longer period and larger spatial extent. As a result, comprehensive spatial data is not yet available.

Given the absence of gridded microclimate data in northern Patagonia and the need for greater spatial and temporal coverage, as well as closer proximity in microclimatic modelling, our study aims to comprehensively analyse and project the microclimates of Andean forests in northern Patagonia. We address both historical changes and vertical variations within the constraints of existing data. Our objectives are to: (1) model the current microclimates of Andean forests in northern Patagonia and identify statistical relationships between predictors and microclimatic variables, (2) project these findings onto the historical period from 1981–2010 to assess past changes, (3) investigate vertical microclimatic variations at 6 cm depth and heights of 15 cm and 2 m, and (4) evaluate data limitations in northern Patagonia’s microclimatic modelling. Our analysis is based on measurements of three key microclimatic variables at different heights: air temperature at 2 m and 15 cm above ground and 6 cm below ground, relative humidity at 2 m, and volumetric water content (VWC) at 6 cm depth. Using a random forest regression

model, we incorporate microclimatic observations from 2022–2024 alongside vegetation and terrain data from satellite imagery and local climate data from weather stations and downscaled ERA5 estimates. This approach enables spatial interpolation at 30-meter resolution and temporal interpolation for the historical period of 1981–2010. The combination of variables at multiple heights and depths allows us to assess initial vertical patterns within the microclimate. Finally, we analyse the current data used in our microclimatic predictions to identify which parts of the model suffer from data shortcomings and to understand the uncertainties these shortcomings cause. Our models, along with supplementary information, aim to characterize local microclimatic patterns and variations, providing essential insights for further studies on ecological processes beneath the canopy.

5.2 Data and methods

5.2.1 Study area

Our study focuses on two selected zones located to the north and west of El Bolsón in the Andes of northern Patagonia (Figure 5.1). One zone, Figure 5.1a, encompasses the Valle del Río Manso Inferior, approximately 50 km by 10 km in extent, while the other, Figure 5.1b, includes parts of the Valle del Río Manso Inferior and areas around Lago Lahuán, measuring about 20 km by 30 km. Both zones overlap in a section covering parts of the Valle del Río Manso Inferior (Figure 5.1c). The investigated landscape is predominantly covered by four native tree species: *Nothofagus pumilio* ((Poepp. & Endl.) Krasser), *N. antarctica* ((Forst.) Oerst.), *N. dombeyi* ((Mirb.) Oerst.), and *Austrocedrus chilensis* (D. Don) Pic.-Ser. & Bizz). The area features a macroclimate that is influenced by its geographical setting in valleys of various sizes within the Andes mountains. Furthermore, the area is characterized by two environmental key gradients: a pronounced precipitation gradient from west to east and an elevational gradient ranging from approximately 450 to 1,700 m. Annual precipitation recorded at the weather station in El Bolsón (1991-2020) at 345 m elevation averages 894 mm, ranging from 30 mm in February to 170 mm in June. The mean annual temperature is 10.3 °C, with the highest monthly mean temperature of 17.7 °C in February and the lowest of 3.8 °C in July (SMN 2024).

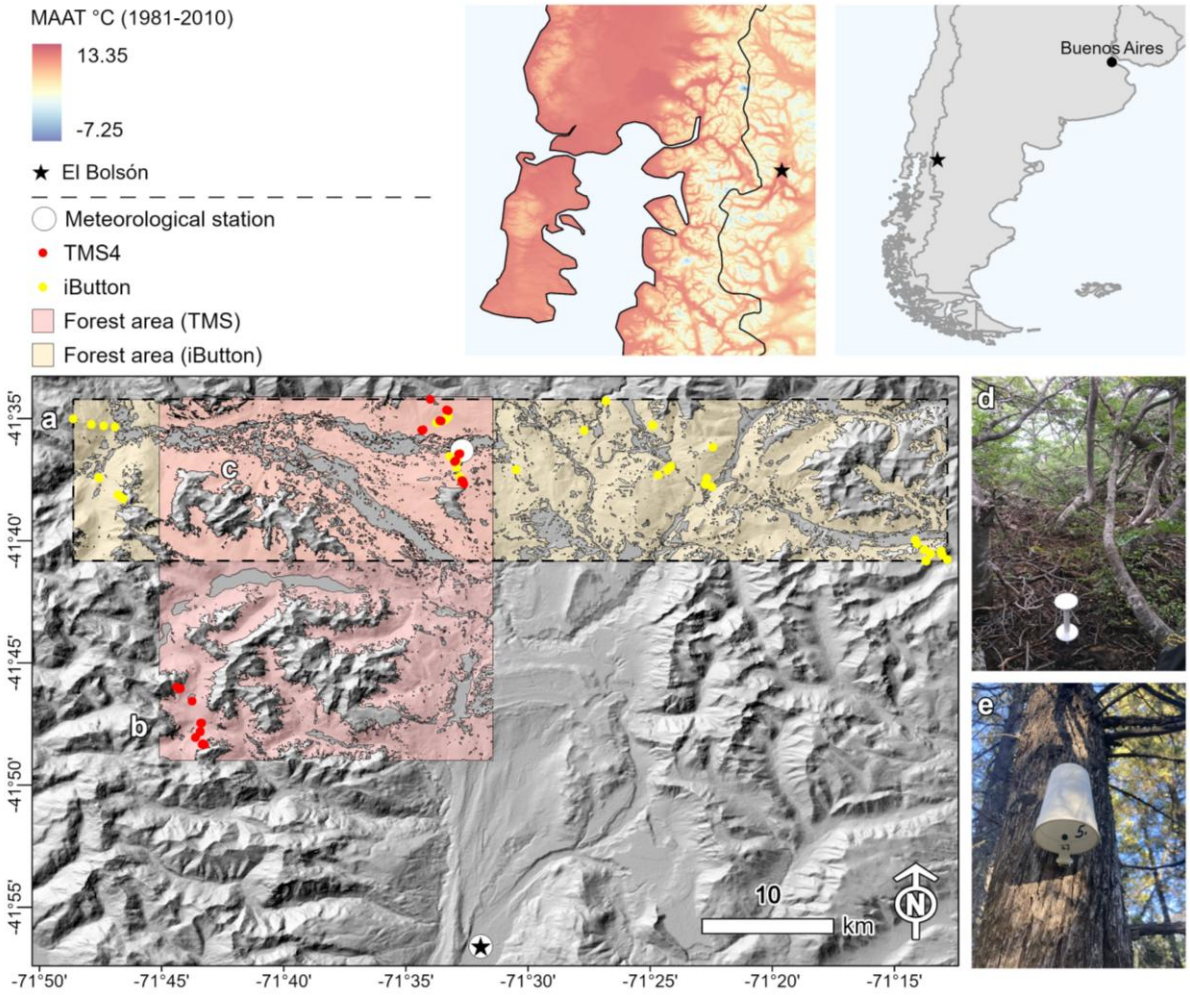

Figure 5.1 *Study area. Where (a) is showing the section of iButton data loggers, (b) the section of TMS-4 data loggers, and (c) the intersection of both. Photos (d) and (e) show exemplary sites of TMS and iButton loggers respectively. Mean Annual Air Temperature (MAAT) of the region is based on climate data of (Karger et al. 2017).*

5.2.2 Microclimatic data

Using TOMST TMS-4 Standard dataloggers (Wild et al. 2019), we recorded temperature at 15 cm height and both temperature and VWC at a soil depth of 6 cm below ground (Figure 5.1d) every 15 minutes across 8 locations (20 loggers) from March 2022 to February 2024, and 8 locations (18 loggers) from March 2023 to February 2024. The dataloggers were installed across forest stands covering an elevational gradient from 600 to 1600 m (Figure 5.1b) with replicates between 600 and 1400 m and individual loggers at the treeline between 1500 m and 1600 m, respectively. Additional temperature and relative humidity data, recorded at 4-hour intervals (02:00, 06:00, 10:00, 14:00, 18:00, and 22:00 UTC-3) from loggers at 2 m height (Figure 5.1e), were collected from 40 sites, partially overlapping with the TMS loggers (Figure 5.1a). This data spans March 2022 to February 2023 Simon et al. (2024) using iButton dataloggers (DS1923 Hygrochron) (Analog Devices, Inc., USA). To ensure reliable measurements, the sensors were shielded from direct sunlight and adverse weather conditions, including precipitation and strong winds, using a white, ventilated enclosure to

minimize environmental impact (Figure 5.1e). All logger data underwent quality checks to remove errors and duplicates. For VWC, we only used daily records where the average soil temperature exceeded 0 °C, excluding 1.6% of days to eliminate frozen soil data (Wild et al. 2019). VWC was estimated using a simplified calibration based on Jačka et al. (2023) , focusing on proportional trends rather than absolute values. Our calibration can be considered simplified because it is based on a single soil sample and average physical properties (e.g. bulk density) according to Simon et al. (in prep.). Calibration details appear in Figure S1, with logger time series shown in Figures S2–S4. We selected soil moisture, air humidity, and soil-, surface-, and air temperature as key variables for this study due to their fundamental roles in shaping microclimatic conditions relevant to organisms and ecological processes. These variables influence critical processes such as water availability, evapotranspiration, and thermal regulation, which are essential for shaping species distributions, physiological traits, and ecosystem functions (Barry 2008a; Geiger et al. 2009; Conant et al. 2011; De Frenne et al. 2021). Furthermore, their widespread use in microclimatic studies (e.g., De Frenne et al. 2021; Kašpar et al. 2021; Aalto et al. 2022; Lembrechts et al. 2022) facilitates direct comparisons with existing datasets, enhancing the broader applicability of our findings.

5.2.3 Macroclimatic data

We retrieved macroclimatic temperature data from a weather station located in the Valle del Río Manso Inferior at -41.61° South and -71.54° West, and macroclimatic precipitation and humidity data from a weather station located in El Bolsón at -41.94° South and -71.53° West. The Valle del Río Manso Inferior station has records from May 2003 to the present, with a gap between 2015 and 2019, while the El Bolsón station has records from January 1992 to the present (SMN 2024). While the station variables were directly integrated into the model calibration for the period from 2022 to 2024, we used ECMWF ERA5 predictors (Hersbach et al. 2020) for statistical downscaling (Table 5.1) to produce macroclimatic variables for the climate normal from 1981 to 2010. These variables measure various atmospheric conditions at different heights and pressure levels, including wind speed, wind direction, geopotential energy, humidity, temperature, and precipitation, essential for understanding and predicting weather patterns (Table S1). The variables were downloaded on a daily basis for the historical period from 1979 to 2014, as provided by the Canadian Centre for Climate Modelling and Analysis (ECCC 2024). By focusing on the historical period 1981-2010, future studies could compare the results of our research with existing models, such as those developed by Karger et al. (2017).

Table 5.1 *Predictor variables for statistical downscaling of ERA5 data. Using even years from 2004 to 2014 for the Valle del Río Manso Inferior station and even years from 1991 to 2014 for the El Bolsón station, predictor variables were selected from the 26 available options (Table S1) based on their partial correlation coefficients (r) and p-values. Where hPa is the atmospheric pressure level in hectopascals.*

Variable (Station)	No.	ERA5 predictor variable	Partial r	P value
TMAX: maximum daily temperature (Valle del Río Manso Inferior)	1	Mean sea level pressure	-0.242	<0.0001
	2	500 hPa Wind speed	-0.139	<0.0001
	3	500 hPa Meridional wind component	0.184	<0.0001
	4	500 hPa Geopotential	0.235	<0.0001
	5	850 hPa Zonal wind component	-0.120	<0.0001
	6	850 hPa Geopotential	0.132	<0.0001
TMIN: minimum daily temperature (Valle del Río Manso Inferior)	1	Mean sea level pressure	-0.195	<0.0001
	2	1000 hPa Wind speed	0.261	<0.0001
	3	1000 hPa Relative vorticity of true wind	0.190	<0.0001
	4	1000 hPa Divergence of true wind	-0.145	<0.0001
	5	500 hPa Geopotential	0.290	<0.0001
	6	Total precipitation	-0.112	<0.0001
	7	850 hPa Specific humidity	0.313	<0.0001
PRCP: daily sum of precipitation (El Bolsón)	1	1000 hPa Zonal wind component	-0.189	<0.0001
	2	500 hPa Wind speed	0.112	<0.0001
	3	850 hPa Wind Speed	0.139	<0.0001
	4	850 hPa Geopotential	-0.240	<0.0001
	5	850 hPa Divergence of true wind	-0.107	<0.0001
RH: relative humidity (El Bolsón)	1	1000 hPa Divergence of true wind	0.157	<0.0001
	2	850 hPa Divergence of true wind	-0.292	<0.0001
	3	850 hPa Specific humidity	0.532	<0.0001
	4	Air temperature at 2 m	-0.667	<0.0001

5.2.4 Vegetation and terrain data

For vegetation-related variables, we used the Enhanced Vegetation Index (EVI) and Normalized Difference Moisture Index (NDMI) based on Landsat 8/9 (USGS 2024), as well as the Leaf Area Index (LAI) and Fraction of Photosynthetically Active Radiation (FAPAR) based upon Sentinel 3/OLCI data (Copernicus Service Information 2022). EVI and NDMI have a spatial resolution of 30 m, whereas LAI and FAPAR feature a resolution of 300 m. All four indices are calculated monthly, based on an iterative interpolation process, during which pixels from months with cloud cover are replaced by data from subsequent available months. For EVI and NDMI, pixels affected by clouds and cloud shadows are excluded, based on the quality assessment file. Additionally, LAI and FAPAR data are already masked to exclude cloud-affected areas. While LAI and FAPAR data are calculated using a ready-to-use product at 10-day intervals from 2022 to 2024, EVI and NDMI data are derived from 135 Landsat 8/9 scenes available between 2022 and 2024. For tree height, we used the product of Tolan et al. (2024) at a spatial resolution of 1 m. Additionally, we assessed forest cover by combining tree height with EVI, using thresholds of 3 m and 0.22, respectively. This approach, similar to that of (Zignol et al. 2023), helped establish the distance and direction to the forest edge with a resolution of 30 m. Our terrain-related variables included elevation, distance to sink, relative elevation, terrain roughness, the Topographic Position Index (TPI), the Topographic Wetness Index (TWI), and monthly solar radiation derived from SRTM data (Farr et al. 2007) with a resolution of approx. 25 m accessed through *elevatr* in RStudio (Hollister et al. 2023). Except

for solar radiation (potential incoming solar radiation, PISR) which was calculated using *RSAGA* (Brenning et al. 2022), all other terrain-related variables were computed using *terra* in RStudio (Hijmans et al. 2024). Where necessary, data was resampled and reprojected to 30 x 30 m^2 spatial resolution and the EPSG:32719 coordinate system. For our model calibration, tree height data was retained at a 1 m spatial resolution to preserve its quality as a predictor variable. Detailed information on all variables and their processing can be found in Figure S5.

5.2.5 Model calibration

We calibrated 8 models using monthly averages of the following observed microclimatic data as response variables: minimum and maximum daily temperatures at 6 cm depth, 15 cm and 2 m height, relative humidity at a height of 2 m, and VWC at a depth of 6 cm. These monthly averages were calculated by averaging the daily minimum and maximum values for each month. This approach was necessitated by the temporal resolution of the predictor variables, which were limited to monthly data. By averaging daily extremes over a month, we aligned the temporal resolution of the response variables with that of the predictors, ensuring consistency across the modelling framework. This method retains the critical information conveyed by extreme values while facilitating robust temporal interpolation. Before fitting the models, we selected 15 biophysical variables (related to vegetation, terrain, and macroclimate) as predictors: EVI, NDMI, LAI, FAPAR, tree height, distance to forest edge, direction to forest edge, elevation, relative elevation, terrain roughness, TPI, TWI, distance to sink, solar radiation, and macroclimate. The macroclimate variables at the meteorological station were customized according to the specific response variable being studied. Maximum and minimum daily temperature records were used for temperature-related variables, mean daily humidity records for humidity, and daily sum of precipitation data for VWC. We excluded collinear predictors by removing one predictor from each pair that exhibited a significant Pearson correlation coefficient greater than ±0.7. This approach led to a removal of terrain roughness and distance to forest edge, as shown in Figure S6. To determine the best fit of variables, we applied recursive feature elimination based on a 10-fold cross-validation to each model and each month. This method helped us eliminate those variables that did not contribute additional explanatory power, measured by R^2, and reduced discrepancies between predicted and observed values, as indicated by the root mean square error (RMSE). To improve model robustness and assess predictive accuracy, we used a combination of 100 ensembles for each monthly model, where each ensemble consists of a randomly selected training and evaluation subset, comprising 80% and 20% of the data, respectively. This yielded us the variance of the individual model performance shown in Figure 5.2. In total, our study design led to a processing of 96 cases from a combination of 8 models with reference to the observed microclimatic variables and 12 months.

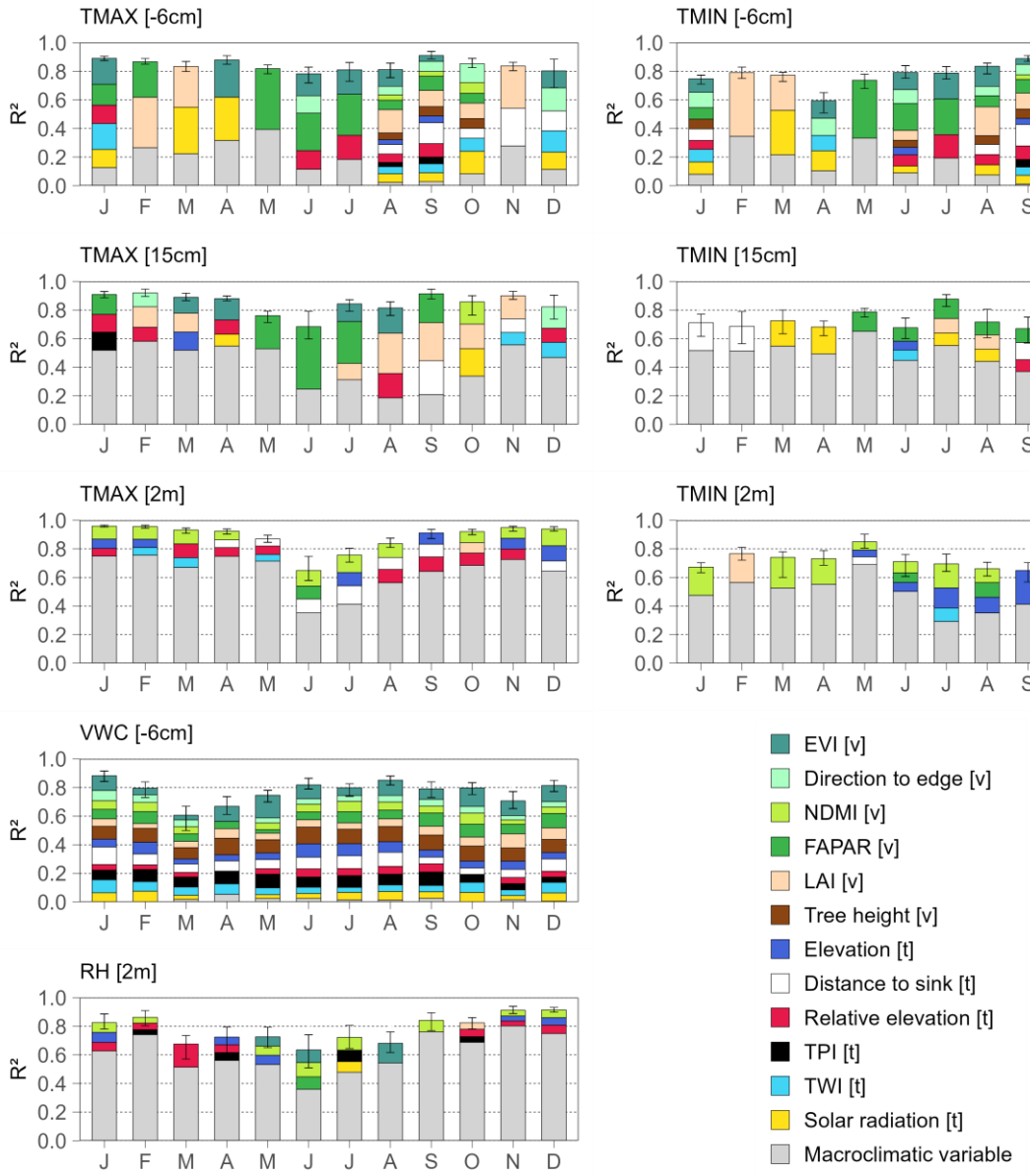

Figure 5.2 *Relative importance of 13 selected biophysical variables for predicting microclimatic observations. Predictors are categorized as related to vegetation (v), topography (t), or macroclimate. The vertical lines in the bar indicate the range (maximum and minimum), while the bars represent the mean R^2 values across 100 ensembles. Each monthly bar corresponds to a specific set of biophysical variables identified after a recursive variable elimination process.*

All calculations were done using the *ranger* function in RStudio (Wright and Ziegler 2017), which applies the algorithm of Breiman (2001). The application of a random forest-based algorithm is based on the assumption that non-linear relationships between predictor and response variables exist (Chen et al. 1999; Zellweger et al. 2019b).

We performed spatiotemporal interpolation on our calibrated models and therefore utilized the Statistical DownScaling Model (SDSM) v.6.1, developed by Wilby et al. (2002) and Wilby and Dawson (2013) to fill data gaps in the weather station records and create a daily time series from 1981 to 2010 based on selected ERA5 predictor variables for statistical downscaling (Table S2). All ERA5 predictands used for downscaling station variables were selected based

on their influence, assessed by partial correlation coefficients (r) and p-values, using the *screen variables* function in the SDSM software. For the recorded periods from 2004 to 2014 at Valle del Río Manso Inferior, and from 1992 to 2014 at El Bolsón respectively, even years were used as training data, while odd years served as validation data (cf. Zignol et al. 2023). Due to insufficient historical precipitation and humidity records at the meteorological station of Valle del Río Manso Inferior, the El Bolsón station was used as a substitute for downscaling these two variables. For each day of the synthesized time series, we generated 100 ensembles using the *weather generator* function and calculated the mean. Once the time series for minimum and maximum daily temperature, as well as mean daily humidity and daily sum of precipitation, were completed, these variables, along with the previously mentioned biophysical variables, served as predictors for temporally interpolating microclimatic variables from 1981 to 2010. Subsequently, we calculated monthly averages from these time series. These averages were then used for spatial interpolation to model microclimatic variables across different zones of our study area. The observation periods covered were 2022-2023 for iButton loggers and 2022-2024 for TMS loggers, in addition to a historical period from 1981-2010. Where one zone was established as an envelope encompassing all iButton loggers (Figure 5.1a), and the other zone by an envelope of all TMS-4 loggers (Figure 5.1b). Spatial interpolation was performed using the *predict* function in terra (Hijmans et al. 2024). Macroclimatic variables of the meteorological stations served as constant variables.

5.3 Results

5.3.1 Model calibration

As shown in Figure 5.2, there is remarkable variability in the explanatory power and influence of predictors across the eight models. This variability can be observed among microclimatic variables (relative humidity, VWC, and minimum and maximum temperatures), their measurement scales (6 cm depth, 15 cm height, and 2 m height), and across different months. While several variables are relevant for predicting monthly VWC at a depth of 6 cm (median of 13 predictors), minimum temperature at 6 cm depth (median of 9 predictors), and maximum temperature at 15 cm height (median of 7 predictors), the number of relevant predictors for minimum temperature at a height of 2 m (median of 2 predictors) and at 15 cm (median of 2 predictors) is relatively low. Table 5.2 presents the three strongest predictor variables for all months in the prediction of VWC at 6 cm depth, minimum and maximum temperatures at 6 cm depth, 15 cm height, and 2 m height, as well as relative humidity at 2 m height.

Table 5.2 *Summary of top predictor variables for microclimatic response variables. Predictor variables are listed according to their relevance, expressed as percentages, across all months.*

Response Variable	No.	Predictor Variable	Importance (%)
VWC [-6cm]	1	Tree height	14.1
	2	EVI	13.5
	3	TPI	10.3
TMIN [-6cm]	1	LAI	26.4
	2	TMIN at station	19.7
	3	FAPAR	19.6
TMAX [-6cm]	1	LAI	25.9
	2	FAPAR	24.1
	3	TMAX at station	21.3
TMIN [15cm]	1	TMIN at station	68.3
	2	Distance to sink	27.0
	3	Solar radiation	22.6
TMAX [15cm]	1	TMAX at station	48.9
	2	FAPAR	33.3
	3	Distance to sink	20.8
RH [2m]	1	RH at station	77.9
	2	EVI	14.4
	3	FAPAR	13.7
TMIN [2m]	1	TMIN station	67.2
	2	LAI	26.5
	3	NDMI	23.5
TMAX [2m]	1	TMAX station	71.5
	2	FAPAR	13.9
	3	NDMI	10.9

Returning to Figure 5.2, the models predicting maximum temperature demonstrate the best performance, with an R^2 of 0.88 at 2 m height, followed by 0.85 at 15 cm height, and 0.84 at 6 cm depth, averaged over all months. In contrast, the models predicting minimum temperature above the surface show the lowest performance, with an R^2 of 0.73 at both 2 m and 15 cm heights, averaged over all months. When considering individual months, R^2 for nearly all models decreases to 0.6 or below, and for the prediction of minimum temperature at a depth of 6 cm in May, it decreases to 0.5. Regarding the error rate of the models, measured by RMSE, the pattern is slightly different. The models predicting maximum temperature at 6 cm depth and 2 m height show RMSE values of 1.1°C and 1.5°C, respectively. Conversely, the models predicting minimum temperature at the same depth and height show RMSE values of 1.2°C and 1.8°C, respectively. However, at 15 cm height, this pattern is reversed, with an RMSE of 1.4°C for the model predicting minimum temperature and an RMSE of 2.4°C for the model predicting maximum temperature. Detailed statistics are provided in Table S3.

5.3.2 Spatiotemporal interpolation

The statistical downscaling of the ERA5 reanalysis data for daily temperature showed an R^2 of 0.69 and R^2 of 0.60 for maximum and minimum temperature respectively; and an R^2 of 0.28 and 0.35 for precipitation and humidity respectively (Figure S7). The results of our spatiotemporal interpolations were monthly models for the maximum and minimum temperature at 2 m height, 15 cm height, and 6 cm depth, as well as relative humidity at 2 m

height and VWC at 6 cm depth. For illustrative presentation (Figure 5.3), we selected three months of an exemplary section in Valle del Río Manso Inferior (Figure 5.1c): February, as a dry and warm extreme, July as a cold extreme, and June as a wet extreme. All other months can be found in the appendix (Figure S8-S23).

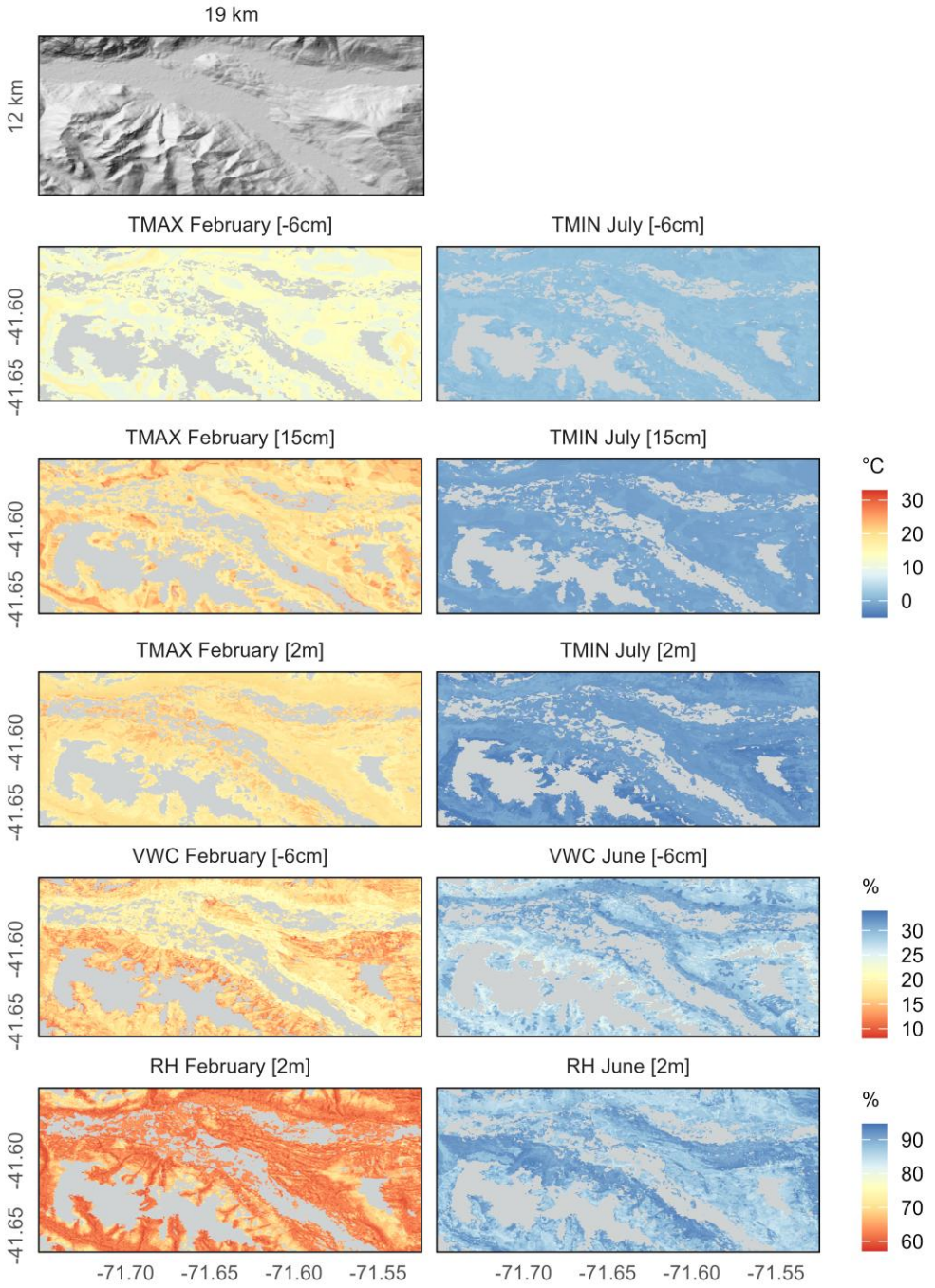

Figure 5.3 *Selected examples of microclimatic maps in Valle del Río Manso Inferior (Figure 5.1c). Depicted variables at a soil depth of 6 cm, as well as at heights of 15 cm and 2 m above ground level, for the period from 1981 to 2010. February represents the warm and dry extreme, July the cold extreme, and June the wet extreme. The section covers an area of 12 by 19 km and spans an elevational gradient from 433 to 2239 m. Grey areas indicate regions not covered by forest.*

5.3.3 Comparison between historical and current microclimate

Figure 5.4 compares microclimatic conditions depicted in our models of the historical period (1981-2010) with those from recent observation periods using iButton data (2022-2023) and TMS data (2022-2024). Most notably, temperatures at 6 cm below ground show a significant change in July's minimum temperatures (Figure 5.4, panel b), with the mean increasing from -0.9°C (SD of 0.4) to 1.8 °C (SD of 0.5), indicating fewer cold extremes. At 15 cm above ground, the strongest change is observed in maximum temperatures (Figure 5.4, panel c), which rose from 20.1 °C (SD of 2.3) to 22.9 °C (SD of 2.6). In terms of VWC below ground, an increase in variance and range (Figure 5.4, panel g) suggests greater variability in VWC during February over the observation period. At a height of 2 m, there is a slight increase in minimum temperatures from -2.0 °C (SD of 1.1) to -1.5 °C (SD of 1.0) during July (Figure 5.4, panel f). Further, maximum temperatures show an increase from 18.7 °C (SD of 1.7) to 19.7 °C (SD of 0.2) during February over the observation period. Regarding relative humidity at 2 m, an increase in variance and standard deviation indicates greater variability during June (Figure 5.4, panel j). Besides these highlighted significant changes, the analysis did not reveal any other significant variations in the climate variables at depths of 6 cm and heights of 15 cm and 2 m between the historical reference period (1981-2010) and the observation period (2022-2024). It is important to consider the temperature accuracy of ±0.5 °C within this comparative analysis (Wild et al. 2019).

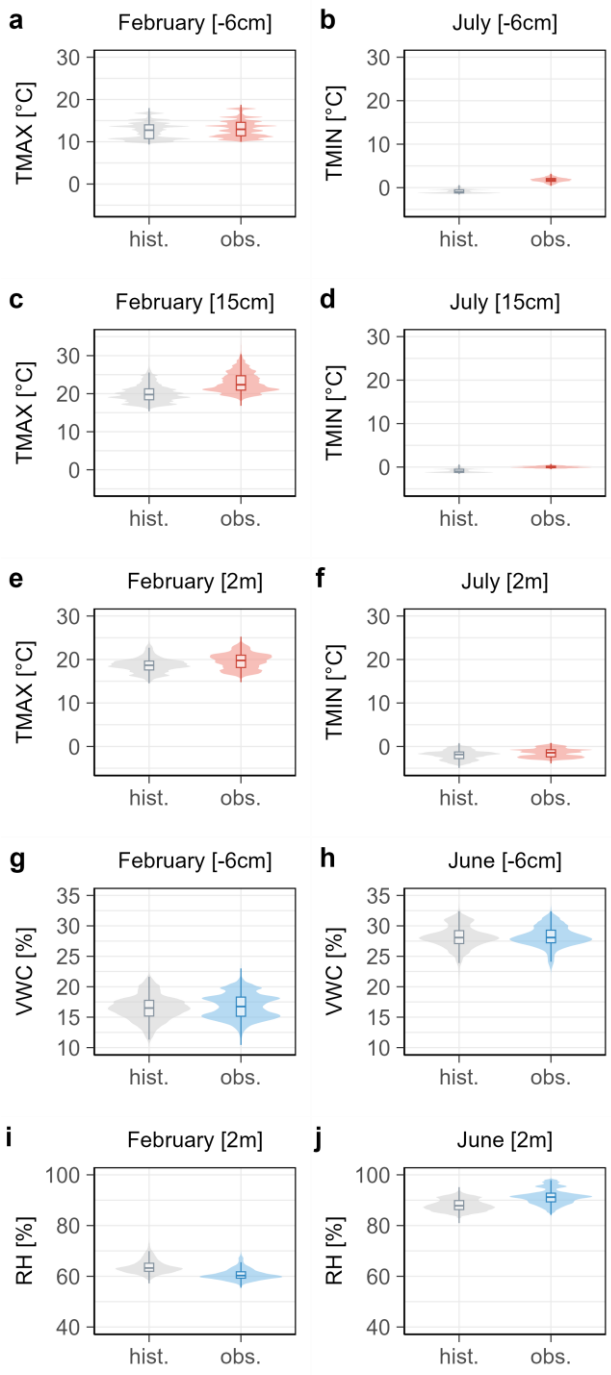

Figure 5.4 *Microclimatic variables across periods and heights. Plots illustrating the distribution of microclimatic variables over historical and observed periods at 2 m and 15 cm heights, as well as 6 cm depth, highlighting the median, quartiles, and the frequency of values at different points. The observation period is 2022-2023 for the iButton loggers and 2022-2024 for the TMS loggers, while the historical reference period spans from 1981 to 2010. Temperature (red) at 6 cm depth and 15 cm height, as well as VWC (blue) at 6 cm depth, represent data from TMS loggers. Temperature (red) and relative humidity (blue) at 2 m height represent data from iButton loggers.*

5.3.4 Vertical temperature variations

Figure 5.5 (panel a) shows the monthly course of mean daily minimum temperatures across three vertical horizons in the section of our study area where the interpolation of iButton data and TMS data overlaps (Figure 5.1c). The minimum temperatures at a height of 15 cm are consistently lower than those at a depth of 6 cm, with an annual mean difference of 2.8 K. A

similar pattern applies to the relation of minimum temperatures at a height of 2 m compared to those at a depth of 6 cm, though only until August. During September and November, minimum temperature at 6 cm depth exceeds that at 2 m height. The largest difference in minimum temperatures between two horizons occurs in November, with temperatures of 2.8 °C at 15 cm height and 9.6 °C at 2 m height, resulting in a difference of 6.7 K.

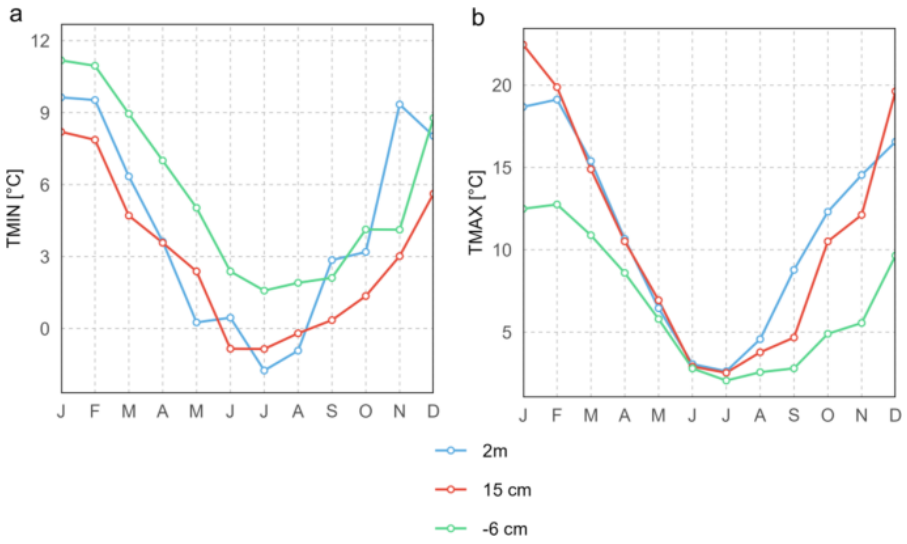

Figure 5.5 *Vertical temperature variations. Where the left panel shows the mean monthly minimum and the right panel the mean monthly maximum temperatures for different vertical horizons at 2 m and 15 cm height, as well as 6 cm depth for the period from 1981 to 2010. Variations are related to a section of our study area where both spatial interpolations of iButton and TMS data overlap (Figure 5.1c).*

Figure 5.5 (panel b) illustrates the monthly course of mean daily maximum temperatures across the same vertical horizons and the same section. The highest maximum temperatures are observed at 15 cm height during December to February, reaching up to 23.6 °C. Intra-annual amplitude of maximum and minimum temperatures is more pronounced at heights of 2 m and 15 cm than those at a depth of 6 cm (Figure 5.5 panel b). The largest differences in maximum temperatures between two horizons occur in January and December, with temperatures of 23.6 °C and 20.0 °C at 15 cm height, and 12.7 °C and 10.0 °C at 6 cm depth, resulting in differences of 10.8 K and 10.0 K, respectively.

5.4 Discussion

We applied a random forest-based regression on microclimatic observations from 2022 to 2024, weather station records, and geospatial vegetation and terrain data to identify drivers of microclimatic variability in northern Patagonia. Additionally, we applied a statistical downscaling of ERA5 data to expand microclimatic models to a historical period (1981–2010). These models characterize local microclimatic patterns, forming a foundation for studies on understory vegetation and soil processes like respiration and nutrient cycling. Nevertheless, inherent uncertainties arise from limited biophysical data, sparse measurements, and the challenges of capturing dynamic ecological processes, as discussed later.

5.4.1 Drivers of microclimatic variability

Our study shows that the statistical relationships between biophysical predictors and microclimatic variability varies significantly by microclimatic variable and season, a finding consistent with Aalto et al. (2022). We observed that predicting VWC at 6 cm depth required the most predictors (15), while estimating minimum temperature at 2 m height required the lowest (4). This discrepancy suggests that many predictors are not effective for estimating minimum temperature and humidity at 2 m. Fewer predictors can make models overly sensitive to those individual variables, leading to variability in our final models. One reason for the different number of predictors can be attributed to the variability of the underlying data. Specifically, lower variability in below-ground data tends to yield more reliable predictions. On the other hand, the high number of predictors needed to model underground temperature, WVC and winter RH, combined with their low consistency along the year, highlights the need for further exploring other predictors that better relate to these variables (Figure 5.2).

For all models, except those focused on below-ground variables, local macroclimatic data, particularly air temperature and RH, exerted the most substantial influence. This result aligns with findings from Zignol et al. (2023), but suggests a slightly stronger macroclimate effect, with its influence ranging from 50% to 80%. This underscores the importance of establishing more local weather stations to capture detailed macroclimatic conditions in this region, which significantly impact microclimatic variations. Beyond macroclimatic drivers, solar radiation, FAPAR, NDMI, and distance to sink emerge as key predictors These factors influenced microclimate either during specific periods (e.g., FAPAR in winter temperature prediction at 15 cm depth) or consistently throughout the year (e.g., NDMI for 2 m temperature). This underscores that, alongside the potential incoming solar radiation, canopy structure and composition reflected through FAPAR, NDMI, and LAI are important factors of microclimatic regulation within forest ecosystems.

The overall explanatory power of monthly predictions and relative importance of predictors also varies substantially between months. This can be attributed to the seasonal climate of northern Patagonia and related changes in plant phenology, which is confirmed by another study in an environment with strong seasonal changes (Aalto et al. 2022). Winter data gaps also amplify seasonal effects, impacting model accuracy for winter months, a topic we will discuss in more detail below. The accuracies of our models also depend strongly on the microclimatic variables and months as it was also recognized in other studies (Lembrechts et al. 2022; Zignol et al. 2023). The highest accuracy was observed in the model predicting maximum temperature at a 2 m height (R^2 = 0.88, RMSE = 1.5 °C), while the lowest accuracy was in the model predicting minimum temperature at the same height (R^2 = 0.73, RMSE = 1.8 °C). In some months, the explanatory power dropped as low as R^2 = 0.6. These variations highlight the complexities of

modelling microclimatic extremes at different heights, likely influenced by unrepresented predictors or those unavailable at an adequate scale.

5.4.2 Microclimatic variability over space and time

Our models capture both landscape-specific variability and, to some extent, the vertical variability within 30-meter microclimate grid cells across our study area. At the landscape level, we observed over 10 K differences in maximum temperatures at 2 m height between exposed, sparsely forested areas at lower elevations and dense forests in higher elevations (e.g., Valle del Río Manso Inferior) during the warmest month from 2022 to 2023. Relative humidity also varied by up to 25% between these landforms in the same month. Such conditions likely impact tree species regeneration (Paritsis et al. 2015), species in the understory (Maclean et al. 2015; Morelli et al. 2016; Rahbek et al. 2019), and patterns of fuel moisture and fire disturbances (Barberá et al. 2023).

During summer (December to February), we recorded the highest maximum temperatures near the ground at 15 cm, while winter minimum temperatures were lower at 2 m than at 15 cm. This suggests that understory species encounter warmer maximum temperatures during the late growing season and less severe minimum temperatures in winter. Late winter and spring showed lower minimum and maximum temperatures at ground level compared to 2 m, contributing to extended winter conditions (Figure 5.5). These conditions likely influence the vertical stratification of understory species (De Frenne et al. 2021; Aalto et al. 2022). The strongest vertical temperature difference occurred between 15 cm above ground and 6 cm below ground, with up to 10.8 K in January, indicating inefficient heat conduction into deeper soil. This significant temperature difference suggests that heat is not efficiently or quickly conducted into deeper soil layers. This could be attributed to the minerals soil's coverage by an ecto-organic humus layer and understory vegetation, or to the generally low bulk density of volcanic ash soils, which inherently possesses lower thermal conductivity (Abu-Hamdeh and Reeder 2000; Buduba et al. 2020).

In addition to the spatial results of our study, our models capture current monthly microclimates from 2022 to 2024, as well as historical microclimates from 1981 to 2010, revealing microclimatic variability over time. We identified significant temperature increases at 15 cm and 2 m in recent years. The maximum temperatures increased from 20.1 °C to 22.9 °C at 15 cm, and from 18.7 °C to 19.7 °C at 2 m, indicating a notable rise in maximum temperatures over the observation period between 2022 and 2024. Subsurface minimum temperatures at 6 cm in July also increased from -0.9 °C to 1.8 °C, indicating reduced cold extremes below ground. These temperature shifts are likely influenced by macroclimatic anomalies associated with mid-level anticyclonic patterns (Stella 2022; Collazo et al. 2024; Stella 2024).

Our high-resolution spatial and temporal modelling provides critical insights for developing bioclimatic envelopes tailored to forest species and ecosystems. These results provide a framework for evaluating forest management strategies that consider both landscape and vertical climate variability, offering insights into species distribution patterns and understory dynamics, including tree regeneration (Kemppinen et al. 2024). Temporal interpolation of our models to 1981–2010 facilitates comparisons with other datasets from that period (cf. Karger et al. 2017) and supports the derivation of correction factors for macroclimatic models, as suggested by De Frenne et al. (2021).

5.4.3 Data scarcity, model uncertainties, and prospects

A significant limitation of our model is its inability to capture intra-annual and multi-year dynamics due to missing or insufficient biophysical data. Key variables absent or only partially available include those related to vegetation, snow, soil properties, and human activities. Many vegetation-related variables, like tree height, are limited to single-year measurements, while cloud cover makes much winter data unusable, resulting in a bias towards capturing the seasonal changes of deciduous forests. Snow cover data, which is essential for understanding how near-surface temperature impacts soil moisture and overwintering organisms, is currently unavailable. This absence is significant, as snow's insulating effect on soil temperatures plays a key role in the survival rates of these organisms (Williams et al. 2015).

Of 20,825 sensor-days analysed, 4,114 (about 19.8%) could have been affected by snow cover (adopting the method of Man et al. 2024), especially at higher altitudes and in winter, where model uncertainty is greatest. Variables like FAPAR and LAI, which provide canopy insights, significantly influence our models but could be enhanced with higher-resolution data, such as airborne LiDAR (Kašpar et al. 2021) or ground-based validation. This lack of dynamic vegetation data limits our ability to explain microclimatic variability across months and seasons, which we expect to impact future microclimates via shifts in disturbance regimes, land use, and species composition (Raffaele et al. 2011; Iglesias et al. 2022; Kitzberger et al. 2022).

Our sampling approach presents additional limitations. We used a random forest-based model, chosen for its ability to capture nonlinear relationships between biophysical predictors and microclimatic variables (Chen et al. 1999; Zellweger et al. 2019b). However, with few measurement points, there is an increased risk of overfitting. Future model enhancements could incorporate focal distance raster, which capture the influence of land cover within varying spatial buffers, to better reflect the broader environmental effects on microclimatic variability. This method, as demonstrated by Shandas et al. (2019), has been shown to improve model precision and predictive power by considering the spatial configuration of landscape features around measurement points. However, the inclusion would require substantial computational resources and processing. Regarding the existing VWC measurements, our study shows

proportional trends rather than absolute values due to simplified calibration, potentially underrepresenting extreme conditions like droughts. This limitation is critical for ecological predictions.

Given these limitations, especially in environmental data quality and measurement scarcity, we recommend testing our gridded data at different spatial resolutions. Even at lower resolutions, our dataset can improve microclimatic representation beneath forest canopies in the northern Patagonian Andes. This refinement is crucial, as Klinges et al. (2024) have demonstrated that not only higher temporal and spatial resolution but particularly proximity, i.e., the change from macro- to microclimate, is essential for enhancing ecological models. Consequently, our datasets could at least enhance prior datasets by Karger et al. (2017) and Fick and Hijmans (2017b), which primarily reflect open atmosphere conditions.

A further limitation is the use of VWC measurements at a shallow 6 cm depth, which raises concerns given the prevalence of summer droughts and deeper soil layers in our area. While 6 cm VWC data is valuable for understanding fuel moisture and wildfire risk (Jensen et al. 2018; Krueger et al. 2023), it may not represent the moisture levels experienced by plant roots in deeper soil. This could limit the effectiveness of these measurements in predicting plant water stress and ecosystem responses, suggesting the need for deeper VWC measurements. However, shallow VWC data does provide insight into the survival and growth of tree seedlings critical for forest regeneration (Caselli et al. 2019).

Addressing these limitations by incorporating dynamic data sources could enhance our models' predictive accuracy, enabling more robust management strategies tailored to changing microclimates. Expanding the model to include disturbed areas could further inform forest regeneration processes and identify tipping points affecting vegetation structure. Simon et al. (2024) showed that microclimate varies significantly within shrub-like vegetation, yet our data does not cover all regional vegetation types. With disturbances projected to increase (Kitzberger et al. 2022), filling these gaps will be crucial for accurately projecting future microclimatic conditions.

Our findings on microclimatic variability provide a foundation for understanding how extreme temperature buffering can guide conservation and land management strategies in northern Patagonia. Identifying areas as potential climate refugia for vulnerable species highlights the critical role of microclimates in mitigating biodiversity loss under climate change (Beugnon et al. 2024; Kemppinen et al. 2024). Future efforts should prioritize integrating microclimatic processes into reforestation and land-use planning to enhance ecosystem resilience. By promoting vertical canopy complexity and minimizing soil exposure, management strategies can help buffer against extreme climatic events, support biodiversity conservation, and foster species adaptation. Additionally, fire risk assessments could be improved by incorporating

microclimatic influences on fuel moisture and flammability. As demonstrated by Barberá et al. (2023), local microclimatic differences, such as cooler and moister conditions in forested areas compared to shrublands, significantly affect fuel moisture content and fire behaviour. Considering these microclimatic effects, alongside local precipitation, topography, and vegetation-related wind patterns, could enhance the accuracy of fire risk predictions and inform land management strategies. These actionable insights underscore the value of this work as a stepping stone for both scientific inquiry and practical applications in addressing climate challenges.

5.5 CRediT authorship contribution statement

Martin Kappas: Project administration, Funding acquisition, Conceptualization, Writing – review & editing, **Helge Walentowski:** Project administration, Funding acquisition, Writing review & editing, **Ernesto Juan Reiter:** Data curation, Writing – review & editing, **Juan Haridis Gowda:** Methodology, Writing – review & editing, **Alois Simon:** Conceptualization, Methodology, Data curation, Writing – review & editing, **Birgitta Putzenlechner:** Conceptualization, Methodology, Data curation, Writing – review & editing, **Jonas Fierke:** Conceptualization, Data curation, Formal analysis, Methodology, Visualization, Writing – original draft.

5.6 Data availability

Derived data supporting the findings of this study are available upon request from the corresponding author. Logger data could also be stored and made available with a DOI via the GRO.data of the eResearch alliance.

5.7 Acknowledgements

We extend our heartfelt thanks to CIEFAP for their invaluable assistance with the logistics of our sampling efforts. Their support played a crucial role in the execution of our fieldwork. We are also grateful to ANP and ANPRALE for their trust and collaboration, which were pivotal in gaining access to the Nahuel Huapi National Park and protected areas. Our deepest appreciation goes to all the landowners who generously allowed us access to their properties for the purpose of our study. Their trust and outstanding cooperation were indispensable. Without their participation, this study would not have been possible.

5.8 Funding

This study is part of the research project *Sustainable forest management of temperate deciduous forests – Northern hemisphere beech and southern hemisphere beech forests (KLIMNEM)*, a cooperation between the universities of Göttingen (Germany), Free University of Bozen-Bolzano (Italy), the University of Applied Sciences and Arts, and the Andean

Patagonian Forest Research and Extension Centre (CIEFAP, Argentina). The project is supported by funds of the Federal Ministry of Food and Agriculture (BMEL) based on a decision of the Parliament of the Federal Republic of Germany via the Federal Office for Agriculture and Food (BLE, grant No. 28I-042-01).

5.9 Supplementary information

Below is the link to the electronic supplementary material.

Supplementary file: https://static-content.springer.com/esm/art%3A10.1007%2Fs10113-024-02278-5/MediaObjects/10113_2024_2278_MOESM1_ESM.docx

5.10 Rights and permissions

6. Study III - Vegetation structure and elevation provide stronger thermal buffering than slope orientation during summer heat in northern Patagonia

Submitted on 11 August 2025 to *Scientific Reports* (Springer Nature)

Jonas Fierke, Juan Haridas Gowda, Gastón Mauro Díaz, Philipp Koal, Helge Walentowski, Martin Kappas & Birgitta Putzenlechner

Abstract

Forests in temperate mountain regions are increasingly exposed to extreme heat. Near-surface microclimates, shaped by vegetation and topography, influence forest regeneration, fuel dynamics, and disturbance feedbacks. We examined how daily warming rates, maximum temperatures, and cooling rates differ between buffered sites (forested, high elevation, south-facing) and exposed sites (shrubland, low elevation, north-facing) in northern Patagonia, and whether buffering strength increases with heat exposure. We deployed a network of temperature loggers in the Río Manso Valley, recording summer temperatures at 15-minute intervals. Using a paired sampling design, we compared six environmental gradients representing vegetation structure, elevation, and slope orientation. We used linear mixed-effects models to assess thermal differences and their sensitivity to local maximum temperatures at exposed sites. Buffering capacity varied across gradients. Forest structure and elevation had the strongest, most consistent effects; low-stature vegetation buffered less than medium-height vegetation, while slope orientation showed weaker, more variable effects. Across all gradients, thermal differences increased under higher maximum temperatures, indicating that microclimatic buffering intensifies during heat extremes. Our findings underscore the multidimensional, temperature-sensitive nature of microclimate regulation. By linking structural and topographic gradients with thermal responses, our study provides insights essential for modelling forest regeneration, fuel moisture dynamics, and disturbance feedbacks in fire-prone landscapes under climate change.

Keywords: Microclimate, Temperate mountain forests, Near-surface temperature, Linear mixed effects models, Patagonia

6.1 Introduction

Forests in temperate mountain regions are increasingly exposed to climate-driven changes in disturbance regimes, including more frequent and severe droughts and wildfires (Bebi et al. 2017; Kulakowski et al. 2017; Albrich et al. 2020). These dynamics are altering forest structure, composition, and post-disturbance recovery processes, with important implications for ecosystem functioning and resilience (Sommerfeld et al. 2018). While these are broad-scale processes, their effects are dampened or amplified through local conditions, with microclimatic variation particularly shaped by vegetation and topography (Carnicer et al. 2021).

Vegetation structure and topography modulate near-surface temperature by influencing radiation, air flow, and moisture conditions, creating heterogeneous microclimates that can buffer or decouple organisms and ecological processes from broader climate trends (De Frenne et al. 2021). As wildfire regimes intensify in temperate mountain landscapes, near-surface temperature dynamics are becoming increasingly important for both forest recovery and fire behaviour. Microclimatic conditions during and after disturbance shape regeneration outcomes by influencing temperature extremes experienced at the seedling to sapling level. Buffered microsites, such as those beneath closed-canopy forest, can reduce thermal stress during sensitive life stages like germination and early establishment (Marsh et al. 2022b; Marsh et al. 2022a; Hill et al. 2024). In contrast, more exposed locations may favour light-demanding species by offering greater irradiance and warmer conditions, but only under adequate moisture availability (Espinosa del Alba et al. 2024). Beyond regeneration, near-surface temperatures also affect surface fuel conditions: cooler and moister microsites reduce fuel drying, potentially lowering ignition risk and slowing fire spread during hot and dry periods (Barberá et al. 2023). These roles are further reinforced by vegetation–microclimate feedbacks. Even modest increases in vegetation height or density can dampen thermal variability, creating a self-reinforcing cooling effect (D'Odorico et al. 2010; D'Odorico et al. 2013). Understanding how vegetation and topography interact to shape near-surface temperatures is therefore essential for anticipating landscape trajectories in a warming, fire-prone climate.

Recent studies have advanced our understanding of forest microclimates by collecting fine-scale temperature data across gradients of vegetation structure, elevation, or topography (Atkins et al. 2023; Máliš et al. 2023; Jia et al. 2024). While these efforts have yielded important insights, comparisons across multiple environmental gradients within the same system remain relatively scarce. Moreover, thermal buffering is frequently characterized using temperature extremes, such as daily maxima, whereas temporal features like the rate and timing of warming and cooling have received comparatively less attention, despite their ecological relevance (Hill et al. 2024). Previous findings also suggest that buffering capacity varies with temperature,

with the strongest effects observed during extreme conditions (Davis et al. 2019; De Frenne et al. 2019; Starck et al. 2025). This underscores the need for comprehensive assessments that span multiple environmental gradients and capture both thermal amplitude and diurnal dynamics. Such efforts are particularly important in mountainous landscapes, where complex terrain creates high microclimatic variability and may reveal context-dependent buffering behaviour.

To address these gaps, we examine how near-surface thermal buffering varies across multiple environmental gradients in a temperate mountain landscape of northern Patagonia, Argentina. By combining paired sites in elevation, slope orientation, and vegetation structure, including both closed-canopy forests and structurally open sites, our study quantifies differences in warming rates, daily maximum, and cooling rates between buffered and more exposed conditions. This allows us to assess how near-surface thermal conditions respond to rising temperatures across diverse but ecologically representative forest and shrubland settings.

Northern Patagonia offers a particularly relevant context for this analysis: while much of the region remains dominated by continuous native forests, recent and projected increases in heat and drought raise concerns about growing wildfire vulnerability (Kitzberger et al. 2022). Understanding how local microclimatic conditions are structured by vegetation and topography is of importance to predict how forest regeneration and disturbance feedbacks will unfold under future climate extremes.

In this study, we pursue two main objectives. First, we examine how daily warming rates, maximum temperatures, and cooling rates near the surface differ between buffered and exposed sites across gradients of elevation, slope orientation, and vegetation structure, and assess the consistency of thermal buffering capacity across these environmental contrasts. Second, we investigate how the magnitude and sensitivity of these thermal dynamics respond to thermal conditions during the summer season. To meet these objectives, we address the following research questions: (1) How do daily warming rates, maximum temperatures, and cooling rates differ between buffered and exposed sites across elevation, aspect, and vegetation structure? (2) Does the strength of microclimatic buffering increase with rising thermal stress, and if so, which environmental gradients contribute most effectively to this response? By disentangling the contribution of topographic and structural features to local thermal regimes, our findings aim to improve process-based understanding of forest microclimates and support spatial predictions of microclimatic variation under climate change.

6.2 Material and methods

6.2.1 Study area

The study was conducted in the Río Manso Valley, northern Patagonia, Argentina (41.60° S, 71.56° W), approximately 5 km west of the town of Río Villegas. This temperate mountain landscape is characterized by steep elevation gradients, varying slope orientations, and a mosaic of vegetation types shaped by both natural disturbance dynamics and historical land use (Gowda et al. 2012; Kitzberger 2012). Over short distances, the valley transitions between dense *Nothofagus pumilio* forests, structurally open shrublands dominated by *Nothofagus antarctica*, and mixed formations, creating high microclimatic and structural heterogeneity. The region experiences a marked seasonality in temperature and precipitation, with increasingly frequent summer heat extremes and wildfire activity (Holz et al. 2012; Kitzberger et al. 2022), making it a representative setting for studying interactions between topography, vegetation structure, and climate stressors.

6.2.2 Microclimatic sampling

To assess thermal buffering across environmental gradients, we deployed a network of 22 TOMST TMS-4 Standard loggers (Wild et al. 2019), each installed along a valley transect of Río Manso Inferior Valley. All sensors recorded temperatures in 15-minute intervals from February 15, 2024, to February 14, 2025, and were shielded from direct solar radiation to ensure consistent and comparable microclimatic measurements. Although the loggers record temperature at three levels (–6 cm below surface, +2 cm at the surface, and +15 cm above surface), we focused our analysis on the 15 cm measurements. This choice reflects both the practical difficulty of maintaining a consistent sensor height at 2 cm across structurally complex vegetation (Aalto et al. 2022) and the limited sensitivity of subsurface temperatures (–6 cm) to short-term warming and cooling dynamics near the surface.

The study was designed to capture three key environmental gradients: (i) elevation (low to high), (ii) slope orientation (north- to south-facing), and (iii) vegetation structure (dense forest to low- and medium-height shrubland). Each gradient was sampled using a paired design, with two nearby sites differing in one focal variable while remaining similar in their topographic and vegetation context. Within each site pair, one site was expected to be more buffered and the other more exposed (e.g., forested vs. shrubby, south- vs. north-facing slopes). These labels are relative, with exposed sites representing the less buffered end of the local gradient rather than fully open or extreme conditions. Each observed site was equipped with three microclimate loggers, resulting in three replicate comparisons per gradient. While we refer to elevation, slope, and vegetation as gradients throughout the study, it is important to note that these were operationalized as binary contrasts.

The spatial layout of the contrasting pairs is shown in Fig. 6.1 and listed in Table 6.1. Loggers used for gradients of elevation and slope orientation (sites 1, 5, 7, and 8) were located at 600 m and 1400 m on both north- and south-facing slopes, all within dense forest. At each elevation, six loggers were deployed (three per slope orientation) totalling 12 units that simultaneously captured both gradients. Forest composition varied along the elevation gradient, with low-elevation stands dominated by *Nothofagus dombeyi* and *Austrocedrus chilensis*, and high-elevation sites by *Nothofagus pumilio* and dense *Chusquea culeou* understory. As shown in Table 1, aspect and elevation gradients were further subdivided to isolate the effect of a single variable while keeping other factors constant. Elevation was replicated at two slope orientations (north and south), and aspect at two elevations (600 m and 1400 m), ensuring that comparisons were not confounded by overlapping gradients.

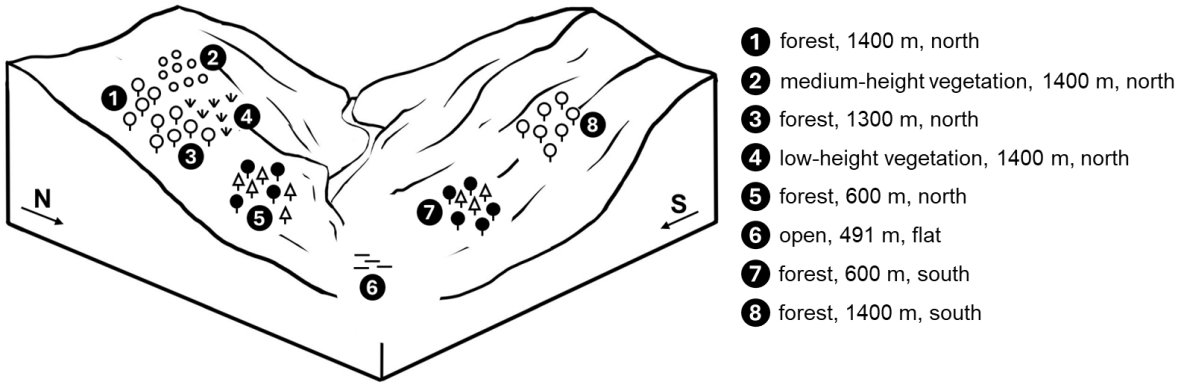

Figure 6.1 *Overview of the study area in the Río Manso Valley showing the locations of microclimate loggers across three environmental gradients: vegetation structure, elevation, and slope orientation. Site numbers correspond to contrasting conditions used in the paired-sampling design (see Table 6.1).*

Table 6.1 *Overview of environmental gradients used in the study, including definitions of buffered and exposed conditions and the corresponding site pairs. Each gradient represents a paired comparison between two sites differing in a single variable (elevation, slope orientation, or vegetation structure) while keeping other factors constant. Site numbers refer to locations shown in Fig. 6.1.*

Gradient label	Definition of gradient (exposed vs. buffered)	Site pairs
E-N	Low vs. high elevation on north-facing slopes	1 and 5
E-S	Low vs. high elevation on south-facing slopes	7 and 8
A-H	North- vs. south-facing slopes at high elevations	1 and 8
A-L	North- vs. south-facing slopes at low elevations	5 and 7
V-M	Medium-height vegetation vs. forest	1 and 2
V-L	Low-height vegetation vs. forest	3 and 4

To examine vegetation effects under high solar exposure, loggers were deployed exclusively on north-facing slopes. This slope orientation also reflects the natural distribution of shrubland in the study area, which is largely confined to north-facing aspects, while south-facing slopes are typically forested (Gowda et al. 2012). At 1300 m, three loggers were installed in *Nothofagus pumilio* forest and three in adjacent low shrubland (sites 3 and 4), which featured sparse *Nothofagus antarctica* individuals under 1 m tall and patches of grass and bare ground. At 1400 m, three more loggers were placed in dense medium-height shrubland (1.5–2.5 m,

dominated by *Nothofagus antarctica*, site 2) and matched to the adjacent forest loggers (site 1). Logger spacing was designed to balance local comparability with the ability to capture fine-scale thermal variation.

In addition, one logger was placed at 491 m in an open, flat area (site 6) to serve as a reference for thermal exposure at the valley bottom, independent of the paired design. The site conditions of the reference logger correspond to those of a standardized weather station on open grassland with regular mowing intervals.

6.2.3 Statistical analysis

Prior to analysis, we imported and pre-processed the temperature time series, including cleaning for missing, duplicated, and temporally misaligned records, and restricted all data to the austral summer months (December–February). To align with the natural diurnal temperature cycle, we computed four daily metrics for each logger: (i) maximum temperature (°C), (ii) minimum temperature (°C), (iii) warming rate (K per hour), and (iv) cooling rate (K per hour). These metrics were selected to characterize different aspects of thermal buffering capacity, capturing both peak temperature conditions and the temporal dynamics of warming and cooling at high temporal resolution. The warming rate was calculated from the last minimum temperature preceding the daily maximum, while the cooling rate was based on the subsequent minimum following the maximum. Importantly, the latter was defined as the first minimum occurring between two consecutive daily maxima, rather than being restricted to a fixed calendar day.

$$W = \frac{T_{max} - T_{min}^{\leftarrow}}{t_{max} - t_{min}^{\leftarrow}}$$

$$C = \frac{T_{max} - T_{min}^{\rightarrow}}{t_{max} - t_{min}^{\rightarrow}}$$

Where W and C are the warming and cooling rates in K/hour, T_{max} is the maximum temperature of the day in °C, $T_{min}^{\leftarrow}$ is the last minimum temperature before T_{max} in °C, $T_{min}^{\rightarrow}$ is the first minimum temperature after T_{max}, and t_{max}, $t_{min}^{\leftarrow}$, $t_{min}^{\rightarrow}$ and are the corresponding timestamps to the measured temperature. For simplicity, we refer to these variables as “Warming”, “TMAX”, and “Cooling” in the figures. In addition to the main thermal metrics, we performed a supplementary analysis of summer frost exposure. For this, we calculated the number of nights with sub-zero temperatures, using a nighttime window from 20:00 to 10:00 the following day.

Based on the paired sampling design, in which each buffered and exposed condition was represented by three replicates, we calculated daily differences in temperature metrics (warming rate, maximum temperature, cooling rate) per pair for each environmental gradient.

$$\Delta Y = Y_{exposed_i} - Y_{buffered_i}$$

Where Y represents W, T_{max}, or C and i is the $i\text{-}th$ pair. This resulted in three ΔY values per day and gradient, reflecting replicate-level thermal differences.

These daily differences were then used as response variables in linear mixed-effects models, fitted using the *nlme* package in RStudio (Pinheiro and Bates 2025). Each gradient was expected to yield 270 replicate-level temperature and rate differences (based on 3 replicates × 90 days), with each value representing the difference between exposed and buffered conditions. To ensure valid rate calculations, days with implausible warming or cooling patterns (e.g., $T_{min}^{\leftarrow}$ after T_{max}) were excluded. This affected at most 7 days per contrast, resulting in minor variation in sample size across gradients (see Supplementary Table 6.1 and 6.2).

To disentangle the influence of environmental gradients from the intensity of thermal forcing, we implemented a two-step modelling approach. In the first step, we fit linear mixed-effects models without covariates to estimate the average effect of each environmental gradient on thermal differences across the summer period. These models provide a baseline assessment of buffering strength under typical conditions. In the second step, we included the maximum temperature at the exposed site T_{max}^{e} as a covariate to test whether thermal differences scaled with external heat load. This variable served as a proxy for localized thermal forcing and allowed us to assess the extent to which microclimatic differences increased under more intense thermal conditions.

In both steps, models were fitted separately for each environmental gradient and thermal metric. To account for residual variability between replicate sites (e.g., microsite effects) and temporal dependence in the data, we included a random intercept per replicate and an autoregressive correlation structure (AR(1)). Model assumptions, including residual normality, homoscedasticity, and autocorrelation, were checked using diagnostic plots and were met within acceptable limits.

The model structure without covariate was:

$$\Delta Y \sim 1 + (1 \mid replicate) + AR(1)$$

The model structure with the covariate was:

$$\Delta Y \sim T_{max}^{e} + (1 \mid replicate) + AR(1)$$

where ΔY represents the daily difference in maximum temperature, warming slope, and cooling slope, respectively.

To evaluate model performance, we calculated marginal and conditional R^2 following the framework proposed by Nakagawa and Schielzeth (2013) and extended by Johnson (2014). These metrics were computed using the *MuMIn* package in RStudio (Bartoń 2025). Model assumptions (normality of residuals, homoscedasticity, temporal structure) were validated using diagnostic plots and were met within acceptable limits.

6.3 Results

6.3.1 Observed thermal patterns and microclimatic differences across gradients

A descriptive analysis of the observed temperature data (Supplementary Table 6.1) reveals that the mean daily maximum temperature across all gradients was 25.2 °C (IQR = 8.0). The highest mean value was recorded at the low elevation north-facing slope (see Fig. 6.1, site 5), reaching 30.8 °C (IQR = 9.4). For comparison, the mean temperature at the reference site (see Fig. 6.1, site 6) was 32.3 °C (IQR = 8.5), indicating that all study sites exhibit some degree of thermal buffering.

The average time of day when maximum temperatures occurred across all gradients was 15:00 (IQR = 1.75 h). The earliest median time of daily maximum temperature was observed in the medium-height vegetation (see Fig. 6.1, site 2) at 13:30 (IQR = 1.5 h), while the latest occurred at high elevations on south-facing slopes (see Fig. 6.1, site 8) at 16:00 (IQR = 2.5 h). At the reference site, the median time of maximum temperature was 14:30 (IQR = 2 h).

In addition to heat exposure, our site-averaged temperature records revealed occasional nighttime frost events during the austral summer (see Supplementary Table 6.2). The highest number of frost nights was recorded at the open valley-bottom reference site (see Fig. 6.1, site 6), with 38 frost nights. Shrubland sites experienced 7 to 9 frost nights, while forest sites ranged from 0 to 9, depending on elevation and aspect.

In models without covariates, warming, maximal temperature, and cooling differences between buffered and exposed microclimates varied substantially across gradients (Fig. 6.2).

For the warming rate differences (Fig. 6.2 panel a and d; Supplementary Table 6.3), gradients V-L (0.97 K/h, $p < 0.001$), V-M (1.07 K/h, $p < 0.05$), E-S (0.86 K/h, $p < 0.001$), and A-H (0.68 K/h, $p < 0.05$) showed significant differences, while E-N (1.00 K/h, $p = 0.213$) and A-L (0.82 K/h, $p = 0.075$) were not statistically significant. Explained variance was heterogeneous, with conditional R^2 ranging from 0.15 (E-S) to 0.55 (V-M).

For maximum temperature (Fig. 6.2 panel b and e; Supplementary Table 6.3), the strongest differences were observed in the elevation gradients, particularly on south-facing slopes (E-S: 8.31 K) and north-facing slopes (E-N: 7.98 K), both statistically significant ($p < 0.001$ and $p < 0.05$). The low-height vegetation gradient (V-L) also showed a large and significant difference of 7.75 K ($p < 0.001$). In contrast, medium-height vegetation (V-M: 3.84 K) and the slope aspect gradients (A-H: 2.76 K, A-L: 2.33 K) displayed smaller differences, with A-L not reaching statistical significance ($p = 0.192$). Despite these pronounced mean differences, conditional R^2 values again varied widely, from very low in A-H (0.004) to high in E-N (0.82).

Cooling rate differences (Fig. 6.2 panel c and f; Supplementary Table 6.3) were generally smaller. Significant differences were detected for both vegetation gradients: V-L (0.67 K/h, $p <$

0.001) and V-M (0.25 K/h, $p < 0.001$), while all other gradients showed lower effect sizes and were not statistically significant ($p > 0.1$). Conditional R^2 values ranged from 0.06 (V-M) to 0.57 (E-N).

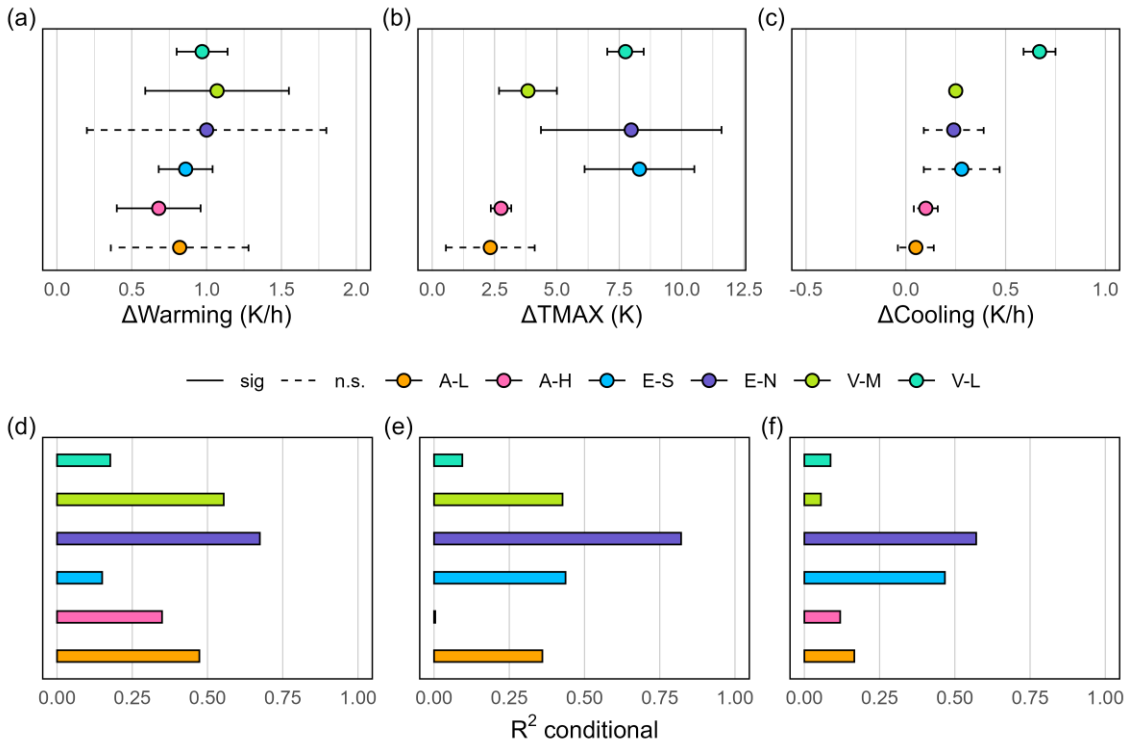

Figure 6.2 *Daily differences in (a, d) warming rate (K/h), (b, e) maximum temperature (K), and (c, f) cooling rate (K/h) between buffered and exposed sites across six environmental gradients: vegetation structure (low-height [V-L], medium-height [V-M]), elevation (north-facing [E-N], south-facing [E-S]), and slope orientation (high elevation [A-H], low elevation [A-L]). Panels (a–c) show marginal means (±95% confidence intervals) estimated from linear mixed-effects models fitted with an autoregressive correlation structure. Solid lines indicate statistically significant differences ($p < 0.05$); dashed lines indicate non-significant results. Panels (d–f) display conditional R^2 values for each model, reflecting the proportion of variance explained by both fixed and random effects.*

6.3.2 Temperature-dependent variation in microclimatic buffering strength

When maximum temperature at the exposed site was included as a covariate, buffering strength showed a significant temperature dependence across all gradients and temperature variables (Fig. 6.3). While significance levels for the V-M and A-L gradients reached $p < 0.05$ and $p < 0.005$, respectively, all other gradients consistently showed stronger effects with $p < 0.001$.

For warming rate differences (Fig. 6.3 panel a and d, Supplementary Table 6.4), all gradients showed significant positive relationships with maximum temperature at the exposed site. Slope estimates ranged from 0.042 (A-H) to 0.074 (E-S), with the strongest explanatory power in the elevation gradient on south-facing slopes (E-S: marginal $R^2 = 0.43$), followed by V-L (0.25). Gradients V-M, A-L, and E-N showed low to moderate relationships (marginal R^2 between 0.07 and 0.11), whereas conditional R^2 values remained high across most gradients.

For maximum temperature differences (Fig. 6.3 panel b and e; Supplementary Table 6.4), all gradients showed highly significant and positive relationships, indicating once again that temperature differences between buffered and exposed sites increased with rising maximum temperatures at the exposed site. The strongest slope was observed in the low-height vegetation gradient (V-L: 0.417), followed by E-S (0.287), A-H (0.243), and A-L (0.195). Weaker but still significant relationships were found in V-M and E-N (both 0.116). The explanatory power varied considerably between gradients: the V-L contrast showed the highest marginal R^2 (0.57), indicating a strong effect of maximum temperature at the exposed site, while the E-N contrast had a low marginal R^2 (0.02) but high conditional R^2 (0.80), suggesting that most variation was explained by random effects rather than temperature-driven differences.

Cooling rate differences (Fig. 6.3 panel c and f; Supplementary Table 6.4) also showed significant positive relationships across all gradients. While slope estimates were consistently smaller than for warming rate differences (ranging from 0.005 in V-M to 0.030 in V-L), most relationships were statistically robust. The V-L gradient stood out with the highest slope (0.030) and marginal R^2 (0.33), while other gradients had weaker effect sizes and marginal R^2 values mostly below 0.17.

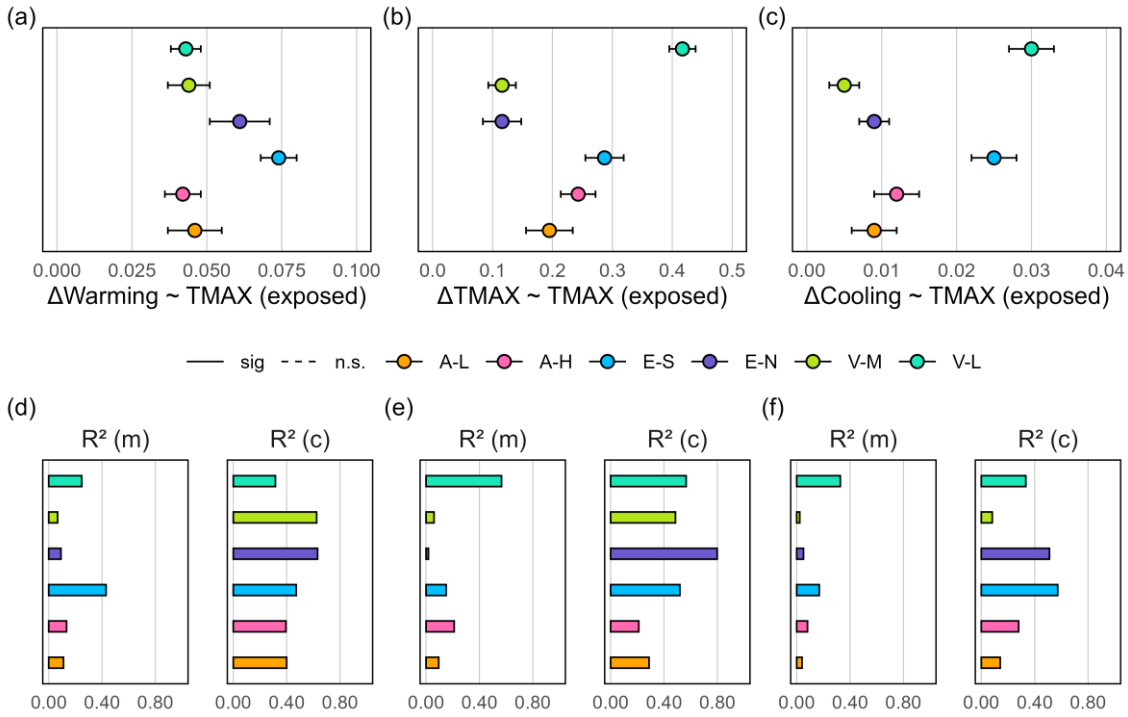

Figure 6.3 *Temperature-dependent amplification of microclimatic differences in (a, d) warming rate (K/h), (b, e) maximum temperature (K), and (c, f) cooling rate (K/h) across six environmental gradients: vegetation structure (low-height [V-L], medium-height [V-M]), elevation (north-facing [E-N], south-facing [E-S]), and slope orientation (high elevation [A-H], low elevation [A-L]). Panels (a–c) show model-estimated slopes (±95% confidence intervals) from linear mixed-effects models with maximum temperature at the exposed site as a covariate. These slopes quantify how thermal differences between buffered and exposed sites scale with increasing heat load. Solid lines indicate statistically significant relationships ($p < 0.05$); dashed lines indicate non-significant trends. Panels (d–f) display marginal (left) and conditional (right) R^2 values for each model.*

To visualize how microclimatic differences change across temperature regimes, we compared model predictions at 15 °C and 30 °C for all three metrics and six gradients (Fig. 6.4). Patterns varied between gradients and metrics. Among all gradients, V-L showed the strongest and most consistent increases at 30 °C, clearly separating it from most other gradients across all comparisons. Elevation gradients showed strong shifts in warming rates, particularly on south-facing slopes (E-S), whereas warming rate differences were more pronounced in the V-M gradient. These patterns illustrate that the magnitude and direction of buffering effects are not constant but vary across gradients and temperature levels.

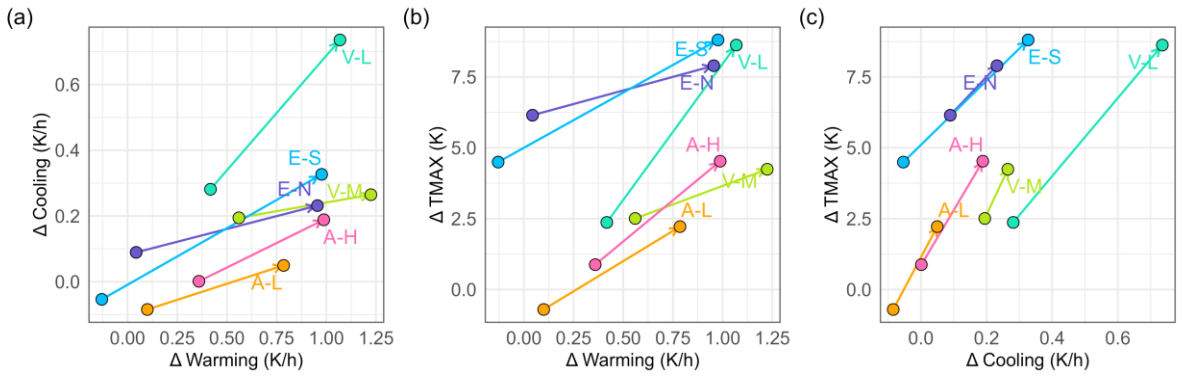

Figure 6.4 *Predicted differences in microclimatic buffering across six environmental contrasts at fixed exposed-site temperatures of 15 °C and 30 °C. Arrows indicate the shift in predicted differences in warming rate, cooling rate, and maximum temperature between buffered and exposed sites as heat load increases. Each point represents model-derived differences at 15 °C (arrow base) and 30 °C (arrow tip) for a given contrast. Results illustrate the temperature-dependent and multidimensional nature of microclimatic buffering (compare Fig. 6.3).*

6.4 Discussion

6.4.1 Differences in thermal buffering capacity and sensitivity across vegetation, elevation, and slope orientation

Our findings confirm that microclimatic buffering near the ground is not a static property but varies with environmental context and thermal load (Davis et al. 2019; De Frenne et al. 2019; Starck et al. 2025). We detected consistent microclimatic differences between buffered and exposed sites, but the magnitude, direction, and statistical significance of these effects varied across gradients and thermal metrics. This variation highlights distinct patterns of microclimatic divergence and thermal sensitivity among vegetation, elevation, and slope gradients.

Vegetation structure exerted the strongest and most consistent buffering effect. Dense forest cover of *Nothofagus pumilio* strongly suppressed thermal maxima and moderated both warming and cooling rates compared to adjacent low-height (<1 m) vegetation. This pattern is consistent with earlier findings on the buffering role of forest structural complexity and canopy closure (Jucker et al. 2018; Díaz-Calafat et al. 2023; Csölleová et al. 2024; John et al. 2024), and further supported by regional observations from Simon et al. (2024), who reported pronounced temperature differences between dense forest stands and canopy gaps. While both low-height (<1 m) and medium-height (1.5-2.5 m) vegetation structures differed

significantly from forests, their buffering capacities varied. Low-height vegetation showed consistently strong differences in warming rate, maximum temperature, and cooling rate, with greater sensitivity under warmer conditions. In contrast, medium-height vegetation showed weaker differences and lower sensitivity, particularly for cooling rate and maximum temperature. This supports findings from post-fire landscapes where sparse or low-stature vegetation allows intense daytime heating and limited nocturnal retention (Marsh et al. 2022b; Marsh et al. 2022a). Even modest increases in vegetation height can reduce thermal variability, a pattern consistent with vegetation–microclimate feedbacks (D'Odorico et al. 2010; D'Odorico et al. 2013). Notably, the frequency of summer frost nights further illustrates these differences in thermal exposure: the low-height vegetation experienced 9 frost nights, compared to just 1 in its paired forest. In contrast, the medium-height vegetation recorded 7 frost nights, slightly fewer than its adjacent forest site with 9. The open valley-bottom reference site showed the highest exposure, with 38 frost nights. These results highlight the dual exposure to both heat and cold extremes in open microsites, particularly those with sparse or low-stature vegetation.

Topographic gradients showed more complex and less consistent buffering patterns. In the elevation contrasts, south-facing slopes exhibited both large differences in maximum temperature and strong temperature dependence. In contrast, north-facing slopes also exhibited large temperature differences but much weaker relationships with maximum temperature. This asymmetry suggests that elevation interacts with slope orientation, with north-facing sites potentially reaching thermal saturation more quickly under strong solar exposure. These findings underscore that elevation alone is not a reliable predictor of buffering, given its interaction with landscape position and atmospheric coupling (Dobrowski 2011). Slope aspect gradients showed limited and variable buffering patterns compared to vegetation and elevation contrasts. Slope aspect gradients showed more limited and variable buffering patterns compared to vegetation and elevation contrasts. In both aspect gradients, differences in maximum temperature between buffered and exposed sites were moderate in magnitude, with only the high-elevation gradient reaching statistical significance. While these effects were smaller than those observed in elevation or vegetation contrasts, the aspect gradient at high elevation showed a significant amplification of thermal differences with rising temperatures at the exposed site. This suggests that slope orientation is a less important driver of microclimatic buffering compared to vegetation structure and elevation, with meaningful effects only emerging under specific conditions such as high elevation and elevated temperatures.

Together, these results underscore that microclimatic buffering is a multidimensional, spatially and temporally variable process. Vegetation structure, elevation, and slope orientation interact to mediate thermal exposure near the surface. Spatially explicit, high-resolution temperature data remain essential for understanding this variability (De Frenne et al. 2021; Csölleová et al.

2024). These insights are especially relevant for improving forest microclimate models, such as those by Fierke et al. (2025) in northern Patagonia, which currently underrepresent fine-scale effects of vegetation structure and topography. By quantifying how buffering capacity varies across environmental gradients and with thermal intensity, our study contributes data essential for parameterizing and validating these models, thereby enhancing their ecological realism and utility.

6.4.2 Potential implications for microclimate-sensitive processes in fire-prone landscapes

Our findings provide a framework for understanding how near-surface microclimates mediate key ecological processes in fire-prone landscapes, particularly forest regeneration and surface flammability. Seedling establishment is highly sensitive to microsite conditions, with near-surface temperature dynamics influencing germination, dehydration risk, and early growth (Espinosa del Alba et al. 2024; Hill et al. 2024). Forested sites, which exhibited consistent thermal buffering, may function as microrefugia for early life stages by protecting seedlings from increasingly frequent heat extremes (von Arx et al. 2013). In contrast, structurally open shrublands showed sharp diurnal temperature fluctuations, combining high daytime heat with rapid nocturnal cooling. These regimes may expose seedlings to multiple stressors, potentially favouring fast-growing, heat-tolerant species, while limiting recruitment of shade- or drought-sensitive taxa and altering successional dynamics. At the same time, exposed microsites such as shrublands and north-facing slopes at low elevation are more prone to surface fuel drying, which increases ignition probability and fire spread during hot and dry conditions (Blackhall et al. 2017; Barberá et al. 2023). These patterns align with fire probability models in northwestern Patagonia, where burn risk is highest in low elevations with intermediate precipitation and flammable vegetation like shrublands. (Barberá et al. 2025). While Barberá et al. (2025) identified statistical relationships between fire occurrence, vegetation, and environmental factors, our results provide microclimatic insight at fine spatial scale. On north-facing slopes, open vegetation promoted high near-surface temperatures and rapid thermal shifts, conditions that intensify fuel drying. Although our vegetation contrasts were limited to north-facing slopes, the consistent patterns observed suggest vegetation structure alone can shape microclimate and fire risk. Moreover, recurrent fires in these environments may reinforce thermal extremes by reducing structural complexity and promoting shrub encroachment, creating feedbacks that sustain flammable landscape states (Paritsis et al. 2015; Tiribelli et al. 2018). These coupled patterns show how microclimate regulates both regeneration and disturbance risk, and how each process may reinforce the other. By quantifying fine-scale thermal variation across vegetation and topographic gradients, our study helps refine spatial predictions of these interacting dynamics under climate change.

6.4.3 Limitations and future directions

While our study provides detailed insights into thermal buffering across vegetation, elevation, and slope orientation, several limitations should be acknowledged. Although our sensor network captures fine-scale near-surface temperature variation, it does not include other variables such as humidity, wind, or radiation, which also influence buffering (Davis et al. 2019) and fire risks. Second, our design focuses on binary contrasts (e.g., forest vs. low- and medium-height vegetation), which limits our ability to assess microclimatic gradients along continuous structural or compositional transitions. This may overlook gradual vegetation changes and edge effects (Meeussen et al. 2021). Finally, while we recorded a full year of data including several heat events, longer-term monitoring is needed to assess interannual variation and cumulative impacts, particularly in relation to large-scale climate drivers such as the El Niño–Southern Oscillation and the Southern Annular Mode.

Future studies should integrate parameters such as soil moisture, humidity, wind, and radiation to allow a more complete evaluation of buffering. The use of remote sensing, including Lidar-based vegetation structure data, could help quantify forest structural complexity and extend the spatial scope of these findings. Linking microclimate data to weather stations would improve upscaling and integration with climate models. Overall, this study represents a first step toward a broader framework for understanding and managing landscape-level climate resilience in forest ecosystems of northern Patagonia.

6.5 CRediT authorship contribution statement

Jonas Fierke: Conceptualization, Formal Analysis, Investigation, Methodology, Writing – Original Draft Preparation. **Juan Haridas Gowda:** Formal Analysis, Methodology, Writing – Review & Editing. **Gastón Mauro Díaz:** Formal Analysis, Methodology, Writing – Review & Editing. **Philipp Koal:** Investigation, Writing – Review & Editing. **Helge Walentowski:** Writing – Review & Editing, Funding acquisition. **Martin Kappas:** Writing – Review & Editing, Funding acquisition. **Birgitta Putzenlechner:** Conceptualization, Investigation, Writing – Review & Editing.

6.6 Data availability

Derived data supporting the findings of this study are available upon request from the corresponding author.

6.7 Funding

This study is part of the research project *Sustainable forest management of temperate deciduous forests – Northern hemisphere beech and southern hemisphere beech forests (KLIMNEM)*, a cooperation between the universities of Göttingen (Germany), Free University

of Bozen-Bolzano (Italy), the University of Applied Sciences and Arts, and the Andean Patagonian Forest Research and Extension Centre (CIEFAP, Argentina). The project is supported by funds of the Federal Ministry of Food and Agriculture (BMEL) based on a decision of the Parliament of the Federal Republic of Germany via the Federal Office for Agriculture and Food (BLE, grant No. 28I-042-01).

6.8 Competing interest

The authors have no relevant financial or non-financial interests to disclose.

6.9 Acknowledgement

We thank CIEFAP for their invaluable help with fieldwork logistics, which greatly supported our sampling efforts. We are also grateful to ANP for their trust and assistance in facilitating access to Nahuel Huapi National Park. Our sincere thanks go to all landowners who kindly granted access to their properties, as their cooperation was essential for this study. We also thank Dario Perez for his expert support in preparing one of the graphics.

6.10 Supplementary information

Supplementary Table 6.1 *Summary statistics of temperature and diurnal metrics recorded at eight study sites in the Río Manso Valley during the austral summer. Variables include daily maximum temperature (TMAX), minimum temperature (TMIN), and their respective times of occurrence (TMAX Time, TMIN Time), as well as warming and cooling rates. For each variable and site, sample size (n), median, interquartile range (IQR), minimum (Min), and maximum (Max) are reported. Time values are presented in HH:MM format.*

Variable	Site	n	Median	IQR	Min	Max
TMAX	1	264	23.16	7.56	6.63	39.75
	2	264	27.28	8.48	7.50	39.94
	3	264	20.63	7.30	6.19	34.25
	4	265	28.50	9.44	6.63	44.00
	5	268	30.75	9.41	10.75	51.38
	6	90	32.28	8.47	17.38	41.50
	7	264	28.56	8.92	12.44	46.81
	8	263	20.19	7.50	6.75	34.69
TMIN	1	264	5.81	5.28	-1.88	13.38
	2	264	4.84	5.58	-2.25	13.13
	3	264	6.16	5.25	-1.13	13.81
	4	265	4.56	5.75	-3.38	13.75
	5	268	9.31	4.33	2.75	16.88
	6	90	1.19	8.61	-5.38	24.63
	7	264	9.00	4.52	2.00	17.13
	8	263	6.38	5.47	-1.56	14.88
TMAX Time	1	264	14:30	1:30	10:00	17:15
	2	264	13:30	1:30 h	10:45	17:15
	3	264	15:15	2:00 h	10:45	19:30
	4	265	15:30	2:00 h	10:30	19:30

	5	268	14:15	2:15 h	10:30	17:30
	6	90	14:30	2:00 h	0:00	22:00
	7	264	15:30	0:45 h	12:30	19:00
	8	263	16:00	2:30 h	10:15	19:30
TMIN Time	1	264	06:30	01:15 h	02:00	08:15
	2	264	06:15	01:15 h	01:30	08:30
	3	264	06:30	01:15 h	02:00	09:15
	4	265	06:15	01:30 h	00:30	09:00
	5	268	07:15	00:45 h	00:30	09:30
	6	90	06:30	01:15 h	00:00	22:45
	7	264	07:00	01:00 h	02:00	09:30
	8	263	06:15	01:37 h	01:15	09:30
WARMING	1	264	1.97	1.05	0.35	4.77
	2	264	3.18	1.30	0.47	5.91
	3	264	1.59	0.61	0.30	3.72
	4	265	2.65	1.42	0.38	5.00
	5	268	2.85	1.63	0.61	7.56
	6	90	3.70	2.14	0.57	6.28
	7	264	2.36	1.22	0.34	4.12
	8	263	1.38	0.59	0.24	3.50
COOLING	1	264	1.07	0.37	0.19	2.00
	2	264	1.33	0.35	0.39	2.06
	3	264	0.92	0.30	0.18	2.24
	4	265	1.57	0.61	0.21	3.44
	5	268	1.27	0.54	0.25	2.60
	6	90	2.02	0.87	0.20	3.26
	7	264	1.20	0.54	0.21	2.64
	8	263	0.93	0.40	0.16	2.04

Supplementary Table 6.2 *Number of summer frost nights (nights with at least one 15-minute interval below 0 °C) recorded at each study site during the period from 15 February 2024 to 13 February 2025, based on site-averaged temperature data. Frost nights were identified using nighttime temperature data (20:00–10:00), and sites are grouped by vegetation structure, elevation, and slope orientation as described in Figure 1.*

Site	Description	Frost nights (n)
1	Forest, 1400 m, north	9
2	Medium-height vegetation, 1400 m, north	7
3	Forest, 1300 m, north	1
4	Low-height vegetation, 1300 m, north	9
5	Forest, 600 m, north	0
6	Open site, 491 m, flat	38
7	Forest, 600 m, south	0
8	Forest, 1400 m, south	8

Supplementary Table 6.3 *Results of linear mixed-effects models quantifying absolute differences in warming rate (K/h), maximum temperature (K), and cooling rate (K/h) between buffered and exposed microclimates across six environmental gradients: vegetation structure (low-height [V-L], medium-height [V-M]), elevation (north-facing [E-N], south-facing [E-S]), and slope orientation (high elevation [A-H], low elevation [A-L]). For each variable and gradient, model estimates (intercept), standard error (SE), t-value, and p-value are shown. Marginal (R^2 m) and conditional (R^2 c) R^2 values indicate the variance explained by fixed effects alone and by the full model including random effects, respectively.*

Variable	Gradient	n (days)	Intercept	SE	t-value	p-value	R^2 (m)	R^2 (c)
Warming	V-L	264	0.97	0.17	5.68	<0.001	0	0.18
	V-M	264	1.07	0.48	2.24	0.0262	0	0.55
	E-N	264	1.00	0.80	1.25	0.2128	0	0.67
	E-S	263	0.86	0.18	4.81	<0.001	0	0.15
	A-H	263	0.68	0.28	2.44	0.0154	0	0.35
	A-L	263	0.82	0.46	1.79	0.0750	0	0.47
TMAX	V-L	264	7.75	0.73	10.64	<0.001	0	0.09
	V-M	264	3.84	1.16	3.31	0.0011	0	0.43
	E-N	264	7.98	3.62	2.20	0.0286	0	0.82
	E-S	263	8.31	2.20	3.77	<0.001	0	0.44
	A-H	263	2.76	0.41	6.70	<0.001	0	0.00
	A-L	263	2.33	1.78	1.31	0.1920	0	0.36
Cooling	V-L	264	0.67	0.08	8.78	<0.001	0	0.09
	V-M	264	0.25	0.03	7.53	<0.001	0	0.06
	E-N	264	0.24	0.15	1.59	0.1138	0	0.57
	E-S	263	0.28	0.19	1.50	0.1350	0	0.47
	A-H	263	0.10	0.06	1.64	0.1028	0	0.12
	A-L	263	0.05	0.09	0.64	0.5214	0	0.17

Supplementary Table 6.4 *Results of linear mixed-effects models including maximum temperature at the exposed site as a covariate. Models quantify absolute differences in warming rate (K/h), maximum temperature (K), and cooling rate (K/h) between buffered and exposed microclimates across six environmental gradients: vegetation structure (low-height [V-L], medium-height [V-M]), elevation (north-facing [E-N], south-facing [E-S]), and slope orientation (high elevation [A-H], low elevation [A-L]). For each variable and gradient, model estimates (intercept and slope), standard error (SE), t-value, and p-value are shown. Marginal (R^2 m) and conditional (R^2 c) R^2 values indicate the variance explained by fixed effects alone and by the full model including random effects, respectively.*

Variable	Gradient	n (days)	Intercept	Slope	SE	t-value	p-value	R^2 (m)	R^2 (c)
Warming	V-L	264	-0.23	0.043	0.005	9.00	<0.001	0.25	0.32
	V-M	264	-0.10	0.044	0.007	6.32	<0.001	0.07	0.63
	E-N	264	-0.87	0.061	0.010	6.19	<0.001	0.09	0.63
	E-S	263	-1.24	0.074	0.006	12.67	<0.001	0.43	0.47
	A-H	263	-0.27	0.042	0.006	6.87	<0.001	0.13	0.40
	A-L	263	-0.59	0.046	0.009	5.36	<0.001	0.11	0.40
TMAX	V-L	264	-3.89	0.417	0.022	18.80	<0.001	0.57	0.57
	V-M	264	0.77	0.116	0.023	5.14	<0.001	0.06	0.49
	E-N	264	4.40	0.116	0.032	3.70	<0.001	0.02	0.80
	E-S	263	0.18	0.287	0.032	9.02	<0.001	0.15	0.52
	A-H	263	-2.78	0.243	0.029	8.27	<0.001	0.21	0.21
	A-L	263	-3.63	0.195	0.039	4.97	<0.001	0.10	0.29
Cooling	V-L	264	-0.17	0.030	0.003	10.52	<0.001	0.33	0.33
	V-M	264	0.12	0.005	0.002	2.44	0.0154	0.02	0.08
	E-N	264	-0.05	0.009	0.002	4.08	<0.001	0.05	0.51
	E-S	263	-0.43	0.025	0.003	8.75	<0.001	0.17	0.57
	A-H	263	-0.19	0.012	0.003	4.82	<0.001	0.08	0.28
	A-L	263	-0.22	0.009	0.003	2.94	0.0036	0.04	0.14

7. Synthesis and outlook

7.1 Synthesis of main findings

This thesis addressed how climate data at different spatial scales can be used to improve our understanding of forest ecosystem responses to climate change in mountainous regions. By addressing research questions Q1-Q5 through three empirical studies, the work examined the interplay between macroclimatic data and their uncertainties (Fierke et al. 2024), microclimatic drivers and the interpolation of in-situ measurements to the landscape scale (Fierke et al. 2025), and thermal buffering processes analysed at a localized scale (Fierke et al. submitted-b). Taken together, the findings show that the regions of highest ecological sensitivity are also those where climate representation is most uncertain and where fine-scale processes exert the greatest control over local conditions.

Addressing Q1 and Q2, the comparison between CHELSA v2.1 and WorldClim v2.1 revealed substantial discrepancies in both temperature- and precipitation-related estimates for northern Patagonia, with precipitation showing the largest divergences. For example, a precipitation-related index representing median conditions in CHELSA corresponds to values at the upper extreme in WorldClim, highlighting the pronounced differences in their estimation of precipitation patterns, particularly in high-elevation zones. These discrepancies translated into notable divergences in projections of bioclimatic zones under future scenarios, with differences in predicted extents varying by zone and reaching up to approximately 20 percent. This indicates that macroclimatic dataset choice can fundamentally alter assessments of forest vulnerability in mountain environments, particularly in steep and data-sparse terrain. On the contrary, certain consistent trends across datasets can still be identified, providing potential guidance for setting research priorities and informing environmental planning (Fierke et al. 2024).

The implications of these macroclimate uncertainties become clearer when integrated with the findings from Q3 and Q4. Spatial modelling of microclimatic conditions across multiple vertical levels at 30 m resolution estimated how monthly temperature and moisture patterns within forests were jointly influenced by macroclimatic, vegetation, and terrain-related drivers. Macroclimatic data from nearby weather stations remained the dominant predictors for aboveground conditions, explaining roughly 50 to 80 percent of the observed variation, yet the inclusion of remote-sensing products substantially improved accuracy. Individual vegetation indices such as FAPAR, NDMI, and LAI, alongside topographic variables including solar radiation and distance to sink, enhanced predictions in ways that reflected seasonal and vertical complexity. These patterns emphasize that vegetation structure and dynamics exert a substantial influence on microclimate and point towards the value of integrating high-resolution

canopy data, such as LiDAR, into future modelling efforts. Nevertheless, the reliability of predictions varied depending on both microclimatic response variable and season. While maximum temperatures were reproduced with relatively high accuracy, minimum temperatures proved harder to capture. The fluctuating importance of predictors across depths and months illustrates the inherently dynamic and heterogeneous nature of forest microclimates, while also highlighting the challenge of identifying suitable satellite-based indices at high spatial and temporal resolution. Taken together with the inconsistencies identified in macroclimatic products, these results suggest that assessments of forest vulnerability cannot rely on regional climate layers alone. Instead, they require explicit integration of vegetation and terrain effects, thus acknowledging the dynamic vegetation processes such as seasonal changes in canopy cover and forest structural development that strongly shape microclimatic conditions but remain difficult to represent at broader scales (Fierke et al. 2025).

These insights correspond to Q5, which examined microclimatic buffering during summer heat events at a localized scale. Buffering strength, defined as the temperature difference between buffered and exposed sites, increased with higher maximum temperatures at exposed sites. In vegetation contrasts, differences exceeded 8 K between forest and adjacent shrubland under hot background conditions, highlighting the strong role of canopy cover in mitigating heat stress. Elevation and slope orientation also contributed to buffering but in less consistent ways. On south-facing slopes, contrasts between high and low elevations became more pronounced with rising heat, whereas north-facing slopes showed weaker or declining differences. At high elevations, slope aspect exerted only modest influence on maximum temperatures. Overall, Q5 underscored that buffering responses are not uniform across the landscape but differ in strength and mechanism depending on the environmental gradient considered. Vegetation provided the strongest and most consistent thermal buffering, while topographic contrasts offered more conditional effects that sometimes weakened under extremes (Fierke et al. submitted-b).

Viewed together, the answers to Q1-Q5 reveal an overarching pattern: the areas where macroclimatic datasets disagree most are often the locations where fine-scale vegetation and terrain effects exert a strong control on microclimate, and where buffering potential is highest during extremes. This alignment suggests that improving ecological assessments in mountain forests requires not only better macroclimate data, but also explicit integration of microclimatic processes. Moreover, the seasonal shifts in predictor importance (Q4) and the amplification of buffering with rising heat (Q5) indicate that spatial patterns alone are insufficient, as temporal dynamics are equally critical. This underscores the need for extensive data on dynamical changes to improve climate models that integrate vegetation.

The synthesis therefore underscores three central conclusions.

First, macroclimatic data in complex terrain carry systematic uncertainties that affect ecological forecasts, making dataset choice a non-trivial decision for modelling forest responses to climate change. This is particularly important in transitional environments such as treelines, forest edges, and canopy gaps, which represent distinct types of transitions but share the characteristic of concentrating key ecological processes including species range shifts, regeneration dynamics, and disturbance responses.

Second, thermal buffering is not a static property but one that intensifies under extreme heat, suggesting that the capacity of mountain forests to act as microrefugia may be greater during the most critical periods, but only in specific landscape settings.

Together, these conclusions provide an integrated response to the overarching thesis aim: understanding forest ecosystem responses in mountain regions requires bridging macro- and microclimatic perspectives, focusing on where the uncertainties in climate representation overlap with the strongest local controls on temperature and moisture. By linking Q1-Q5 into a unified perspective, this thesis shows that such integration is essential for advancing both ecological theory and applied conservation planning in the face of climate change.

7.2 From macroclimatic uncertainty to microclimatic evidence: Implications for forest dynamics and management in northern Patagonia

The following section appears as originally written in the book chapter ***Climate variations across landscape gradients of northern Patagonian Andean forests: lessons from high-resolution climate datasets and microclimatic records***, submitted to Springer Nature as part of the edited volume *Ecology, Structure and Dynamics of the Central Patagonian Andean Forest and Derivations for Ecosystem-Based Management*. It outlines how microclimatic processes influence forest dynamics in northern Patagonia and what this implies for ecosystem-based management (Fierke et al. submitted-a). For smoother integration, the opening paragraph of the original chapter has been omitted.

In northern Patagonia, ecological processes such as fire dynamics, post-disturbance regeneration, and long-term vegetation change are closely related to climatic conditions. The region’s complex topography and vegetation mosaic create distinct thermal and moisture conditions that influence the probability, behaviour, and ecological impact of wildfires (Barberá et al. 2025). While large-scale climatic drivers like El Niño-Southern Oscillation (ENSO), the Antarctic Oscillation (AAO), and interannual climatic variability set the stage for fire-prone periods (Kitzberger and Veblen 1997; Holz and Veblen 2011; Holz et al. 2012; Barberá et al. 2023), local vegetation structure and site conditions modulate flammability and fire severity. For example, continuous canopy cover and productive forest types are often associated with

cooler and moister understorey conditions, which reduce fuel flammability and can reduce fire occurrence and frequency (Mermoz et al. 2005; Blackhall et al. 2017; Barberá et al. 2023; Tiribelli et al. 2024). Following disturbance, microclimatic conditions such as light availability, temperature, and moisture regimes strongly affect plant development and phenological processes (Paritsis et al. 2006). Canopy cover, in particular, influences the thermal environment that determine regeneration success (Paritsis et al. 2015; Tepley et al. 2018). Over time, these fine-scale drivers contribute to divergent vegetation trajectories: repeated fires, combined with warmer, drier microclimates, can favour a shift from forest to shrub-dominated systems, especially where regeneration is limited by post-disturbance stress (Paritsis et al. 2015; Kitzberger et al. 2016). With ongoing climate change, fire activity in northern Patagonia is expected to intensify (Kitzberger et al. 2022; Barberá et al. 2025), further reinforcing these feedbacks and accelerating vegetation transitions (Landesmann et al. 2021).

Recognizing the ecological importance of microclimatic variation also opens up opportunities for proactive forest and ecosystem management (Kemppinen et al. 2024). Rather than viewing microclimate as a static setting, it can be actively considered and shaped to buffer ecosystems against climate change impacts (Hylander et al. 2022). In forested landscapes with high topographic heterogeneity such as northern Patagonia, this could include the identification and protection of areas that function as microclimatic refugia, which are cooler and moister sites that offer stable conditions for regeneration and species persistence (Scheffers et al. 2014; Keppel et al. 2015; Suggitt et al. 2018; Wolf et al. 2021). Forest cover plays a central role in creating such refugia, with tall, mature forest stands enhancing local thermal buffering (Fierke et al. submitted-b; Frey et al. 2016b) and moisture buffering (Davis et al. 2019; Simon et al. 2024). Management strategies that retain canopy cover (e.g., continuous cover forestry) and minimize fragmentation, particularly in habitats that harbour cold-adapted species, can help preserve these beneficial microclimates in a warmer and drier future of northern Patagonia. Moreover, recent work in European beech forests suggests that promoting landscape-scale heterogeneity through a mix of managed and unmanaged forest types, rather than focusing solely on structural complexity within stands, can enhance microclimatic diversity and support biodiversity and resilience goals (Menge et al. 2023). While these findings offer relevant insights, their applicability to Patagonian *Nothofagus* forests remains uncertain, particularly given the potential influence of bamboo-dominated understories in canopy gaps, which may affect both microclimate and fire risk. Further studies are needed to assess these dynamics in the southern Andes. Nevertheless, existing studies from Patagonia demonstrate that spatially variable canopy retention can recreate diverse microenvironments within harvested *N. pumilio* stands, supporting both regeneration and resilience under changing climatic conditions (Martínez Pastur et al. 2011; Martínez Pastur et al. 2014). Beyond forested habitats, non-forested features may also function as microrefugia; for instance, rock outcrops on south-

facing slopes were found to harbour cooler conditions and cold-adapted species in northern Patagonia (Speziale and Ezcurra 2015). Taken together, these examples show that managing for microclimatic diversity through structural retention, landscape heterogeneity, and the protection of natural refugia offers a tangible yet often overlooked opportunity to foster resilience in the forests of northern Patagonia.

Beyond these long-term benefits, microclimatic data also offer practical value for operational fire management. Local measurements of temperature and humidity within forests can improve the spatial resolution and predictive power of fire danger indices, especially in structurally diverse or topographically complex areas. This is particularly relevant for components such as the fuel moisture codes of the Canadian Forest Fire Weather Index (FWI) system, which estimate the moisture content of surface and subsurface fuels (Wagner 1987) and are highly sensitive to localized microclimatic conditions. Thus, incorporating microclimate into fire monitoring systems may help anticipate ignition risk, refine suppression strategies, and identify areas where natural fire breaks or refugia could be preserved or enhanced (Just et al. 2016). In this way, microclimatic information becomes not only a conservation asset but a tool for early warning and more targeted wildfire control.

The recognition that microclimates can be actively shaped through management not only offers practical tools for adaptation but also points to a broader need: to better integrate microclimatic knowledge into both science and practice. This chapter has shown that microclimatic insights are essential for understanding ecological processes in northern Patagonia, and for potentially influencing them to adapt forest management to the realities of climate change. However, microclimate research in the region is still in its early stages. Data availability, methodological consistency, and modelling capacity remain limited. Against this background, five key lessons emerge from this chapter that can guide both forest management and future research efforts.

(1) Macroclimatic datasets have value but also limitations: While widely used datasets such as CHELSA and WorldClim capture general climatic gradients, they can diverge in absolute values, especially for precipitation, and often miss fine-scale variation critical for ecological applications.

(2) Microclimatic variability is ecologically meaningful: Forest microclimates in northern Patagonia show strong and consistent patterns across elevation, vegetation types, and slope orientation, shaping exposure to thermal extremes.

(3) Vegetation height is a key driver of thermal buffering: High-growing *N. pumilio* forests consistently reduced daytime temperature maxima and moderated diurnal fluctuations compared to adjacent *N. antarctica* shrublands, particularly those of low stature (<1 m) with

open vegetation. These results suggest that taller, more vertically developed vegetation formations provide stronger microclimatic buffering than shorter shrublands.

(4) Microclimate responds dynamically to climate forcing: The strength of microclimatic contrasts increases under hot conditions, underlining their importance for understanding and managing climate extremes.

(5) Modelling microclimate at landscape scale is feasible: In northern Patagonia, spatial models that combine high resolution observations with satellite-based predictors such as local macroclimatic data including air temperature and relative humidity, vegetation indices like NDMI and FAPAR, and topographic variables including distance to sink and solar radiation have successfully estimated microclimatic conditions across different vertical levels and seasons. However, to fully unlock the ecological and management value of such models, two types of complementary data are needed: first, improved predictor variables to enhance model performance, such as vegetation structure derived from airborne laser scanning or other high-resolution remote sensing sources; and second, ecological target variables such as species occurrences and fuel moisture to ensure that model outputs are relevant for biodiversity assessments and management planning.

7.3 Conceptual and methodological contributions

This thesis contributes to the conceptual integration of landscape ecology and microclimatology by showing how heterogeneity and scale shape the climatic conditions organisms experience in mountain forests, and how uncertainty affects their measurement and representation. A first contribution lies in highlighting the role of uncertainty as an integral part of bioclimatology. Differences between climate datasets were not only a technical obstacle but reflected the difficulty of representing processes in complex terrain (Fierke et al. 2024). Recognizing uncertainty in this way aligns with landscape ecology's emphasis on heterogeneity and underlines the need to treat data limitations and inherent variability as part of ecological inference rather than as external to it. While one could argue that all uncertainty ultimately reflects limitations of data and knowledge, ecological complexity ensures that some degree of uncertainty will always remain, even with improved datasets and models (Beckage et al. 2011). Importantly, acknowledging uncertainty in this way does not exclude continued work to fill uncertainty gaps through better data and models (Simmonds et al. 2024), but situates these efforts within a framework that sees uncertainty as intrinsic to ecological systems. For conservation planning and resource management, this implies that uncertainty should be treated not only as a challenge to be reduced, but also as a condition to be actively managed (Burgman et al. 2005). Strategies that emphasize adaptive management, scenario planning, and resilience-building are particularly valuable in systems where uncertainty cannot be eliminated (Peterson et al. 2003; Berkes 2007; Williams 2011). A second contribution

concerns the multi-scalar nature of microclimatic variation. By considering both horizontal differences across vegetation and topography as well as vertical differences above and below ground, the work illustrates that scale is not only spatial extent but also vertical layering. These vertical contrasts, sometimes exceeding 10 K, demonstrate that the scale at which organisms interact with their environment differs markedly from the scales usually represented in macroclimatic products (Fierke et al. 2025). This perspective supports findings from landscape ecology, where analyses that neglect variation along vertical structures of landscape elements are often less convincing and harder to relate to ecological processes (Liding et al. 2008; Turner and Gardner 2015). Incorporating such vertical patterns into multi-dimensional analyses therefore strengthens the ecological relevance of both landscape and microclimate research. A third conceptual contribution is the recognition that buffering is a dynamic and context-dependent process. Across gradients, buffering strength varied with external thermal load and local conditions, showing that it cannot be assumed as a static property of vegetation or terrain (Fierke et al. submitted-b). This provides a more nuanced view of how fine-scale landscape features interact with broader climatic forcing, emphasizing both the influence of spatial heterogeneity on abiotic processes and the role of spatio-temporal interactions (Risser et al. 1984). Taken together, these conceptual contributions refine existing ideas in landscape ecology and microclimatology by showing how uncertainty, vertical and horizontal scale, and context-dependence manifest in empirical data from northern Patagonia.

Methodologically, this thesis advances approaches for analysing microclimatic variability in mountainous landscapes where data are sparse and conditions highly heterogeneous. A first contribution lies in the systematic comparison and validation of gridded climate datasets. By assessing two widely used high-resolution products against local station records, the work demonstrates how a comparative evaluation of datasets can be used to identify inconsistent variables while also exposing systematic uncertainties, particularly in precipitation (Fierke et al. 2024). This approach shows that drawing reliable conclusions requires not only selecting appropriate datasets but also acknowledging the degree of confidence that can be placed in them (Bobrowski et al. 2021; Abdulwahab et al. 2022; Hemp and Hemp 2024). A second contribution is the integration of ground-based loggers with geospatial data and statistical modelling to link macroclimate and microclimate across scales. The use of random forest regression to identify predictor importance, combined with the downscaling of reanalysis data, provided a framework for reconstructing spatial and temporal microclimate patterns beyond the short time span of logger deployments (Fierke et al. 2025). This combination illustrates how field-based observations can be leveraged to bridge scales, producing microclimatic information at both local and regional levels (Zellweger et al. 2019a; Zignol et al. 2023). A third contribution arises from the empirical design of paired contrasts across vegetation, elevation, and slope orientation. Deploying loggers in replicate pairs enabled the isolation of specific

environmental effects on near-surface temperature, while the inclusion of multiple thermal metrics such as warming and cooling rates and frost occurrence extended the analysis beyond mean conditions (Fierke et al. submitted-b). This design made it possible to capture both the magnitude and the dynamics of buffering, and to do so in a way that is replicable and transferable to other landscapes. Taken together, these methodological contributions illustrate how diverse data sources, machine learning techniques, and carefully designed field comparisons can be combined to reveal fine-scale climatic variability in mountain forests. They provide a foundation for future work that seeks to integrate microclimatic processes into ecological modelling and climate impact assessments, particularly in regions like northern Patagonia where long-term and high-resolution measurements remain limited. At the same time, the challenges of scaling up microclimate monitoring are increasingly recognized, including issues of spatial representativeness, sensor choice, and financial feasibility (Lembrechts et al. 2021). Addressing these challenges will be critical for embedding fine-scale climatic insights more systematically into regional and global observation networks.

7.4 Methodological reflections, limitations, and outlook

Several methodological limitations need to be acknowledged when interpreting the findings of this thesis. First, the spatial coverage of the logger network was unavoidably limited. Although the paired design across vegetation, elevation, and slope contrasts allowed for direct comparisons, measurements were restricted to selected valleys and to binary contrasts. This design captured distinct differences between buffered and exposed sites but could not fully represent the gradual transitions (Meeussen et al. 2021; Máliš et al. 2023) and edge effects (Baker et al. 2016; Hofmeister et al. 2019) that are common in mountain landscapes and of considerable ecological importance. The restriction to a relatively small number of sites also limits the extent to which results can be generalized across the wider Andean region. Second, the temporal scope of the logger deployments was confined to one (Study 3) or two (Study 2) years. This enabled the analysis of seasonal patterns and several extreme summer events but does not cover interannual variability or the influence of large-scale climate modes such as ENSO or the Southern Annular Mode (Grimm et al. 2000; Kayano and Andreoli 2007; Garreaud et al. 2013). Downscaling ERA5 data provided a longer baseline for comparison, yet reanalysis products and statistical downscaling cannot fully substitute for multi-year in-situ observations, particularly in complex terrain. Finally, methodological simplifications and uncertainties must be considered. Random forest models proved effective for identifying complex and nonlinear relationships but remain sensitive to overfitting when based on relatively few logger points (Schonlau and Zou 2020). In Study 2, uncertainties therefore remain both in the empirical data and in the modelling process. From an ecological point of view, it should also be noted that the scope of this dissertation is restricted to analysing climatic and microclimatic variability itself. The ecological implications of these patterns, such as how plants or other organisms respond

to macroclimatic and microclimatic changes, are beyond the scope of this work and require further research. For example, Reiter et al. (2024), Reiter et al. (2025a), and Reiter et al. (2025b) investigate the effects of climate on tree species within the Río Puelo watershed using dendrochronological approaches, illustrating how species-specific responses can only be assessed with additional ecological and physiological information. In a similar way, recent studies by Joelson et al. (2025b) and Joelson et al. (2025a) provide detailed insights into understory species composition in the region. A priority for future research would be to integrate such species-level datasets with fine-scale microclimatic measurements to better understand how near-ground thermal and moisture conditions shape understory biodiversity within the Río Puelo watershed.

Taken together, these methodological reflections clarify the boundaries within which the research questions (Q1–Q5) were addressed. The macroclimatic comparisons (Q1, Q2) provide robust insights into dataset differences, yet these differences unavoidably introduce uncertainty into ecological predictions for forest ecosystems in the Río Puelo watershed. The microclimatic modelling (Q3, Q4) identifies key predictors with strong explanatory power, but further testing across longer periods and more diverse conditions is needed to confirm their generality. The buffering analysis (Q5) demonstrates clear, temperature-dependent buffering effects, though its reliance on binary contrasts and a single warm season limits its transferability. These considerations point directly toward the next steps: expanding temporal and spatial coverage of macro- and microclimatic measurements, integrating mechanistic understanding into predictive frameworks, and developing approaches that bridge macro- and microclimatic processes not only analytically but also in operational modelling. Addressing these priorities would enhance the capacity to forecast forest ecosystem responses to climate change with greater accuracy and ecological realism.

References

Aalto J, Riihimäki H, Meineri E, Hylander K, Luoto M (2017) Revealing topoclimatic heterogeneity using meteorological station data. Intl Journal of Climatology 37:544–556. https://doi.org/10.1002/joc.5020

Aalto J, Tyystjärvi V, Niittynen P, Kemppinen J, Rissanen T, Gregow H, Luoto M (2022) Microclimate temperature variations from boreal forests to the tundra. Agricultural and Forest Meteorology 323:109037. https://doi.org/10.1016/j.agrformet.2022.109037

Abdulwahab UA, Hammill E, Hawkins CP (2022) Choice of climate data affects the performance and interpretation of species distribution models. Ecological Modelling 471:110042. https://doi.org/10.1016/j.ecolmodel.2022.110042

Abu-Hamdeh NH, Reeder RC (2000) Soil Thermal Conductivity Effects of Density, Moisture, Salt Concentration, and Organic Matter. Soil Science Soc of Amer J 64:1285–1290. https://doi.org/10.2136/sssaj2000.6441285x

Ackerly DD, Loarie SR, Cornwell WK, Weiss SB, Hamilton H, Branciforte R, Kraft NJB (2010) The geography of climate change: implications for conservation biogeography. Diversity and Distributions 16:476–487. https://doi.org/10.1111/j.1472-4642.2010.00654.x

Adler C, Wester P, Bhatt I, Huggel C, Insarov GE, Morecroft MD, Muccione V, Prakash A (2022) Cross-Chapter Paper 5: Mountains. In: Pörtner HO, Roberts DC, Tignor M, Poloczanska ES, Mintenbeck K, Alegría A, Craig M, Langsdorf S, Löschke S, Möller V, Okem A, Rama B (eds) Climate Change 2022: Impacts, Adaptation and Vulnerability. Contribution of Working Group II to the Sixth Assessment Report of the Intergovernmental Panel on Climate Change. Cambridge University Press, Cambridge, UK and New York, NY, USA, pp 2273–2318. https://doi.org/10.1017/9781009325844.022

Adler C, Wester P, Bhatt I, Huggel C, Insarov GE, Morecroft MD, Muccione V, Prakash A (2023) Cross-Chapter Paper 5: Mountains. In: Pörtner HO, Roberts DC, Tignor M, Poloczanska ES, Mintenbeck K, Alegría A, Craig M, Langsdorf S, Löschke S, Möller V, Okem A, Rama B (eds) Climate Change 2022: Impacts, Adaptation and Vulnerability: Contribution of Working Group II to the Sixth Assessment Report of the Intergovernmental Panel on Climate Change. Cambridge University Press, Cambridge, UK and New York, NY, USA, pp 2273–2318. https://doi.org/10.1017/9781009325844.022

Agnew JA (2011) Space and Place. In: Agnew J, Livingstone DN (eds) The SAGE Handbook of Geographical Knowledge. SAGE Publications Ltd, 1 Oliver's Yard, 55 City Road, London EC1Y 1SP United Kingdom, pp 316–330. https://doi.org/10.4135/9781446201091.n24

Agosta EA, Hurtado SI, Martin PB (2020) “Easterlies”-induced precipitation in eastern Patagonia: Seasonal influences of ENSO'S FLAVOURS and SAM. Int J Climatol 40:5464–5484. https://doi.org/10.1002/joc.6529

Aguayo R, León-Muñoz J, Vargas-Baecheler J, Montecinos A, Garreaud R, Urbina M, Soto D, Iriarte JL (2019) The glass half-empty: climate change drives lower freshwater input in the coastal system of the Chilean Northern Patagonia. Climatic Change 155:417–435. https://doi.org/10.1007/s10584-019-02495-6

Albrich K, Rammer W, Seidl R (2020) Climate change causes critical transitions and irreversible alterations of mountain forests. Glob Chang Biol 26:4013–4027. https://doi.org/10.1111/gcb.15118

Alexander JM, Diez JM, Levine JM (2015) Novel competitors shape species' responses to climate change. Nature 525:515–518. https://doi.org/10.1038/nature14952

Allen CD, Macalady AK, Chenchouni H, Bachelet D, McDowell N, Vennetier M, Kitzberger T, Rigling A, Breshears DD, Hogg EH, Gonzalez P, Fensham R, Zhang Z, Castro J, Demidova N, Lim J-H, Allard G, Running SW, Semerci A, Cobb N (2010) A global overview of drought and heat-induced tree mortality reveals emerging climate change risks for forests. Forest Ecology and Management 259:660–684. https://doi.org/10.1016/j.foreco.2009.09.001

Allen TF, Starr TB (1988) Hierarchy: Perspectives for ecological complexity, 2nd edn. Univ. of Chicago Press, Chicago, Ill. u.a.

Allen CR, Angeler DG, Cumming GS, Folke C, Twidwell D, Uden DR (2016) Quantifying spatial resilience. Journal of Applied Ecology 53:625–635. https://doi.org/10.1111/1365-2664.12634

Amigo J, Rodríguez-Guitián MA (2011) Bioclimatic and phytosociological diagnosis of the species of the Nothofagus genus (Nothofagaceae) in South America. IJGR 1:1–20. https://doi.org/10.5616/ijgr110001

Analog Devices, Inc., USA 2023 DS1923 iButton Hygrochron temperature/ humidity logger with 8KB data-log memory. https://www.analog.com/en/products/ds1923.html#product-overview

Anderegg WRL, Trugman AT, Badgley G, Konings AG, Shaw J (2020) Divergent forest sensitivity to repeated extreme droughts. Nat. Clim. Chang. 10:1091–1095. https://doi.org/10.1038/s41558-020-00919-1

Andrade C, Contente J (2020) Climate change projections for the Worldwide Bioclimatic Classification System in the Iberian Peninsula until 2070. Int J Climatol 40:5863–5886. https://doi.org/10.1002/joc.6553

Andrian LG, Osman M, Vera CS (2024) The role of the Indian Ocean Dipole in modulating the austral spring ENSO teleconnection to the Southern Hemisphere. Weather Clim. Dynam. 5:1505–1522. https://doi.org/10.5194/wcd-5-1505-2024

Aschero V, Srur AM, Guerrido C, Villalba R (2022) Contrasting climate influences on Nothofagus pumilio establishment along elevational gradients. Plant Ecol 223:369–380. https://doi.org/10.1007/s11258-021-01211-8

Ashcroft MB (2010) Identifying refugia from climate change. J Biogeogr 37:1407–1413. https://doi.org/10.1111/j.1365-2699.2010.02300.x

Ashcroft MB, Gollan JR (2012) Fine-resolution (25 m) topoclimatic grids of near-surface (5 cm) extreme temperatures and humidities across various habitats in a large (200 × 300 km) and diverse region. Intl Journal of Climatology 32:2134–2148. https://doi.org/10.1002/joc.2428

Atkins JW, Shiklomanov A, Mathes KC, Bond-Lamberty B, Gough CM (2023) Effects of forest structural and compositional change on forest microclimates across a gradient of disturbance severity. Agricultural and Forest Meteorology 339:109566. https://doi.org/10.1016/j.agrformet.2023.109566

Austin M (2002) Spatial prediction of species distribution: an interface between ecological theory and statistical modelling. Ecological Modelling 157:101–118. https://doi.org/10.1016/S0304-3800(02)00205-3

Baker TP, Jordan GJ, Baker SC (2016) Microclimatic edge effects in a recently harvested forest: Do remnant forest patches create the same impact as large forest areas? Forest Ecology and Management 365:128–136. https://doi.org/10.1016/j.foreco.2016.01.022

Barberá I, Paritsis J, Ammassari L, Morales JM, Kitzberger T (2023) Microclimate and species composition shape the contribution of fuel moisture to positive fire-vegetation feedbacks. Agricultural and Forest Meteorology 330:109289. https://doi.org/10.1016/j.agrformet.2022.109289

Barberá I, Cingolani AM, Tiribelli F, Mermoz MA, Morales JM, Kitzberger T (2025) Biotic and physical drivers of fire in northwestern Patagonia. fire ecol 21. https://doi.org/10.1186/s42408-025-00353-8

Barrueto AK, Merz J, Hodel E, Eckert S (2018) The suitability of Macadamia and Juglans for cultivation in Nepal: an assessment based on spatial probability modelling using climate

scenarios and in situ data. Reg Environ Change 18:859–871. https://doi.org/10.1007/s10113-017-1225-2

Barry R, Blanken P (2016) Microclimate and Local Climate. Cambridge University Press. https://doi.org/10.1017/CBO9781316535981

Barry RG (2008a) Mountain weather and climate, 3rd edn. Cambridge Univ. Press, Cambridge

Barry RG (2008b) Mountain Weather and Climate Third Edition. Cambridge University Press, Cambridge. https://doi.org/10.1017/CBO9780511754753

Bartoń K (2025) MuMIn: Multi-Model Inference. https://cran.r-project.org/web/packages/MuMIn/MuMIn.pdf. Accessed 9 July 2025

Bastian O, Steinhardt U (eds) (2002) Development and Perspectives of Landscape Ecology. Springer Netherlands, Dordrecht. https://doi.org/10.1007/978-94-017-1237-8

Bebi P, Seidl R, Motta R, Fuhr M, Firm D, Krumm F, Conedera M, Ginzler C, Wohlgemuth T, Kulakowski D (2017) Changes of forest cover and disturbance regimes in the mountain forests of the Alps. Forest Ecology and Management 388:43–56. https://doi.org/10.1016/j.foreco.2016.10.028

Beck HE, Wood EF, McVicar TR, Zambrano-Bigiarini M, Alvarez-Garreton C, Baez-Villanueva OM, Sheffield J, Karger DN (2020) Bias Correction of Global High-Resolution Precipitation Climatologies Using Streamflow Observations from 9372 Catchments. Journal of Climate 33:1299–1315. https://doi.org/10.1175/JCLI-D-19-0332.1

Beckage B, Gross LJ, Kauffman S (2011) The limits to prediction in ecological systems. Ecosphere 2:art125. https://doi.org/10.1890/ES11-00211.1

Berkes F (2007) Understanding uncertainty and reducing vulnerability: lessons from resilience thinking. Nat Hazards 41:283–295. https://doi.org/10.1007/s11069-006-9036-7

Beugnon R, Le Guyader N, Milcu A, Lenoir J, Puissant J, Morin X, Hättenschwiler S (2024) Microclimate modulation: An overlooked mechanism influencing the impact of plant diversity on ecosystem functioning. Glob Chang Biol 30:e17214. https://doi.org/10.1111/gcb.17214

Billings WD, Golley F, Lange OL, Olson JS, Remmert H, Turner MG (1987) Landscape Heterogeneity and Disturbance, vol 64. Springer New York, New York, NY. https://doi.org/10.1007/978-1-4612-4742-5

Bivand R, Keitt T, Rowlingson B (2023) rgdal: Bindings for the 'Geospatial' Data Abstraction Library: R package version 1.6-7. https://CRAN.R-project.org/package=rgdal

Blackhall M, Raffaele E, Paritsis J, Tiribelli F, Morales JM, Kitzberger T, Gowda JH, Veblen TT (2017) Effects of biological legacies and herbivory on fuels and flammability traits: A long-term experimental study of alternative stable states. Journal of Ecology 105:1309–1322. https://doi.org/10.1111/1365-2745.12796

Blois S de, Domon G, Bouchard A (2002) Landscape issues in plant ecology. Ecography 25:244–256. https://doi.org/10.1034/j.1600-0587.2002.250212.x

Bobrowski M, Schickhoff U (2017) Why input matters: Selection of climate data sets for modelling the potential distribution of a treeline species in the Himalayan region. Ecological Modelling 359:92–102. https://doi.org/10.1016/j.ecolmodel.2017.05.021

Bobrowski M, Weidinger J, Schickhoff U (2021) Is New Always Better? Frontiers in Global Climate Datasets for Modeling Treeline Species in the Himalayas. Atmosphere 12:543. https://doi.org/10.3390/atmos12050543

Box GEP (1966) Use and abuse of regression. Technometrics 8:625–629

Bramer I, Anderson BJ, Bennie J, Bladon AJ, Frenne P de, Hemming D, Hill RA, Kearney MR, Körner C, Korstjens AH, Lenoir J, Maclean IM, Marsh CD, Morecroft MD, Ohlemüller R, Slater HD, Suggitt AJ, Zellweger F, Gillingham PK (2018) Advances in Monitoring and Modelling Climate at Ecologically Relevant Scales. In: Next Generation Biomonitoring: Part 1, vol 58. Elsevier, pp 101–161. https://doi.org/10.1016/bs.aecr.2017.12.005

Breiman L (2001) Random Forests. Machine Learning 45:5–32. https://doi.org/10.1023/A:1010933404324

Bremer S, Wardekker A, Dessai S, Sobolowski S, Slaattelid R, van der Sluijs J (2019) Toward a multi-faceted conception of co-production of climate services. Climate Services 13:42–50. https://doi.org/10.1016/j.cliser.2019.01.003

Brenning A, Bangs D, Becker M, Schratz P, Polakowski F (2022) RSAGA: SAGA Geoprocessing and Terrain Analysis. https://doi.org/10.32614/CRAN.package.RSAGA

Briscoe NJ, Morris SD, Mathewson PD, Buckley LB, Jusup M, Levy O, Maclean IMD, Pincebourde S, Riddell EA, Roberts JA, Schouten R, Sears MW, Kearney MR (2023) Mechanistic forecasts of species responses to climate change: The promise of biophysical ecology. Glob Chang Biol 29:1451–1470. https://doi.org/10.1111/gcb.16557

Brun P, Zimmermann NE, Hari C, Pellissier L, Karger DN (2022) CHELSA-BIOCLIM+ A novel set of global climate-related predictors at kilometre-resolution. https://doi.org/10.16904/ENVIDAT.332

Buduba C, La Manna L, Irisarri JA (2020) El suelo y el bosque en la Región Andino Patagónica. In: Imbellone PA, Barbosa OA (eds) Libro Suelos y Vulcanismo, Argentina. Asociación Argentina de la Ciencia del Suelo, pp 361–390

Burgman MA, Lindenmayer DB, Elith J (2005) MANAGING LANDSCAPES FOR CONSERVATION UNDER UNCERTAINTY. Ecology 86:2007–2017. https://doi.org/10.1890/04-0906

Burton PJ, Jentsch A, Walker LR (2020) The Ecology of Disturbance Interactions. BioScience 70:854–870. https://doi.org/10.1093/biosci/biaa088

Cabral JS, Valente L, Hartig F (2017) Mechanistic simulation models in macroecology and biogeography: state-of-art and prospects. Ecography 40:267–280. https://doi.org/10.1111/ecog.02480

Cagnacci J, Estravis-Barcala M, Lia MV, Martínez-Meier A, Gonzalez Polo M, Arana MV (2020) The impact of different natural environments on the regeneration dynamics of two Nothofagus species across elevation in the southern Andes. Forest Ecology and Management 464:118034. https://doi.org/10.1016/j.foreco.2020.118034

Cai W, McPhaden MJ, Grimm AM, Rodrigues RR, Taschetto AS, Garreaud RD, Dewitte B, Poveda G, Ham Y-G, Santoso A, Ng B, Anderson W, Wang G, Geng T, Jo H-S, Marengo JA, Alves LM, Osman M, Li S, Wu L, Karamperidou C, Takahashi K, Vera C (2020) Climate impacts of the El Niño–Southern Oscillation on South America. Nat Rev Earth Environ 1:215–231. https://doi.org/10.1038/s43017-020-0040-3

Carnicer J, Vives-Ingla M, Blanquer L, Méndez-Camps X, Rosell C, Sabaté S, Gutiérrez E, Sauras T, Peñuelas J, Barbeta A (2021) Forest resilience to global warming is strongly modulated by local-scale topographic, microclimatic and biotic conditions. Journal of Ecology 109:3322–3339. https://doi.org/10.1111/1365-2745.13752

Caselli M, Urretavizcaya MF, Loguercio GÁ, Defossé GE (2019) Light and Moisture Conditions Suitable for Establishing Andean Cypress and Coihue Beech Seedlings in Patagonia: A Nursery Approach. Forest Science 65:27–39. https://doi.org/10.1093/forsci/fxy032

Chen J, Saunders SC, Crow TR, Naiman RJ, Brosofske KD, Mroz GD, Brookshire BL, Franklin JF (1999) Microclimate in Forest Ecosystem and Landscape Ecology. BioScience 49:288–297. https://doi.org/10.2307/1313612

CIEFAP-MAyDS (2016) Actualización de la Clasificación de Tipos Forestales y Cobertura del Suelo de la Región Bosque Andino Patagónico: Informe Final. https://drive.google.com/open?id=0BxfNQUtfxxeaUHNCQm9lYmk5RnM

Collazo S, Suli S, Zaninelli PG, García-Herrera R, Barriopedro D, Garrido-Perez JM (2024) Influence of large-scale circulation and local feedbacks on extreme summer heat in Argentina in 2022/23. Commun Earth Environ 5. https://doi.org/10.1038/s43247-024-01386-8

Conant RT, Ryan MG, Ågren GI, Birge HE, Davidson EA, Eliasson PE, Evans SE, Frey SD, Giardina CP, Hopkins FM, Hyvönen R, Kirschbaum MUF, Lavallee JM, Leifeld J, Parton WJ, Megan Steinweg J, Wallenstein MD, Martin Wetterstedt JÅ, Bradford MA (2011) Temperature and soil organic matter decomposition rates - synthesis of current knowledge and a way forward. Glob Chang Biol 17:3392–3404. https://doi.org/10.1111/j.1365-2486.2011.02496.x

Condom T, Martínez R, Pabón JD, Costa F, Pineda L, Nieto JJ, López F, Villacis M (2020) Climatological and Hydrological Observations for the South American Andes: In situ Stations, Satellite, and Reanalysis Data Sets. Front. Earth Sci. 8. https://doi.org/10.3389/feart.2020.00092

Coop JD, Massatti RT, Schoettle AW (2010) Subalpine vegetation pattern three decades after stand-replacing fire: effects of landscape context and topography on plant community composition, tree regeneration, and diversity. J Vegetation Science 21:472–487. https://doi.org/10.1111/j.1654-1103.2009.01154.x

Copernicus Service Information (2022) Collection 300m LAI & FAPAR. https://land.copernicus.vgt.vito.be/geonetwork/srv/eng/catalog.search#/search

Coûteaux MM, Bottner P, Berg B (1995) Litter decomposition, climate and liter quality. Trends Ecol Evol 10:63–66. https://doi.org/10.1016/S0169-5347(00)88978-8

Crockett JL, Hurteau MD (2022) Post-fire early successional vegetation buffers surface microclimate and increases survival of planted conifer seedlings in the southwestern United States. Can. J. For. Res. 52:416–425. https://doi.org/10.1139/cjfr-2021-0221

Csölleová L, Kotrík M, Kupček D, Knopp V, Máliš F (2024) Post-harvest recovery of microclimate buffering and associated temporary xerophilization of vegetation in sub-continental oak forests. Forest Ecology and Management 572:122238. https://doi.org/10.1016/j.foreco.2024.122238

Cutini M, Flavio M, Giuliana B, Guido R, Jean-Paul T (2021) Bioclimatic pattern in a Mediterranean mountain area: assessment from a classification approach on a regional scale. Int J Biometeorol 65:1085–1097. https://doi.org/10.1007/s00484-021-02089-x

Dale MRT (2009) Spatial Pattern Analysis in Plant Ecology. Cambridge University Press. https://doi.org/10.1017/CBO9780511612589

Datta A, Schweiger O, Kühn I (2020) Origin of climatic data can determine the transferability of species distribution models. NB 59:61–76. https://doi.org/10.3897/neobiota.59.36299

Davis KT, Dobrowski SZ, Holden ZA, Higuera PE, Abatzoglou JT (2019) Microclimatic buffering in forests of the future: the role of local water balance. Ecography 42:1–11. https://doi.org/10.1111/ecog.03836

De Frenne P de, Rodríguez-Sánchez F, Coomes DA, Baeten L, Verstraeten G, Vellend M, Bernhardt-Römermann M, Brown CD, Brunet J, Cornelis J, Decocq GM, Dierschke H, Eriksson O, Gilliam FS, Hédl R, Heinken T, Hermy M, Hommel P, Jenkins MA, Kelly DL, Kirby KJ, Mitchell FJG, Naaf T, Newman M, Peterken G, Petrík P, Schultz J, Sonnier G, van Calster H, Waller DM, Walther G-R, White PS, Woods KD, Wulf M, Graae BJ, Verheyen K (2013) Microclimate moderates plant responses to macroclimate warming. Proc Natl Acad Sci U S A 110:18561–18565. https://doi.org/10.1073/pnas.1311190110

De Frenne P, Zellweger F, Rodríguez-Sánchez F, Scheffers BR, Hylander K, Luoto M, Vellend M, Verheyen K, Lenoir J (2019) Global buffering of temperatures under forest canopies. Nat Ecol Evol 3:744–749. https://doi.org/10.1038/s41559-019-0842-1

De Frenne P, Lenoir J, Luoto M, Scheffers BR, Zellweger F, Aalto J, Ashcroft MB, Christiansen DM, Decocq G, Pauw K de, Govaert S, Greiser C, Gril E, Hampe A, Jucker T, Klinges DH, Koelemeijer IA, Lembrechts JJ, Marrec R, Meeussen C, Ogée J, Tyystjärvi V, Vangansbeke P, Hylander K (2021) Forest microclimates and climate change: Importance, drivers and future research agenda. Glob Chang Biol 27:2279–2297. https://doi.org/10.1111/gcb.15569

Del Arco Aguilar MJ, Rodríguez Delgado O (2018) Vegetation of the Canary Islands, vol 16. Springer International Publishing, Cham. https://doi.org/10.1007/978-3-319-77255-4

Delcourt HR, Delcourt PA (1988) Quaternary landscape ecology: Relevant scales in space and time. Landsc Ecol 2:23–44. https://doi.org/10.1007/BF00138906

Denney DA, Jameel MI, Bemmels JB, Rochford ME, Anderson JT (2020) Small spaces, big impacts: contributions of micro-environmental variation to population persistence under climate change. AoB Plants 12:plaa005. https://doi.org/10.1093/aobpla/plaa005

Derguy MR, Martinuzzi S, Arturi M (2022) Bioclimatic changes in ecoregions of southern South America: Trends and projections based on Holdridge life zones. Austral Ecology 47:580–589. https://doi.org/10.1111/aec.13142

Díaz-Calafat J, Uria-Diez J, Brunet J, Frenne P de, Vangansbeke P, Felton A, Öckinger E, Cousins SA, Bauhus J, Ponette Q, Hedwall P-O (2023) From broadleaves to conifers: The effect of tree composition and density on understory microclimate across latitudes.

Agricultural and Forest Meteorology 341:109684. https://doi.org/10.1016/j.agrformet.2023.109684

Dobrowski SZ (2011) A climatic basis for microrefugia: the influence of terrain on climate. Glob Chang Biol 17:1022–1035. https://doi.org/10.1111/j.1365-2486.2010.02263.x

D'Odorico P, Fuentes JD, Pockman WT, Collins SL, He Y, Medeiros JS, DeWekker S, Litvak ME (2010) Positive feedback between microclimate and shrub encroachment in the northern Chihuahuan desert. Ecosphere 1:1–11. https://doi.org/10.1890/ES10-00073.1

D'Odorico P, He Y, Collins S, Wekker SFJ de, Engel V, Fuentes JD (2013) Vegetation–microclimate feedbacks in woodland–grassland ecotones. Global Ecol Biogeogr 22:364–379. https://doi.org/10.1111/geb.12000

Driscoll DA, Armenteras D, Bennett AF, Brotons L, Clarke MF, Doherty TS, Haslem A, Kelly LT, Sato CF, Sitters H, Aquilué N, Bell K, Chadid M, Duane A, Meza-Elizalde MC, Giljohann KM, González TM, Jambhekar R, Lazzari J, Morán-Ordóñez A, Wevill T (2021) How fire interacts with habitat loss and fragmentation. Biol Rev Camb Philos Soc 96:976–998. https://doi.org/10.1111/brv.12687

ECCC (2024) CMIP6 ensemble of daily predictor variables. https://climate-scenarios.canada.ca/?page=pred-cmip6#table-1. Accessed 15 April 2024

Eskuche U (1973) Estudios fitosociológicos en el norte de Patagonia I. Investigacion de algunos factores de ambiente en comunidades de bosque y de chaparral. phyto 1:64–113. https://doi.org/10.1127/phyto/1/1973/64

Espinosa del Alba C, Fernández-Pascual E, Jiménez-Alfaro B (2024) Microclimatic variation regulates seed germination phenology in alpine plant communities. Journal of Ecology 113:249–262. https://doi.org/10.1111/1365-2745.14461

Fadrique B, Báez S, Duque Á, Malizia A, Blundo C, Carilla J, Osinaga-Acosta O, Malizia L, Silman M, Farfán-Ríos W, Malhi Y, Young KR, Cuesta C F, Homeier J, Peralvo M, Pinto E, Jadan O, Aguirre N, Aguirre Z, Feeley KJ (2018) Widespread but heterogeneous responses of Andean forests to climate change. Nature 564:207–212. https://doi.org/10.1038/s41586-018-0715-9

Falkowski P, Scholes RJ, Boyle E, Canadell J, Canfield D, Elser J, Gruber N, Hibbard K, Högberg P, Linder S, Mackenzie FT, Moore B, Pedersen T, Rosenthal Y, Seitzinger S, Smetacek V, Steffen W (2000) The global carbon cycle: a test of our knowledge of earth as a system. Science 290:291–296. https://doi.org/10.1126/science.290.5490.291

Farr TG, Rosen PA, Caro E, Crippen R, Duren R, Hensley S, Kobrick M, Paller M, Rodriguez E, Roth L, Seal D, Shaffer S, Shimada J, Umland J, Werner M, Oskin M, Burbank D,

Alsdorf D (2007) The Shuttle Radar Topography Mission. Reviews of Geophysics 45. https://doi.org/10.1029/2005RG000183

Fei S, Desprez JM, Potter KM, Jo I, Knott JA, Oswalt CM (2017) Divergence of species responses to climate change. Sci Adv 3:e1603055. https://doi.org/10.1126/sciadv.1603055

Ferrier S, Harwood TD, Ware C, Hoskins AJ (2020) A globally applicable indicator of the capacity of terrestrial ecosystems to retain biological diversity under climate change: The bioclimatic ecosystem resilience index. Ecological Indicators 117:106554. https://doi.org/10.1016/j.ecolind.2020.106554

Fick SE, Hijmans RJ (2017a) WorldClim 2: new 1-km spatial resolution climate surfaces for global land areas. Int J Climatol 37:4302–4315

Fick SE, Hijmans RJ (2017b) WorldClim 2: new 1-km spatial resolution climate surfaces for global land areas. Intl Journal of Climatology 37:4302–4315. https://doi.org/10.1002/joc.5086

Fierke J, Simon A, Putzenlechner B, Neri Winter A, Gowda JH, Kappas M (submitted-a) Climate variations across landscape gradients of northern Patagonian Andean forests: lessons from high-resolution climate datasets and microclimatic records. In: Walentowski H, Kitzberger T, Kappas M, Zerbe S, Loguercio GA (eds) Ecology, Structure and Dynamics of the Central Patagonian Andean Forest and Derivations for Ecosystem-Based Management. Springer

Fierke J, Gowda JH, Díaz GM, Koal P, Walentowski H, Kappas M, Putzenlechner B (submitted-b) Vegetation structure and elevation provide stronger thermal buffering than slope orientation during summer heat in northern Patagonia

Fierke J, Joelson NZ, Loguercio GA, Putzenlechner B, Simon A, Wyss D, Kappas M, Walentowski H (2024) Assessing uncertainty in bioclimatic modelling: a comparison of two high-resolution climate datasets in northern Patagonia. Reg Environ Change 24. https://doi.org/10.1007/s10113-024-02278-5

Fierke J, Putzenlechner B, Simon A, Gowda JH, Reiter EJ, Walentowski H, Kappas M (2025) Modelling microclimatic variability in Andean forests of northern Patagonia. Int J Biometeorol 69:1279–1295. https://doi.org/10.1007/s00484-025-02891-x

Fogt RL, Marshall GJ (2020) The Southern Annular Mode: Variability, trends, and climate impacts across the Southern Hemisphere. WIREs Climate Change 11. https://doi.org/10.1002/wcc.652

Forman RTT (1995) Some general principles of landscape and regional ecology. Landsc Ecol 10:133–142. https://doi.org/10.1007/BF00133027

Forman RTT, Godron M (1986) Landscape ecology. Wiley, New York, NY

Forzieri G, Dakos V, McDowell NG, Ramdane A, Cescatti A (2022) Emerging signals of declining forest resilience under climate change. Nature 608:534–539. https://doi.org/10.1038/s41586-022-04959-9

Franklin J, Davis FW, Ikegami M, Syphard AD, Flint LE, Flint AL, Hannah L (2013) Modeling plant species distributions under future climates: how fine scale do climate projections need to be? Glob Chang Biol 19:473–483. https://doi.org/10.1111/gcb.12051

Frey SJK, Hadley AS, Betts MG (2016a) Microclimate predicts within-season distribution dynamics of montane forest birds. Diversity and Distributions 22:944–959. https://doi.org/10.1111/ddi.12456

Frey SJK, Hadley AS, Johnson SL, Schulze M, Jones JA, Betts MG (2016b) Spatial models reveal the microclimatic buffering capacity of old-growth forests. Sci Adv 2:e1501392. https://doi.org/10.1126/sciadv.1501392

Fuentes-Castillo T, Hernández HJ, Pliscoff P (2020) Hotspots and ecoregion vulnerability driven by climate change velocity in Southern South America. Reg Environ Change 20. https://doi.org/10.1007/s10113-020-01595-9

Garcia RA, Cabeza M, Rahbek C, Araújo MB (2014) Multiple dimensions of climate change and their implications for biodiversity. Science 344:1247579. https://doi.org/10.1126/science.1247579

Garreaud R, Lopez P, Minvielle M, Rojas M (2013) Large-Scale Control on the Patagonian Climate. Journal of Climate 26:215–230. https://doi.org/10.1175/JCLI-D-12-00001.1

Garreaud RD, Vuille M, Compagnucci R, Marengo J (2009) Present-day South American climate. Palaeogeography, Palaeoclimatology, Palaeoecology 281:180–195. https://doi.org/10.1016/j.palaeo.2007.10.032

Gateño F, Mendoza PA, Vásquez N, Lagos-Zúñiga M, Jiménez H, Jerez C, Vargas X, Rubio-Álvarez E, Montserrat S (2024) Screening CMIP6 models for Chile based on past performance and code genealogy. Climatic Change 177. https://doi.org/10.1007/s10584-024-03742-1

GBIF.org (2021) GBIF Occurrence Download: accessed between 2021/11/11 and 2021/11/13. N. dombeyi: https://doi.org/10.15468/dl.qakkqz; A. chilensis: https://doi.org/10.15468/dl.yhjxcu; N. antarctica: https://doi.org/10.15468/dl.7ku59f; N. pumilio: https://doi.org/10.15468/dl.hn4gbf

Geiger R, Aron RH, Todhunter P (2009) The climate near the ground, 7th edn. Rowman & Littlefield, Lanham, Md

Gowda JH, Kitzberger T, Premoli AC (2012) Landscape responses to a century of land use along the northern Patagonian forest-steppe transition. Plant Ecol 213:259–272. https://doi.org/10.1007/s11258-011-9972-5

Graae BJ, Vandvik V, Armbruster WS, Eiserhardt WL, Svenning J-C, Hylander K, Ehrlén J, Speed JD, Klanderud K, Bråthen KA, Milbau A, Opedal ØH, Alsos IG, Ejrnæs R, Bruun HH, Birks HJB, Westergaard KB, Birks HH, Lenoir J (2018) Stay or go – how topographic complexity influences alpine plant population and community responses to climate change. Perspectives in Plant Ecology, Evolution and Systematics 30:41–50. https://doi.org/10.1016/j.ppees.2017.09.008

Gregor K, Knoke T, Krause A, Reyer CPO, Lindeskog M, Papastefanou P, Smith B, Lansø A-S, Rammig A (2022) Trade-Offs for Climate-Smart Forestry in Europe Under Uncertain Future Climate. Earth's Future 10. https://doi.org/10.1029/2022EF002796

Greiser C, Hederová L, Vico G, Wild J, Macek M, Kopecký M (2024) Higher soil moisture increases microclimate temperature buffering in temperate broadleaf forests. Agricultural and Forest Meteorology 345:109828. https://doi.org/10.1016/j.agrformet.2023.109828

Grimm AM, Barros VR, Doyle ME (2000) Climate Variability in Southern South America Associated with El Niño and La Niña Events. Journal of Climate 13:35–58. https://doi.org/10.1175/1520-0442(2000)013<0035:CVISSA>2.0.CO;2

Haesen S, Lembrechts JJ, Frenne P de, Lenoir J, Aalto J, Ashcroft MB, Kopecký M, Luoto M, Maclean I, Nijs I, Niittynen P, van den Hoogen J, Arriga N, Brůna J, Buchmann N, Čiliak M, Collalti A, Lombaerde E de, Descombes P, Gharun M, Goded I, Govaert S, Greiser C, Grelle A, Gruening C, Hederová L, Hylander K, Kreyling J, Kruijt B, Macek M, Máliš F, Man M, Manca G, Matula R, Meeussen C, Merinero S, Minerbi S, Montagnani L, Muffler L, Ogaya R, Penuelas J, Plichta R, Portillo-Estrada M, Schmeddes J, Shekhar A, Spicher F, Ujházyová M, Vangansbeke P, Weigel R, Wild J, Zellweger F, Van Meerbeek K (2021) ForestTemp - Sub-canopy microclimate temperatures of European forests. Glob Chang Biol 27:6307–6319. https://doi.org/10.1111/gcb.15892

Hardwick SR, Toumi R, Pfeifer M, Turner EC, Nilus R, Ewers RM (2015) The relationship between leaf area index and microclimate in tropical forest and oil palm plantation: Forest disturbance drives changes in microclimate. Agricultural and Forest Meteorology 201:187–195. https://doi.org/10.1016/j.agrformet.2014.11.010

Hemp A, Hemp J (2024) Weather or not-Global climate databases: Reliable on tropical mountains? PLoS One 19:e0299363. https://doi.org/10.1371/journal.pone.0299363

Hersbach H, Bell B, Berrisford P, Hirahara S, Horányi A, Muñoz-Sabater J, Nicolas J, Peubey C, Radu R, Schepers D, Simmons A, Soci C, Abdalla S, Abellan X, Balsamo G, Bechtold P, Biavati G, Bidlot J, Bonavita M, Chiara G de, Dahlgren P, Dee D, Diamantakis M, Dragani R, Flemming J, Forbes R, Fuentes M, Geer A, Haimberger L, Healy S, Hogan RJ, Hólm E, Janisková M, Keeley S, Laloyaux P, Lopez P, Lupu C, Radnoti G, Rosnay P de, Rozum I, Vamborg F, Villaume S, Thépaut J-N (2020) The ERA5 global reanalysis. Quart J Royal Meteoro Soc 146:1999–2049. https://doi.org/10.1002/qj.3803

Hijmans RJ (2023) raster: Geographic Data Analysis and Modeling: R pacakage version 3.6-20. https://CRAN.R-project.org/package=raster

Hijmans RJ, Bivand R, Dyba K, Pebesma E, Sumner MD (2024) terra: Spatial Data Analysis. https://doi.org/10.32614/CRAN.package.terra

Hill EM, Cannon JB, Ex S, Ocheltree TW, Redmond MD (2024) Canopy-mediated microclimate refugia do not match narrow regeneration niches in a managed dry conifer forest. Forest Ecology and Management 553:121566. https://doi.org/10.1016/j.foreco.2023.121566

Hofmeister J, Hošek J, Brabec M, Střalková R, Mýlová P, Bouda M, Pettit JL, Rydval M, Svoboda M (2019) Microclimate edge effect in small fragments of temperate forests in the context of climate change. Forest Ecology and Management 448:48–56. https://doi.org/10.1016/j.foreco.2019.05.069

Hollister J, Shah T, Nowosad J, Robitaille AL, Beck MW, Johnson M (2023) elevatr: Access Elevation Data from Various APIs. https://doi.org/10.32614/CRAN.package.elevatr

Holz A, Veblen TT (2011) Variability in the Southern Annular Mode determines wildfire activity in Patagonia. Geophys. Res. Lett. 38:n/a-n/a. https://doi.org/10.1029/2011GL047674

Holz A, Kitzberger T, Paritsis J, Veblen TT (2012) Ecological and climatic controls of modern wildfire activity patterns across southwestern South America. Ecosphere 3:1–25. https://doi.org/10.1890/ES12-00234.1

Holz A, Paritsis J, Mundo IA, Veblen TT, Kitzberger T, Williamson GJ, Aráoz E, Bustos-Schindler C, González ME, Grau HR, Quezada JM (2017) Southern Annular Mode drives multicentury wildfire activity in southern South America. Proc Natl Acad Sci U S A 114:9552–9557. https://doi.org/10.1073/pnas.1705168114

Hunziker M, Buchecker M, Hartig T (2007) Space and Place – Two Aspects of the Human-landscape Relationship. In: Décamps H, Tress B, Tress G, Kienast F, Wildi O, Ghosh S

(eds) A Changing World, vol 8. Springer Netherlands, Dordrecht, pp 47–62. https://doi.org/10.1007/978-1-4020-4436-6_5

Hylander K, Greiser C, Christiansen DM, Koelemeijer IA (2022) Climate adaptation of biodiversity conservation in managed forest landscapes. Conserv Biol 36:e13847. https://doi.org/10.1111/cobi.13847

Iglesias AL, Nuñez MA, Paritsis J (2022) The potential effect of climate change on the establishment of invasive pines in Patagonia. Plant Ecol 223:1207–1218. https://doi.org/10.1007/s11258-022-01268-z

Iseli E, Diaz Zeugin N, Brioschi C, Alexander J, Lenoir J (2025) Early detection of plant community responses to climate warming along mountain roads. Journal of Ecology. https://doi.org/10.1111/1365-2745.70114

Jačka L, Kovář M, Kuželková M (2023) TMS Calibration Handbook. https://tomst.com/web/wp-content/uploads/2023/05/TMS-calibration-handbook.pdf. Accessed 5 October 2024

Jensen D, Reager JT, Zajic B, Rousseau N, Rodell M, Hinkley E (2018) The sensitivity of US wildfire occurrence to pre-season soil moisture conditions across ecosystems. Environ Res Lett 13. https://doi.org/10.1088/1748-9326/aa9853

Jia J, Hughes AC, Nunes MH, Santos EG, Pellikka PK, Kalliovirta L, Mwang ombe J, Maeda EE (2024) Forest structural and microclimatic patterns along an elevational gradient in Mount Kenya. Agricultural and Forest Meteorology 356:110188. https://doi.org/10.1016/j.agrformet.2024.110188

Joelson NZ, Schneider E, Heinrichs S, Zerbe S, Leuschner C, Reiter EJ, Fierke J, Walentowski H (2025a) A 50-year perspective on conservation challenges and legacy effects in temperate Patagonian forests. Biological Conservation 306:111124. https://doi.org/10.1016/j.biocon.2025.111124

Joelson NZ, Simon A, Lampe F von, Loguercio GÁ, Zerbe S, Leuschner C, Walentowski H (2025b) Floristic patterns in the Andes of northern Patagonia’s forests, Argentina: towards integrating ecological responses with expert-based and unsupervised classification methods. VCS 6:37–56. https://doi.org/10.3897/VCS.134621

John A, Pradhan K, Case MJ, Ettinger AK, Hille Ris Lambers J (2024) Forest canopy cover affects microclimate buffering during an extreme heat event. Environ. Res. Commun. 6:91015. https://doi.org/10.1088/2515-7620/ad7705

Johnson PC (2014) Extension of Nakagawa & Schielzeth's R2GLMM to random slopes models. Methods Ecol Evol 5:944–946. https://doi.org/10.1111/2041-210X.12225

Jucker T, Hardwick SR, Both S, Elias DMO, Ewers RM, Milodowski DT, Swinfield T, Coomes DA (2018) Canopy structure and topography jointly constrain the microclimate of human-modified tropical landscapes. Glob Chang Biol 24:5243–5258. https://doi.org/10.1111/gcb.14415

Just MG, Hohmann MG, Hoffmann WA (2016) Where fire stops: vegetation structure and microclimate influence fire spread along an ecotonal gradient. Plant Ecology 217:631–644

Karger DN, Conrad O, Böhner J, Kawohl T, Kreft H, Soria-Auza RW, Zimmermann NE, Linder HP, Kessler M (2017) Climatologies at high resolution for the earth's land surface areas. Sci Data 4:170122. https://doi.org/10.1038/sdata.2017.122

Karger DN, Conrad O, Böhner J, Kawohl T, Kreft H, Soria-Auza RW, Zimmermann NE, Linder HP, Kessler M (2021) Climatologies at high resolution for the earth’s land surface areas. https://doi.org/10.16904/envidat.228.v2.1

Kašpar V, Hederová L, Macek M, Müllerová J, Prošek J, Surový P, Wild J, Kopecký M (2021) Temperature buffering in temperate forests: Comparing microclimate models based on ground measurements with active and passive remote sensing. Remote Sensing of Environment 263:112522. https://doi.org/10.1016/j.rse.2021.112522

Kayano MT, Andreoli RV (2007) Relations of South American summer rainfall interannual variations with the Pacific Decadal Oscillation. Int J Climatol 27:531–540. https://doi.org/10.1002/joc.1417

Kearney M, Porter W (2009) Mechanistic niche modelling: combining physiological and spatial data to predict species' ranges. Ecol Lett 12:334–350. https://doi.org/10.1111/j.1461-0248.2008.01277.x

Kemppinen J, Lembrechts JJ, Van Meerbeek K, Carnicer J, Chardon NI, Kardol P, Lenoir J, Liu D, Maclean I, Pergl J, Saccone P, Senior RA, Shen T, Słowińska S, Vandvik V, Oppen J von, Aalto J, Ayalew B, Bates O, Bertelsmeier C, Bertrand R, Beugnon R, Borderieux J, Brůna J, Buckley L, Bujan J, Casanova-Katny A, Christiansen DM, Collart F, De Lombaerde E, De Pauw K, Depauw L, Di Musciano M, Díaz Borrego R, Díaz-Calafat J, Ellis-Soto D, Esteban R, Jong GF de, Gallois E, Garcia MB, Gillerot L, Greiser C, Gril E, Haesen S, Hampe A, Hedwall P-O, Hes G, Hespanhol H, Hoffrén R, Hylander K, Jiménez-Alfaro B, Jucker T, Klinges D, Kolstela J, Kopecký M, Kovács B, Maeda EE, Máliš F, Man M, Mathiak C, Meineri E, Naujokaitis-Lewis I, Nijs I, Normand S, Nuñez M, Orczewska A, Peña-Aguilera P, Pincebourde S, Plichta R, Quick S, Renault D, Ricci L, Rissanen T, Segura-Hernández L, Selvi F, Serra-Diaz JM, Soifer L, Spicher F, Svenning J-C, Tamian A, Thomaes A, Thoonen M, Trew B, Van de Vondel S, van den Brink L,

Vangansbeke P, Verdonck S, Vitkova M, Vives-Ingla M, Schmalensee L von, Wang R, Wild J, Williamson J, Zellweger F, Zhou X, Zuza EJ, De Frenne P (2024) Microclimate, an important part of ecology and biogeography. Global Ecol Biogeogr 33. https://doi.org/10.1111/geb.13834

Keppel G, Mokany K, Wardell-Johnson GW, Phillips BL, Welbergen JA, Reside AE (2015) The capacity of refugia for conservation planning under climate change. Frontiers in Ecol & Environ 13:106–112. https://doi.org/10.1890/140055

Keppel G, Stralberg D, Morelli TL, Bátori Z (2024) Managing climate-change refugia to prevent extinctions. Trends Ecol Evol 39:800–808. https://doi.org/10.1016/j.tree.2024.05.002

Kitzberger T (2012) Ecotones as Complex Arenas of Disturbance, Climate, and Human Impacts: The Trans-Andean Forest-Steppe Ecotone of Northern Patagonia. In: Myster RW (ed) Ecotones Between Forest and Grassland. Springer New York, New York, NY, pp 59–88. https://doi.org/10.1007/978-1-4614-3797-0_3

Kitzberger T, Veblen TT (1997) Influences of humans and ENSO on fire history of Austrocedrus chilensis woodlands in northern Patagonia, Argentina. Écoscience 4:508–520. https://doi.org/10.1080/11956860.1997.11682430

Kitzberger T, Perry GL, Paritsis J, Gowda JH, Tepley AJ, Holz A, Veblen TT (2016) Fire–vegetation feedbacks and alternative states: common mechanisms of temperate forest vulnerability to fire in southern South America and New Zealand. New Zealand Journal of Botany 54:247–272. https://doi.org/10.1080/0028825X.2016.1151903

Kitzberger T, Tiribelli F, Barberá I, Gowda JH, Morales JM, Zalazar L, Paritsis J (2022) Projections of fire probability and ecosystem vulnerability under 21st century climate across a trans-Andean productivity gradient in Patagonia. Sci Total Environ 839:156303. https://doi.org/10.1016/j.scitotenv.2022.156303

Klinges DH, Baecher JA, Lembrechts JJ, Maclean IMD, Lenoir J, Greiser C, Ashcroft M, Evans LJ, Kearney MR, Aalto J, Barrio IC, De Frenne P, Guillemot J, Hylander K, Jucker T, Kopecký M, Luoto M, Macek M, Nijs I, Urban J, van den Brink L, Vangansbeke P, Von Oppen J, Wild J, Boike J, Canessa R, Nosetto M, Rubtsov A, Sallo-Bravo J, Scheffers BR (2024) Proximal microclimate: Moving beyond spatiotemporal resolution improves ecological predictions. Global Ecol Biogeogr 33. https://doi.org/10.1111/geb.13884

Kochendorfer J, Earle ME, Hodyss D, Reverdin A, Roulet Y-A, Nitu R, Rasmussen R, Landolt S, Buisán S, Laine T (2020) Undercatch Adjustments for Tipping-Bucket Gauge Measurements of Solid Precipitation. Journal of Hydrometeorology 21:1193–1205. https://doi.org/10.1175/JHM-D-19-0256.1

Kopáček J, Bače R, Hejzlar J, Kaňa J, Kučera T, Matějka K, Porcal P, Turek J (2020) Changes in microclimate and hydrology in an unmanaged mountain forest catchment after insect-induced tree dieback. Sci Total Environ 720:137518. https://doi.org/10.1016/j.scitotenv.2020.137518

Körner C (2004) Mountain Biodiversity, Its Causes and Function. AMBIO: A Journal of the Human Environment 33:11. https://doi.org/10.1007/0044-7447-33.sp13.11

Körner C, Paulsen J, Spehn EM (2011) A definition of mountains and their bioclimatic belts for global comparisons of biodiversity data. Alp Botany 121. https://doi.org/10.1007/s00035-011-0094-4

Krueger ES, Levi MR, Achieng KO, Bolten JD, Carlson JD, Coops NC, Holden ZA, Magi BI, Rigden AJ, Ochsner TE (2023) Using soil moisture information to better understand and predict wildfire danger: a review of recent developments and outstanding questions. Int. J. Wildland Fire 32:111–132. https://doi.org/10.1071/WF22056

Kulakowski D, Seidl R, Holeksa J, Kuuluvainen T, Nagel TA, Panayotov M, Svoboda M, Thorn S, Vacchiano G, Whitlock C, Wohlgemuth T, Bebi P (2017) A walk on the wild side: Disturbance dynamics and the conservation and management of European mountain forest ecosystems. Forest Ecology and Management 388:120–131. https://doi.org/10.1016/j.foreco.2016.07.037

Ladau J, Eloe-Fadrosh EA (2019) Spatial, Temporal, and Phylogenetic Scales of Microbial Ecology. Trends Microbiol 27:662–669. https://doi.org/10.1016/j.tim.2019.03.003

Landesmann JB, Tiribelli F, Paritsis J, Veblen TT, Kitzberger T (2021) Increased fire severity triggers positive feedbacks of greater vegetation flammability and favors plant community-type conversions. J Vegetation Science 32. https://doi.org/10.1111/jvs.12936

Lange S (2021) ISIMIP3b bias adjustment fact sheet

Legendre P, Fortin MJ (1989) Spatial pattern and ecological analysis. Vegetatio 80:107–138. https://doi.org/10.1007/BF00048036

Lembrechts JJ, Lenoir J (2020) Microclimatic conditions anywhere at any time! Glob Chang Biol 26:337–339. https://doi.org/10.1111/gcb.14942

Lembrechts JJ, Nijs I, Lenoir J (2019) Incorporating microclimate into species distribution models. Ecography 42:1267–1279. https://doi.org/10.1111/ecog.03947

Lembrechts JJ, Aalto J, Ashcroft MB, Frenne P de, Kopecký M, Lenoir J, Luoto M, Maclean IMD, Roupsard O, Fuentes-Lillo E, García RA, Pellissier L, Pitteloud C, Alatalo JM, Smith SW, Björk RG, Muffler L, Ratier Backes A, Cesarz S, Gottschall F, Okello J, Urban J, Plichta R, Svátek M, Phartyal SS, Wipf S, Eisenhauer N, Puşcaş M, Turtureanu PD,

Varlagin A, Dimarco RD, Jump AS, Randall K, Dorrepaal E, Larson K, Walz J, Vitale L, Svoboda M, Finger Higgens R, Halbritter AH, Curasi SR, Klupar I, Koontz A, Pearse WD, Simpson E, Stemkovski M, Jessen Graae B, Vedel Sørensen M, Høye TT, Fernández Calzado MR, Lorite J, Carbognani M, Tomaselli M, Forte TGW, Petraglia A, Haesen S, Somers B, Van Meerbeek K, Björkman MP, Hylander K, Merinero S, Gharun M, Buchmann N, Dolezal J, Matula R, Thomas AD, Bailey JJ, Ghosn D, Kazakis G, Pablo MA de, Kemppinen J, Niittynen P, Rew L, Seipel T, Larson C, Speed JDM, Ardö J, Cannone N, Guglielmin M, Malfasi F, Bader MY, Canessa R, Stanisci A, Kreyling J, Schmeddes J, Teuber L, Aschero V, Čiliak M, Máliš F, Smedt P de, Govaert S, Meeussen C, Vangansbeke P, Gigauri K, Lamprecht A, Pauli H, Steinbauer K, Winkler M, Ueyama M, Nuñez MA, Ursu T-M, Haider S, Wedegärtner REM, Smiljanic M, Trouillier M, Wilmking M, Altman J, Brůna J, Hederová L, Macek M, Man M, Wild J, Vittoz P, Pärtel M, Barančok P, Kanka R, Kollár J, Palaj A, Barros A, Mazzolari AC, Bauters M, Boeckx P, Benito Alonso J-L, Zong S, Di Cecco V, Sitková Z, Tielbörger K, van den Brink L, Weigel R, Homeier J, Dahlberg CJ, Medinets S, Medinets V, Boeck HJ de, Portillo-Estrada M, Verryckt LT, Milbau A, Daskalova GN, Thomas HJD, Myers-Smith IH, Blonder B, Stephan JG, Descombes P, Zellweger F, Frei ER, Heinesch B, Andrews C, Dick J, Siebicke L, Rocha A, Senior RA, Rixen C, Jimenez JJ, Boike J, Pauchard A, Scholten T, Scheffers B, Klinges D, Basham EW, Zhang J, Zhang Z, Géron C, Fazlioglu F, Candan O, Sallo Bravo J, Hrbacek F, Laska K, Cremonese E, Haase P, Moyano FE, Rossi C, Nijs I (2020) SoilTemp: A global database of near-surface temperature. Glob Chang Biol 26:6616–6629. https://doi.org/10.1111/gcb.15123

Lembrechts JJ, Lenoir J, R. Scheffers B, Frenne P de (2021) Designing countrywide and regional microclimate networks. Global Ecol Biogeogr 30:1168–1174. https://doi.org/10.1111/geb.13290

Lembrechts JJ, van den Hoogen J, Aalto J, Ashcroft MB, Frenne P de, Kemppinen J, Kopecký M, Luoto M, Maclean IMD, Crowther TW, Bailey JJ, Haesen S, Klinges DH, Niittynen P, Scheffers BR, Van Meerbeek K, Aartsma P, Abdalaze O, Abedi M, Aerts R, Ahmadian N, Ahrends A, Alatalo JM, Alexander JM, Allonsius CN, Altman J, Ammann C, Andres C, Andrews C, Ardö J, Arriga N, Arzac A, Aschero V, Assis RL, Assmann JJ, Bader MY, Bahalkeh K, Barančok P, Barrio IC, Barros A, Barthel M, Basham EW, Bauters M, Bazzichetto M, Marchesini LB, Bell MC, Benavides JC, Benito Alonso JL, Berauer BJ, Bjerke JW, Björk RG, Björkman MP, Björnsdóttir K, Blonder B, Boeckx P, Boike J, Bokhorst S, Brum BNS, Brůna J, Buchmann N, Buysse P, Camargo JL, Campoe OC, Candan O, Canessa R, Cannone N, Carbognani M, Carnicer J, Casanova-Katny A, Cesarz S, Chojnicki B, Choler P, Chown SL, Cifuentes EF, Čiliak M, Contador T, Convey P, Cooper EJ, Cremonese E, Curasi SR, Curtis R, Cutini M, Dahlberg CJ,

Daskalova GN, Pablo MA de, Della Chiesa S, Dengler J, Deronde B, Descombes P, Di Cecco V, Di Musciano M, Dick J, Dimarco RD, Dolezal J, Dorrepaal E, Dušek J, Eisenhauer N, Eklundh L, Erickson TE, Erschbamer B, Eugster W, Ewers RM, Exton DA, Fanin N, Fazlioglu F, Feigenwinter I, Fenu G, Ferlian O, Fernández Calzado MR, Fernández-Pascual E, Finckh M, Higgens RF, Forte TGW, Freeman EC, Frei ER, Fuentes-Lillo E, García RA, García MB, Géron C, Gharun M, Ghosn D, Gigauri K, Gobin A, Goded I, Goeckede M, Gottschall F, Goulding K, Govaert S, Graae BJ, Greenwood S, Greiser C, Grelle A, Guénard B, Guglielmin M, Guillemot J, Haase P, Haider S, Halbritter AH, Hamid M, Hammerle A, Hampe A, Haugum SV, Hederová L, Heinesch B, Helfter C, Hepenstrick D, Herberich M, Herbst M, Hermanutz L, Hik DS, Hoffrén R, Homeier J, Hörtnagl L, Høye TT, Hrbacek F, Hylander K, Iwata H, Jackowicz-Korczynski MA, Jactel H, Järveoja J, Jastrzębowski S, Jentsch A, Jiménez JJ, Jónsdóttir IS, Jucker T, Jump AS, Juszczak R, Kanka R, Kašpar V, Kazakis G, Kelly J, Khuroo AA, Klemedtsson L, Klisz M, Kljun N, Knohl A, Kobler J, Kollár J, Kotowska MM, Kovács B, Kreyling J, Lamprecht A, Lang SI, Larson C, Larson K, Laska K, Le Maire G, Leihy RI, Lens L, Liljebladh B, Lohila A, Lorite J, Loubet B, Lynn J, Macek M, Mackenzie R, Magliulo E, Maier R, Malfasi F, Máliš F, Man M, Manca G, Manco A, Manise T, Manolaki P, Marciniak F, Matula R, Mazzolari AC, Medinets S, Medinets V, Meeussen C, Merinero S, Mesquita RdCG, Meusburger K, Meysman FJR, Michaletz ST, Milbau A, Moiseev D, Moiseev P, Mondoni A, Monfries R, Montagnani L, Moriana-Armendariz M, Di Morra Cella U, Mörsdorf M, Mosedale JR, Muffler L, Muñoz-Rojas M, Myers JA, Myers-Smith IH, Nagy L, Nardino M, Naujokaitis-Lewis I, Newling E, Nicklas L, Niedrist G, Niessner A, Nilsson MB, Normand S, Nosetto MD, Nouvellon Y, Nuñez MA, Ogaya R, Ogée J, Okello J, Olejnik J, Olesen JE, Opedal ØH, Orsenigo S, Palaj A, Pampuch T, Panov AV, Pärtel M, Pastor A, Pauchard A, Pauli H, Pavelka M, Pearse WD, Peichl M, Pellissier L, Penczykowski RM, Penuelas J, Petit Bon M, Petraglia A, Phartyal SS, Phoenix GK, Pio C, Pitacco A, Pitteloud C, Plichta R, Porro F, Portillo-Estrada M, Poulenard J, Poyatos R, Prokushkin AS, Puchalka R, Puşcaş M, Radujković D, Randall K, Ratier Backes A, Remmele S, Remmers W, Renault D, Risch AC, Rixen C, Robinson SA, Robroek BJM, Rocha AV, Rossi C, Rossi G, Roupsard O, Rubtsov AV, Saccone P, Sagot C, Sallo Bravo J, Santos CC, Sarneel JM, Scharnweber T, Schmeddes J, Schmidt M, Scholten T, Schuchardt M, Schwartz N, Scott T, Seeber J, Segalin de Andrade AC, Seipel T, Semenchuk P, Senior RA, Serra-Diaz JM, Sewerniak P, Shekhar A, Sidenko NV, Siebicke L, Siegwart Collier L, Simpson E, Siqueira DP, Sitková Z, Six J, Smiljanic M, Smith SW, Smith-Tripp S, Somers B, Sørensen MV, Souza JJLL, Souza BI, Souza Dias A, Spasojevic MJ, Speed JDM, Spicher F, Stanisci A, Steinbauer K, Steinbrecher R, Steinwandter M, Stemkovski M, Stephan JG, Stiegler C, Stoll S, Svátek M, Svoboda M,

Tagesson T, Tanentzap AJ, Tanneberger F, Theurillat J-P, Thomas HJD, Thomas AD, Tielbörger K, Tomaselli M, Treier UA, Trouillier M, Turtureanu PD, Tutton R, Tyystjärvi VA, Ueyama M, Ujházy K, Ujházyová M, Uogintas D, Urban AV, Urban J, Urbaniak M, Ursu T-M, Vaccari FP, Van de Vondel S, van den Brink L, van Geel M, Vandvik V, Vangansbeke P, Varlagin A, Veen GF, Veenendaal E, Venn SE, Verbeeck H, Verbrugggen E, Verheijen FGA, Villar L, Vitale L, Vittoz P, Vives-Ingla M, Oppen J von, Walz J, Wang R, Wang Y, Way RG, Wedegärtner REM, Weigel R, Wild J, Wilkinson M, Wilmking M, Wingate L, Winkler M, Wipf S, Wohlfahrt G, Xenakis G, Yang Y, Yu Z, Yu K, Zellweger F, Zhang J, Zhang Z, Zhao P, Ziemblińska K, Zimmermann R, Zong S, Zyryanov VI, Nijs I, Lenoir J (2022) Global maps of soil temperature. Glob Chang Biol 28:3110–3144. https://doi.org/10.1111/gcb.16060

Lenoir J, Hattab T, Pierre G (2017) Climatic microrefugia under anthropogenic climate change: implications for species redistribution. Ecography 40:253–266. https://doi.org/10.1111/ecog.02788

León-Muñoz J, Urbina MA, Garreaud R, Iriarte JL (2018) Hydroclimatic conditions trigger record harmful algal bloom in western Patagonia (summer 2016). Sci Rep 8:1330. https://doi.org/10.1038/s41598-018-19461-4

Levin SA (1992) The Problem of Pattern and Scale in Ecology: The Robert H. MacArthur Award Lecture. Ecology 73:1943–1967. https://doi.org/10.2307/1941447

Liding C, Yang L, Yihe L, Xiaoming F, Bojie F (2008) Pattern analysis in landscape ecology: progress, challenges and outlook. Acta Ecologica Sinica 28:5521–5531. https://doi.org/10.1016/S1872-2032(09)60011-1

Littell JS, McKenzie D, Kerns BK, Cushman S, Shaw CG (2011) Managing uncertainty in climate-driven ecological models to inform adaptation to climate change. Ecosphere 2:art102. https://doi.org/10.1890/ES11-00114.1

Lombaerde E de, Vangansbeke P, Lenoir J, Van Meerbeek K, Lembrechts J, Rodríguez-Sánchez F, Luoto M, Scheffers B, Haesen S, Aalto J, Christiansen DM, Pauw K de, Depauw L, Govaert S, Greiser C, Hampe A, Hylander K, Klinges D, Koelemeijer I, Meeussen C, Ogée J, Sanczuk P, Vanneste T, Zellweger F, Baeten L, Frenne P de (2022) Maintaining forest cover to enhance temperature buffering under future climate change. Sci Total Environ 810:151338. https://doi.org/10.1016/j.scitotenv.2021.151338

Lumley T (2020) leaps: Regression Subset Selection: R package version 3.1. https://CRAN.R-project.org/package=leaps

MacKenzie WH, Mahony CR (2021) An ecological approach to climate change-informed tree species selection for reforestation. Forest Ecology and Management 481:118705. https://doi.org/10.1016/j.foreco.2020.118705

Maclean IMD, Hopkins JJ, Bennie J, Lawson CR, Wilson RJ (2015) Microclimates buffer the responses of plant communities to climate change. Global Ecol Biogeogr 24:1340–1350. https://doi.org/10.1111/geb.12359

Maclean IMD, Mosedale JR, Bennie JJ (2019) Microclima: An r package for modelling meso- and microclimate. Methods Ecol Evol 10:280–290. https://doi.org/10.1111/2041-210X.13093

Máliš F, Ujházy K, Hederová L, Ujházyová M, Csölleová L, Coomes DA, Zellweger F (2023) Microclimate variation and recovery time in managed and old-growth temperate forests. Agricultural and Forest Meteorology 342:109722. https://doi.org/10.1016/j.agrformet.2023.109722

Man M, Kalčík V, Macek M, Brůna J, Hederová L, Wild J, Kopecký M (2024) myClim: Microclimatic Data Processing. https://doi.org/10.32614/CRAN.package.myClim

Marsh C, Krofcheck D, Hurteau MD (2022a) Identifying microclimate tree seedling refugia in post-wildfire landscapes. Agricultural and Forest Meteorology 313:108741. https://doi.org/10.1016/j.agrformet.2021.108741

Marsh C, Crockett JL, Krofcheck D, Keyser A, Allen CD, Litvak M, Hurteau MD (2022b) Planted seedling survival in a post-wildfire landscape: From experimental planting to predictive probabilistic surfaces. Forest Ecology and Management 525:120524. https://doi.org/10.1016/j.foreco.2022.120524

Martínez Pastur GJ, Cellini JM, Lencinas MV, Barrera M, Peri PL (2011) Environmental variables influencing regeneration of Nothofagus pumilio in a system with combined aggregated and dispersed retention. Forest Ecology and Management 261:178–186. https://doi.org/10.1016/j.foreco.2010.10.002

Martínez Pastur GJ, Esteban RS, Cellini JM, Lencinas MV, Peri PL, Neyland MG (2014) Survival and growth of Nothofagus pumilio seedlings under several microenvironments after variable retention harvesting in southern Patagonian forests. Annals of Forest Science 71:349–362. https://doi.org/10.1007/s13595-013-0343-3

McGarigal K, Tagil S, Cushman SA (2009) Surface metrics: an alternative to patch metrics for the quantification of landscape structure. Landsc Ecol 24:433–450. https://doi.org/10.1007/s10980-009-9327-y

Meeussen C, Govaert S, Vanneste T, Bollmann K, Brunet J, Calders K, Cousins SA, Pauw K de, Diekmann M, Gasperini C, Hedwall P-O, Hylander K, Iacopetti G, Lenoir J, Lindmo S, Orczewska A, Ponette Q, Plue J, Sanczuk P, Selvi F, Spicher F, Verbeeck H, Zellweger F, Verheyen K, Vangansbeke P, Frenne P de (2021) Microclimatic edge-to-interior gradients of European deciduous forests. Agricultural and Forest Meteorology 311:108699. https://doi.org/10.1016/j.agrformet.2021.108699

Meineri E, Hylander K (2017) Fine-grain, large-domain climate models based on climate station and comprehensive topographic information improve microrefugia detection. Ecography 40:1003–1013. https://doi.org/10.1111/ecog.02494

Menge JH, Magdon P, Wöllauer S, Ehbrecht M (2023) Impacts of forest management on stand and landscape-level microclimate heterogeneity of European beech forests. Landsc Ecol 38:903–917. https://doi.org/10.1007/s10980-023-01596-z

Mermoz M, Kitzberger T, Veblen TT (2005) Landscape Influences on Occurrence and Spread of Wildfires in Patagonian Forests and Shrublands. Ecology 86:2705–2715

Millar CI, Stephenson NL (2015) Temperate forest health in an era of emerging megadisturbance. Science 349:823–826. https://doi.org/10.1126/science.aaa9933

Mindlin J, Shepherd TG, Vera CS, Osman M, Zappa G, Lee RW, Hodges KI (2020) Storyline description of Southern Hemisphere midlatitude circulation and precipitation response to greenhouse gas forcing. Clim Dyn 54:4399–4421. https://doi.org/10.1007/s00382-020-05234-1

Mindlin J, Shepherd TG, Vera C, Osman M (2021) Combined Effects of Global Warming and Ozone Depletion/Recovery on Southern Hemisphere Atmospheric Circulation and Regional Precipitation. Geophys. Res. Lett. 48. https://doi.org/10.1029/2021GL092568

Morales-Barbero J, Vega-Álvarez J (2019) Input matters matter: Bioclimatic consistency to map more reliable species distribution models. Methods Ecol Evol 10:212–224. https://doi.org/10.1111/2041-210X.13124

Morelli TL, Daly C, Dobrowski SZ, Dulen DM, Ebersole JL, Jackson ST, Lundquist JD, Millar CI, Maher SP, Monahan WB, Nydick KR, Redmond KT, Sawyer SC, Stock S, Beissinger SR (2016) Managing Climate Change Refugia for Climate Adaptation. PLoS One 11:e0159909. https://doi.org/10.1371/journal.pone.0159909

Moure M, Jacobsen JB, Smith-Hall C (2023) Uncertainty and Climate Change Adaptation: a Systematic Review of Research Approaches and People's Decision-Making. Curr Clim Change Rep 9:1–26. https://doi.org/10.1007/s40641-023-00189-x

Nakagawa S, Schielzeth H (2013) A general and simple method for obtaining R2 from generalized linear mixed-effects models. Methods Ecol Evol 4:133–142. https://doi.org/10.1111/j.2041-210x.2012.00261.x

Newell FL, Ausprey IJ, Robinson SK (2022) Spatiotemporal climate variability in the Andes of northern Peru: Evaluation of gridded datasets to describe cloud forest microclimate and local rainfall. International Journal of Climatology 42:5892–5915. https://doi.org/10.1002/joc.7567

Newton AC, Hill RA, Echeverría C, Golicher D, Rey Benayas JM, Cayuela L, Hinsley SA (2009) Remote sensing and the future of landscape ecology. Progress in Physical Geography: Earth and Environment 33:528–546. https://doi.org/10.1177/0309133309346882

Nowakowski AJ, Frishkoff LO, Agha M, Todd BD, Scheffers BR (2018) Changing Thermal Landscapes: Merging Climate Science and Landscape Ecology through Thermal Biology. Curr Landscape Ecol Rep 3:57–72. https://doi.org/10.1007/s40823-018-0034-8

Oliveira-Júnior JF de, Correia Filho WLF, Barros Santiago D de, Gois G de, da Silva Costa M, da Silva Junior CA, Teodoro PE, Freire FM (2021) Rainfall in Brazilian Northeast via in situ data and CHELSA product: mapping, trends, and socio-environmental implications. Environ Monit Assess 193:263. https://doi.org/10.1007/s10661-021-09043-9

O'Neill BC, Tebaldi C, van Vuuren DP, Eyring V, Friedlingstein P, Hurtt G, Knutti R, Kriegler E, Lamarque J-F, Lowe J, Meehl GA, Moss R, Riahi K, Sanderson BM (2016) The Scenario Model Intercomparison Project (ScenarioMIP) for CMIP6. Geosci. Model Dev. 9:3461–3482. https://doi.org/10.5194/gmd-9-3461-2016

Opdam P, Foppen R, Vos C (2001) Bridging the gap between ecology and spatial planning in landscape ecology. Landsc Ecol 16:767–779. https://doi.org/10.1023/A:1014475908949

Otto J, Brown C, Buontempo C, Doblas-Reyes F, Jacob D, Juckes M, Keup-Thiel E, Kurnik B, Schulz J, Taylor A, Verhoelst T, Walton P (2016) Uncertainty: Lessons Learned for Climate Services. Bulletin of the American Meteorological Society 97:ES265-ES269. https://doi.org/10.1175/BAMS-D-16-0173.1

Pacifici M, Foden WB, Visconti P, Watson JEM, Butchart SH, Kovacs KM, Scheffers BR, Hole DG, Martin TG, Akçakaya HR, Corlett RT, Huntley B, Bickford D, Carr JA, Hoffmann AA, Midgley GF, Pearce-Kelly P, Pearson RG, Williams SE, Willis SG, Young B, Rondinini C (2015) Assessing species vulnerability to climate change. Nat. Clim. Chang. 5:215–224. https://doi.org/10.1038/NCLIMATE2448

Paritsis J, Raffaele E, Veblen TT (2006) Vegetation disturbance by fire affects plant reproductive phenology in a shrubland community in northwestern Patagonia, Argentina. New Zealand Journal of Ecology:387–395

Paritsis J, Veblen TT, Holz A (2015) Positive fire feedbacks contribute to shifts from N othofagus pumilio forests to fire-prone shrublands in P atagonia. J Vegetation Science 26:89–101. https://doi.org/10.1111/jvs.12225

Paruelo J, Beltrán AB, Jobbágy E, Sala OE, Golluscio R (1998) The climate of Patagonia: General patterns and controls on biotic processes. Ecologia Austral 8:85–101

Pebesma E (2018) Simple Features for R: Standardized Support for Spatial Vector Data. The R Journal 10:439. https://doi.org/10.32614/RJ-2018-009

Pebesma E, Bivand R (2023) Spatial Data Science. Chapman and Hall/CRC, Boca Raton. https://doi.org/10.1201/9780429459016

Penalba OC, Rivera JA (2016) Precipitation response to El Niño/La Niña events in Southern South America – emphasis in regional drought occurrences. Adv. Geosci. 42:1–14. https://doi.org/10.5194/adgeo-42-1-2016

Pesaresi S, Biondi E, Casavecchia S (2017) Bioclimates of Italy. Journal of Maps 13:955–960. https://doi.org/10.1080/17445647.2017.1413017

Pessacg N, Flaherty S, Solman S, Pascual M (2020) Climate change in northern Patagonia: critical decrease in water resources. Theor Appl Climatol 140:807–822. https://doi.org/10.1007/s00704-020-03104-8

Peters DPC, Bestelmeyer BT, Turner MG (2007) Cross–Scale Interactions and Changing Pattern–Process Relationships: Consequences for System Dynamics. Ecosystems 10:790–796. https://doi.org/10.1007/s10021-007-9055-6

Peterson GD, Cumming GS, Carpenter SR (2003) Scenario Planning: a Tool for Conservation in an Uncertain World. Conservation Biology 17:358–366. https://doi.org/10.1046/j.1523-1739.2003.01491.x

Pham TM, Nguyen HC, van Nguyen K, Pham HH, Nguyen NT, Dang GTH, Dinh HT, Pham TA (2023) Application of the Worldwide Bioclimatic Classification System to determine bioclimatic features and potential natural vegetation distribution in Van Chan district, Vietnam. Trop Ecol

Pickett ST, Cadenasso ML (1995) Landscape ecology: spatial heterogeneity in ecological systems. Science 269:331–334. https://doi.org/10.1126/science.269.5222.331

Pielke RA, Pitman A, Niyogi D, Mahmood R, McAlpine C, Hossain F, Goldewijk KK, Nair U, Betts R, Fall S, Reichstein M, Kabat P, Noblet N de (2011) Land use/land cover changes

and climate: modeling analysis and observational evidence. WIREs Climate Change 2:828–850. https://doi.org/10.1002/wcc.144

Pinheiro J, Bates D (2025) nlme: Linear and Nonlinear Mixed Effects Models. https://cran.r-project.org/web/packages/nlme/nlme.pdf. Accessed 9 July 2025

Piraino S, Molina JA, Hadad MA, Juñent FAR (2022) Resilience capacity of Araucaria araucana to extreme drought events. Dendrochronologia 75:125996. https://doi.org/10.1016/j.dendro.2022.125996

Porter WP, Mitchell JW, Beckman WA, DeWitt CB (1973) Behavioral implications of mechanistic ecology : Thermal and behavioral modeling of desert ectotherms and their microenvironment. Oecologia 13:1–54. https://doi.org/10.1007/BF00379617

Potter KA, Arthur Woods H, Pincebourde S (2013) Microclimatic challenges in global change biology. Glob Chang Biol 19:2932–2939. https://doi.org/10.1111/gcb.12257

Premke K, Attermeyer K, Augustin J, Cabezas A, Casper P, Deumlich D, Gelbrecht J, Gerke HH, Gessler A, Grossart H-P, Hilt S, Hupfer M, Kalettka T, Kayler Z, Lischeid G, Sommer M, Zak D (2016) The importance of landscape diversity for carbon fluxes at the landscape level: small-scale heterogeneity matters. WIREs Water 3:601–617. https://doi.org/10.1002/wat2.1147

Raffaele E, Veblen TT, Blackhall M, Tercero-Bucardo N (2011) Synergistic influences of introduced herbivores and fire on vegetation change in northern Patagonia, Argentina. Journal of Vegetation Science 22:59–71. https://doi.org/10.1111/j.1654-1103.2010.01233.x

Raffaele E, Nuñez MA, Eneström J, Blackhall M (2016) Fire as mediator of pine invasion: evidence from Patagonia, Argentina. Biol Invasions 18:597–601. https://doi.org/10.1007/s10530-015-1038-5

Rahbek C, Borregaard MK, Colwell RK, Dalsgaard B, Holt BG, Morueta-Holme N, Nogues-Bravo D, Whittaker RJ, Fjeldså J (2019) Humboldt's enigma: What causes global patterns of mountain biodiversity? Science 365:1108–1113. https://doi.org/10.1126/science.aax0149

Rangwala I, Miller JR (2012) Climate change in mountains: a review of elevation-dependent warming and its possible causes. Climatic Change 114:527–547. https://doi.org/10.1007/s10584-012-0419-3

Rebaudo F, Soulard T, Condori B, Quispe-Tarqui R, Calatayud P-A, Chavez Vino S, Tonnang HEZ, Bessière L (2023) A low-cost IoT network to monitor microclimate

variables in ecosystems. Methods Ecol Evol 14:1025–1034. https://doi.org/10.1111/2041-210X.14062

Reiter EJ, Weigel R, Walentowski H, Loguercio GA, Fierke J, Winter AFN, Simon A, Kotowska MM, Joelson NZ, Caselli M, Leuschner C (2024) Climate vulnerability of Nothofagus pumilio, Nothofagus dombeyi and Austrocedrus chilensis in northern Patagonia's temperate forests. Forest Ecology and Management 572:122261. https://doi.org/10.1016/j.foreco.2024.122261

Reiter EJ, Weigel R, Leuschner C (2025a) Losing half the crown hardly affects the stem growth of a xeric southern beech population. Sci Rep 15:5721. https://doi.org/10.1038/s41598-025-90061-9

Reiter EJ, Weigel R, Walentowski H, Rago MM, Simon A, Pissolito C, Leuschner C (2025b) Exotic pine plantations vs. native forests in northern Patagonia: Comparing growth patterns and climate change vulnerability. Forest Ecology and Management 595:122966. https://doi.org/10.1016/j.foreco.2025.122966

Renaud V, Rebetez M (2009) Comparison between open-site and below-canopy climatic conditions in Switzerland during the exceptionally hot summer of 2003. Agricultural and Forest Meteorology 149:873–880. https://doi.org/10.1016/j.agrformet.2008.11.006

Risser PG, Karr JR, Forman RTT (1984) Landscape ecology: directions and approaches: a workshop held at Allerton Park, Piatt County, Illinois, April 1983. Illinois Natural History Survey Special Publication no. 02

Rita A, Bonanomi G, Allevato E, Borghetti M, Cesarano G, Mogavero V, Rossi S, Saulino L, Zotti M, Saracino A (2021) Topography modulates near-ground microclimate in the Mediterranean Fagus sylvatica treeline. Sci Rep 11:8122. https://doi.org/10.1038/s41598-021-87661-6

Rivas-Martínez S, Sáenz S, Penas A (2011) Worldwide Bioclimatic Classification System. Global Geobotany 1:1-634+4 Maps. https://doi.org/10.5616/gg110001

Rivera A, Aravena JC, Urra A, Reid B (2023) Chilean Patagonian Glaciers and Environmental Change. In: Castilla JC, Armesto Zamudio JJ, Martínez-Harms MJ, Tecklin D (eds) Conservation in Chilean Patagonia, vol 19. Springer International Publishing, Cham, pp 393–407. https://doi.org/10.1007/978-3-031-39408-9_15

Rodríguez-Catón M, Villalba R, Morales M, Srur A (2016) Influence of droughts on Nothofagus pumilio forest decline across northern Patagonia, Argentina. Ecosphere 7. https://doi.org/10.1002/ecs2.1390

Sala OE, Chapin FS, Armesto JJ, Berlow E, Bloomfield J, Dirzo R, Huber-Sanwald E, Huenneke LF, Jackson RB, Kinzig A, Leemans R, Lodge DM, Mooney HA, Oesterheld M, Poff NL, Sykes MT, Walker BH, Walker M, Wall DH (2000) Global biodiversity scenarios for the year 2100. Science 287:1770–1774. https://doi.org/10.1126/science.287.5459.1770

Salazar Á, Thatcher M, Goubanova K, Bernal P, Gutiérrez J, Squeo F (2024) CMIP6 precipitation and temperature projections for Chile. Clim Dyn 62:2475–2498. https://doi.org/10.1007/s00382-023-07034-9

Sanczuk P, Govaert S, Meeussen C, Pauw K de, Vanneste T, Depauw L, Moreira X, Schoelynck J, Boevre M de, Saeger S de, Bollmann K, Brunet J, Cousins SAO, Plue J, Diekmann M, Graae BJ, Hedwall P-O, Iacopetti G, Lenoir J, Orczewska A, Ponette Q, Selvi F, Spicher F, Vermeir P, Calders K, Verbeeck H, Verheyen K, Vangansbeke P, Frenne P de (2021) Small scale environmental variation modulates plant defence syndromes of understorey plants in deciduous forests of Europe. Global Ecol Biogeogr 30:205–219. https://doi.org/10.1111/geb.13216

Saslis-Lagoudakis CH, Cowman PF, Cardillo M, Catullo RA, Rosauer DF, Warren DL (2014) Biogeography: multidisciplinary approaches in space and time. Frontiers of Biogeography 6. https://doi.org/10.21425/F5FBG21749

Scheffers BR, Edwards DP, Diesmos A, Williams SE, Evans TA (2014) Microhabitats reduce animal's exposure to climate extremes. Glob Chang Biol 20:495–503. https://doi.org/10.1111/gcb.12439

Schonlau M, Zou RY (2020) The random forest algorithm for statistical learning. The Stata Journal: Promoting communications on statistics and Stata 20:3–29. https://doi.org/10.1177/1536867X20909688

Seidl R, Turner MG (2022) Post-disturbance reorganization of forest ecosystems in a changing world. Proc Natl Acad Sci U S A 119:e2202190119. https://doi.org/10.1073/pnas.2202190119

Seidl R, Rammer W, Spies TA (2014) Disturbance legacies increase the resilience of forest ecosystem structure, composition, and functioning. Ecol Appl 24:2063–2077. https://doi.org/10.1890/14-0255.1

Seidl R, Thom D, Kautz M, Martin-Benito D, Peltoniemi M, Vacchiano G, Wild J, Ascoli D, Petr M, Honkaniemi J, Lexer MJ, Trotsiuk V, Mairota P, Svoboda M, Fabrika M, Nagel TA, Reyer CPO (2017) Forest disturbances under climate change. Nat. Clim. Chang. 7:395–402. https://doi.org/10.1038/NCLIMATE3303

Seidl R, Albrich K, Thom D, Rammer W (2018) Harnessing landscape heterogeneity for managing future disturbance risks in forest ecosystems. J Environ Manage 209:46–56. https://doi.org/10.1016/j.jenvman.2017.12.014

Senf C, Seidl R (2018) Natural disturbances are spatially diverse but temporally synchronized across temperate forest landscapes in Europe. Glob Chang Biol 24:1201–1211. https://doi.org/10.1111/gcb.13897

Servicio Meteorológico Nacional (2023) Servicio Meteorológico Nacional. https://www.smn.gob.ar/. Accessed 13 July 2023

Shandas V, Voelkel J, Williams J, Hoffman J (2019) Integrating Satellite and Ground Measurements for Predicting Locations of Extreme Urban Heat. Climate 7:5. https://doi.org/10.3390/cli7010005

Silvestri G, Vera C (2009) Nonstationary Impacts of the Southern Annular Mode on Southern Hemisphere Climate. Journal of Climate 22:6142–6148. https://doi.org/10.1175/2009JCLI3036.1

Simmonds EG, Adjei KP, Cretois B, Dickel L, González-Gil R, Laverick JH, Mandeville CP, Mandeville EG, Ovaskainen O, Sicacha-Parada J, Skarstein ES, O'Hara B (2024) Recommendations for quantitative uncertainty consideration in ecology and evolution. Trends Ecol Evol 39:328–337. https://doi.org/10.1016/j.tree.2023.10.012

Simon A, Fierke J, Reiter EJ, Loguercio GA, Heinrichs S, Putzenlechner B, Joelson NZ, Walentowski H (2024) The interior climate and its microclimatic variation of temperate forests in Northern Patagonia, Argentina. Int J Biometeorol 68:719–730. https://doi.org/10.1007/s00484-024-02617-5

Simon et al. (in prep.) Unravelling the pedogenetic development of forest soils in northern Patagonia, Argentina

Sistema Nacional de Información Hídrica (2023) Sistema Nacional de Información Hídrica. https://snih.hidricosargentina.gob.ar/Filtros.aspx. Accessed 13 July 2023

Slavich E, Warton DI, Ashcroft MB, Gollan JR, Ramp D (2014) Topoclimate versus macroclimate: how does climate mapping methodology affect species distribution models and climate change projections? Diversity and Distributions 20:952–963. https://doi.org/10.1111/ddi.12216

SMN (2024) Servicio Meteorologico Nacional Argentina. https://www.smn.gob.ar/

Sokal RR (2009) Introduction to biostatistics, 2nd edn. Dover Publ, Mineola, N.Y

Soliani C, Ceccarelli V, Lantschner MV, Thomas E, Marchelli P (2024) Predicting the distribution of plant species from southern South America: are the hotspots of genetic

diversity threatened by climate change? Biodivers Conserv 33:725–757. https://doi.org/10.1007/s10531-023-02770-0

Sommerfeld A, Senf C, Buma B, D'Amato AW, Després T, Díaz-Hormazábal I, Fraver S, Frelich LE, Gutiérrez ÁG, Hart SJ, Harvey BJ, He HS, Hlásny T, Holz A, Kitzberger T, Kulakowski D, Lindenmayer D, Mori AS, Müller J, Paritsis J, Perry GLW, Stephens SL, Svoboda M, Turner MG, Veblen TT, Seidl R (2018) Patterns and drivers of recent disturbances across the temperate forest biome. Nat Commun 9:4355. https://doi.org/10.1038/s41467-018-06788-9

Speziale KL, Ezcurra C (2015) Rock outcrops as potential biodiversity refugia under climate change in North Patagonia. Plant Ecology & Diversity 8:353–361. https://doi.org/10.1080/17550874.2014.983200

Srur AM, Villalba R, Rodríguez-Catón M, Amoroso MM, Marcotti E (2016) Establishment of Nothofagus pumilio at Upper Treelines Across a Precipitation Gradient in the Northern Patagonian Andes. Arctic, Antarctic, and Alpine Research 48:755–766. https://doi.org/10.1657/AAAR0016-015

Srur AM, Villalba R, Rodríguez-Catón M, Amoroso MM, Marcotti E (2018) Climate and Nothofagus pumilio Establishment at Upper Treelines in the Patagonian Andes. Front. Earth Sci. 6. https://doi.org/10.3389/feart.2018.00057

Starck I, Aalto J, Hancock S, Valkonen S, Kalliovirta L, Maeda E (2025) Slow recovery of microclimate temperature buffering capacity after clear-cuts in boreal forests. Agricultural and Forest Meteorology 363:110434. https://doi.org/10.1016/j.agrformet.2025.110434

Stark JR, Fridley JD (2022) Microclimate-based species distribution models in complex forested terrain indicate widespread cryptic refugia under climate change. Global Ecol Biogeogr 31:562–575. https://doi.org/10.1111/geb.13447

Stein A, Gerstner K, Kreft H (2014) Environmental heterogeneity as a universal driver of species richness across taxa, biomes and spatial scales. Ecol Lett 17:866–880. https://doi.org/10.1111/ele.12277

Stella JL (2022) Informe Especial N°2 Por Ola de Calor / Atlas Temperaturas Temporada 2022-2023

Stella JL (2024) Informe Especial N°4 Por Ola de Calor / Atlas Temperaturas Temporada 2023-2024. https://www.smn.gob.ar/sites/default/files/informe_oladecalor_21ene_al_12feb_2024.pdf

Suding KN, Gross KL, Houseman GR (2004) Alternative states and positive feedbacks in restoration ecology. Trends Ecol Evol 19:46–53. https://doi.org/10.1016/j.tree.2003.10.005

Suggitt AJ, Platts PJ, Barata IM, Bennie JJ, Burgess MD, Bystriakova N, Duffield S, Ewing SR, Gillingham PK, Harper AB, Hartley AJ, Hemming DL, Maclean IMD, Maltby K, Marshall HH, Morecroft MD, Pearce-Higgins JW, Pearce-Kelly P, Phillimore AB, Price JT, Pyke A, Stewart JE, Warren R, Hill JK (2017) Conducting robust ecological analyses with climate data. Oikos 126:1533–1541. https://doi.org/10.1111/oik.04203

Suggitt AJ, Wilson RJ, Isaac NJB, Beale CM, Auffret AG, August T, Bennie JJ, Crick HQP, Duffield S, Fox R, Hopkins JJ, Macgregor NA, Morecroft MD, Walker KJ, Maclean IMD (2018) Extinction risk from climate change is reduced by microclimatic buffering. Nat. Clim. Chang. 8:713–717. https://doi.org/10.1038/s41558-018-0231-9

Szabó AI, Ács F, Breuer H (2021) Larger Carpathian region climate according to Köppen, Feddema and the Worldwide Bioclimatic Classification System methods. Int J Climatol 41. https://doi.org/10.1002/joc.6859

Tang G, Clark MP, Papalexiou SM (2022) EM-Earth: The Ensemble Meteorological Dataset for Planet Earth. Bulletin of the American Meteorological Society 103:E996-E1018. https://doi.org/10.1175/BAMS-D-21-0106.1

Tepley AJ, Thomann E, Veblen TT, Perry GLW, Holz A, Paritsis J, Kitzberger T, Anderson-Teixeira KJ (2018) Influences of fire–vegetation feedbacks and post-fire recovery rates on forest landscape vulnerability to altered fire regimes. Journal of Ecology 106:1925–1940. https://doi.org/10.1111/1365-2745.12950

Tewksbury JJ, Levey DJ, Haddad NM, Sargent S, Orrock JL, Weldon A, Danielson BJ, Brinkerhoff J, Damschen EI, Townsend P (2002) Corridors affect plants, animals, and their interactions in fragmented landscapes. Proc Natl Acad Sci U S A 99:12923–12926. https://doi.org/10.1073/pnas.202242699

Thom D, Rammer W, Seidl R (2017) The impact of future forest dynamics on climate: interactive effects of changing vegetation and disturbance regimes. Ecol Monogr 87:665–684. https://doi.org/10.1002/ecm.1272

Thom D, Sommerfeld A, Sebald J, Hagge J, Müller J, Seidl R (2020) Effects of disturbance patterns and deadwood on the microclimate in European beech forests. Agricultural and Forest Meteorology 291. https://doi.org/10.1016/j.agrformet.2020.108066

Thornton JM, Pepin N, Shahgedanova M, Adler C (2022) Coverage of In Situ Climatological Observations in the World's Mountains. Front. Clim. 4. https://doi.org/10.3389/fclim.2022.814181

Tilman D, Kareiva P (1997) Spatial ecology: the role of space in population dynamics and interspecific interactions, vol 30. Princeton University Press

Tiribelli F, Kitzberger T, Morales JM (2018) Changes in vegetation structure and fuel characteristics along post-fire succession promote alternative stable states and positive fire–vegetation feedbacks. J Vegetation Science 29:147–156. https://doi.org/10.1111/jvs.12620

Tiribelli F, Paritsis J, Barberá I, Kitzberger T (2024) Spatial and temporal opportunities for forest resilience promoted by burn severity attenuation across a productivity gradient in north western Patagonia. Int. J. Wildland Fire 33. https://doi.org/10.1071/WF23098

Tolan J, Yang H-I, Nosarzewski B, Couairon G, Vo HV, Brandt J, Spore J, Majumdar S, Haziza D, Vamaraju J, Moutakanni T, Bojanowski P, Johns T, White B, Tiecke T, Couprie C (2024) Very high resolution canopy height maps from RGB imagery using self-supervised vision transformer and convolutional decoder trained on aerial lidar. Remote Sensing of Environment 300:113888. https://doi.org/10.1016/j.rse.2023.113888

Torregrosa A, Taylor MD, Flint LE, Flint AL (2013) Present, future, and novel bioclimates of the San Francisco, California region. PLoS One 8:e58450. https://doi.org/10.1371/journal.pone.0058450

Tovar C, Carril AF, Gutiérrez AG, Ahrends A, Fita L, Zaninelli P, Flombaum P, Abarzúa AM, Alarcón D, Aschero V, Báez S, Barros A, Carilla J, Ferrero ME, Flantua SGA, Gonzáles P, Menéndez CG, Pérez-Escobar OA, Pauchard A, Ruscica RC, Särkinen T, Sörensson AA, Srur A, Villalba R, Hollingsworth PM (2022) Understanding climate change impacts on biome and plant distributions in the Andes: Challenges and opportunities. J Biogeogr 49:1420–1442. https://doi.org/10.1111/jbi.14389

Turner MG (1990) Spatial and temporal analysis of landscape patterns. Landsc Ecol 4:21–30. https://doi.org/10.1007/BF02573948

Turner MG (2010) Disturbance and landscape dynamics in a changing world. Ecology 91:2833–2849. https://doi.org/10.1890/10-0097.1

Turner MG, Gardner RH (2015) Landscape Ecology in Theory and Practice. Springer New York, New York, NY. https://doi.org/10.1007/978-1-4939-2794-4

Turner MG, Romme WH, Gardner RH, O'Neill RV, Kratz TK (1993) A revised concept of landscape equilibrium: Disturbance and stability on scaled landscapes. Landsc Ecol 8:213–227. https://doi.org/10.1007/BF00125352

Turner MG, Baker WL, Peterson CJ, Peet RK (1998) Factors Influencing Succession: Lessons from Large, Infrequent Natural Disturbances. Ecosystems 1:511–523. https://doi.org/10.1007/s100219900047

Turner MG (1989) Landscape ecology: the effect of pattern on process. Annual review of ecology and systematics:171–197

UNFCCC (2015) Paris Agreement. adopted on 12 December 2015 and in force since 4 November 2016. https://treaties.un.org/pages/ViewDetails.aspx?src=TREATY&mtdsg_no=XXVII-7-d&chapter=27&clang=_en. Accessed 22 August 2023

USGS (2024) Earth Resources Observation and Science (EROS) Center Science Processing Architecture (ESPA) On Demand Interface. https://www.usgs.gov/centers/eros

Veblen TT (2007) Temperate Forests of the Southern Andean Region. In: Veblen TT, Orme AR, Young KR (eds) The physical geography of South America. Oxford University Press, Oxford, New York. https://doi.org/10.1093/oso/9780195313413.003.0021

Veblen TT, Lorenz DC (1987) Post-fire stand development of Austrocedrus-Nothofagus forests in northern Patagonia. Vegetatio 71:113–126. https://doi.org/10.1007/BF00044825

Veblen TT, Donoso C, Kitzberger T, Rebertus AJ (1996) Ecology of southern Chilean and Argentinean Nothofagus forests. The ecology and biogeography of Nothofagus forests 10:93–353

Vera CS, Osman M (2018) Activity of the Southern Annular Mode during 2015–2016 El Niño event and its impact on Southern Hemisphere climate anomalies. Int J Climatol 38. https://doi.org/10.1002/joc.5419

Villalba R, Lara A, Boninsegna JA, Masiokas M, Delgado S, Aravena JC, Roig FA, Schmelter A, Wolodarsky A, Ripalta A (2003) Large-Scale Temperature Changes across the Southern Andes: 20th-Century Variations in the Context of the Past 400 Years. Climatic Change 59:177–232. https://doi.org/10.1023/A:1024452701153

Vinod N, Slot M, McGregor IR, Ordway EM, Smith MN, Taylor TC, Sack L, Buckley TN, Anderson-Teixeira KJ (2023) Thermal sensitivity across forest vertical profiles: patterns, mechanisms, and ecological implications. New Phytol 237:22–47. https://doi.org/10.1111/nph.18539

von Arx G von, Graf Pannatier E, Thimonier A, Rebetez M (2013) Microclimate in forests with varying leaf area index and soil moisture: potential implications for seedling

establishment in a changing climate. Journal of Ecology 101:1201–1213. https://doi.org/10.1111/1365-2745.12121

Wagner CE (1987) Development and structure of the Canadian forest fire weather index system

Wang J, Zhao W, Ding J, Liu Y (2025) Shifting research paradigms in landscape ecology: insights from bibliometric analysis. Landsc Ecol 40. https://doi.org/10.1007/s10980-025-02082-4

Wiens JA (1989) Spatial Scaling in Ecology. Functional Ecology 3:385. https://doi.org/10.2307/2389612

Wiens JA (1992) What is landscape ecology, really? Landsc Ecol 7:149–150. https://doi.org/10.1007/BF00133306

Wilby RL, Dawson CW (2013) The Statistical DownScaling Model: insights from one decade of application. Intl Journal of Climatology 33:1707–1719. https://doi.org/10.1002/joc.3544

Wilby RL, Dawson CW, Barrow EM (2002) sdsm — a decision support tool for the assessment of regional climate change impacts. Environmental Modelling & Software 17:145–157. https://doi.org/10.1016/S1364-8152(01)00060-3

Wild J, Kopecký M, Macek M, Šanda M, Jankovec J, Haase T (2019) Climate at ecologically relevant scales: A new temperature and soil moisture logger for long-term microclimate measurement. Agricultural and Forest Meteorology 268:40–47. https://doi.org/10.1016/j.agrformet.2018.12.018

Wilke CO (2022) ggridges: Ridgeline Plots in 'ggplot2': R package version 0.5.4. https://CRAN.R-project.org/package=ggridges

Williams BK (2011) Adaptive management of natural resources--framework and issues. J Environ Manage 92:1346–1353. https://doi.org/10.1016/j.jenvman.2010.10.041

Williams CM, Henry HAL, Sinclair BJ (2015) Cold truths: how winter drives responses of terrestrial organisms to climate change. Biol Rev Camb Philos Soc 90:214–235. https://doi.org/10.1111/brv.12105

Wolf C, Bell DM, Kim H, Nelson MP, Schulze M, Betts MG (2021) Temporal consistency of undercanopy thermal refugia in old-growth forest. Agricultural and Forest Meteorology 307:108520. https://doi.org/10.1016/j.agrformet.2021.108520

Wright MN, Ziegler A (2017) ranger : A Fast Implementation of Random Forests for High Dimensional Data in C++ and R. J. Stat. Soft. 77. https://doi.org/10.18637/jss.v077.i01

Wu J (2013) Key concepts and research topics in landscape ecology revisited: 30 years after the Allerton Park workshop. Landsc Ecol 28:1–11. https://doi.org/10.1007/s10980-012-9836-y

Wu J, Addai J, Consolata M, Gao Z, Martin E, Yasutake ES, Wang Y (2025) Landscape sustainability science and the Sustainable Development Goals. Geography and Sustainability 6:100309. https://doi.org/10.1016/j.geosus.2025.100309

Xie S-P, Deser C, Vecchi GA, Collins M, Delworth TL, Hall A, Hawkins E, Johnson NC, Cassou C, Giannini A, Watanabe M (2015) Towards predictive understanding of regional climate change. Nat. Clim. Chang. 5:921–930. https://doi.org/10.1038/NCLIMATE2689

Yu H, Liu X, Kong B, Li R, Wang G (2019) Landscape ecology development supported by geospatial technologies: A review. Ecological Informatics 51:185–192. https://doi.org/10.1016/j.ecoinf.2019.03.006

Zellweger F, Frenne P de, Lenoir J, Rocchini D, Coomes D (2019a) Advances in Microclimate Ecology Arising from Remote Sensing. Trends Ecol Evol 34:327–341. https://doi.org/10.1016/j.tree.2018.12.012

Zellweger F, Coomes D, Lenoir J, Depauw L, Maes SL, Wulf M, Kirby KJ, Brunet J, Kopecký M, Máliš F, Schmidt W, Heinrichs S, Ouden J den, Jaroszewicz B, Buyse G, Spicher F, Verheyen K, Frenne P de (2019b) Seasonal drivers of understorey temperature buffering in temperate deciduous forests across Europe. Global Ecol Biogeogr 28:1774–1786. https://doi.org/10.1111/geb.12991

Zellweger F, Frenne P de, Lenoir J, Vangansbeke P, Verheyen K, Bernhardt-Römermann M, Baeten L, Hédl R, Berki I, Brunet J, van Calster H, Chudomelová M, Decocq G, Dirnböck T, Durak T, Heinken T, Jaroszewicz B, Kopecký M, Máliš F, Macek M, Malicki M, Naaf T, Nagel TA, Ortmann-Ajkai A, Petřík P, Pielech R, Reczyńska K, Schmidt W, Standovár T, Świerkosz K, Teleki B, Vild O, Wulf M, Coomes D (2020) Forest microclimate dynamics drive plant responses to warming. Science 368:772–775. https://doi.org/10.1126/science.aba6880

Zignol F, Kjellström E, Hylander K, Ayalew B, Zewdie B, Rodríguez-Gijón A, Tack AJ (2023) The understory microclimate in agroforestry now and in the future – a case study of Arabica coffee in its native range. Agricultural and Forest Meteorology 340:109586. https://doi.org/10.1016/j.agrformet.2023.109586

Zomer RJ, Trabucco A, Metzger MJ, Wang M, Oli KP, Xu J (2014) Projected climate change impacts on spatial distribution of bioclimatic zones and ecoregions within the Kailash Sacred Landscape of China, India, Nepal. Climatic Change 125:445–460. https://doi.org/10.1007/s10584-014-1176-2

Zweifel R, Steppe K, Sterck FJ (2007) Stomatal regulation by microclimate and tree water relations: interpreting ecophysiological field data with a hydraulic plant model. J Exp Bot 58:2113–2131. https://doi.org/10.1093/jxb/erm050

Annex

Table A.1 *List of all TMS-4 Standard loggers used in Studies 2 and 3 of this thesis, with their respective locality IDs, serial numbers, aspects, elevations, and coordinates.*

No.	ID	Serial No.	Aspect	Elevation	Longitude	Latitude
1	S800C	94226061	south	798	-71.5597010	-41.5849924
2	S800W	94226062	south	801	-71.5602366	-41.5847029
3	S800E	94226063	south	807	-71.5592778	-41.5848869
4	S600E	94226064	south	616	-71.5716028	-41.5909133
5	S600C	94226065	south	591	-71.5721019	-41.5913257
6	S600W	94226066	south	591	-71.5725121	-41.5911325
7	N1400W	94226067	north	1392	-71.5452303	-41.6256508
8	N1400W	94226067	north	1401	-71.7224535	-41.8055570
9	N1400C	94226068	north	1395	-71.5448101	-41.6256821
10	N1400C	94226068	north	1400	-71.7220378	-41.8051567
11	N1400E	94226069	north	1411	-71.5445779	-41.6258806
12	N1400E	94226069	north	1396	-71.7218853	-41.8049390
13	N800E	94226070	north	817	-71.5494252	-41.6122089
14	N800C	94226071	north	826	-71.5498402	-41.6125135
15	N800W	94226072	north	822	-71.5501786	-41.6126454
16	N600W	94226073	north	614	-71.5474864	-41.6074891
17	N600E	94226074	north	597	-71.5464403	-41.6074311
18	N600C	94226075	north	595	-71.5468910	-41.6075684
19	N1500M	94226076	north	1469	-71.5438594	-41.6279210
20	N1500M	94226076	north	1504	-71.7206217	-41.8057944
21	S1400C	94226077	south	1399	-71.5551135	-41.5777863
22	S1400C	94226077	south	1395	-71.7376018	-41.7675115
23	S1400E	94226078	south	1392	-71.5545327	-41.5780191
24	S1400E	94226078	south	1389	-71.7372070	-41.7673577
25	S1400W	94226079	south	1396	-71.5556646	-41.5774316
26	S1400W	94226079	south	1388	-71.7379255	-41.7676528
27	S1600M	94226080	south	1598	-71.5667745	-41.5701671
28	N1300E	94244841	north	1314	-71.5449265	-41.6230159
29	N1300Wd	94244843	north	1307	-71.5470767	-41.6229355
30	N1300C	94244844	north	1328	-71.5450206	-41.6229559
31	N1400Wd	94244845	north	1401	-71.5457448	-41.6253838
32	N1400Cd	94244846	north	1400	-71.5456743	-41.6254478
33	N1300Cd	94244847	north	1307	-71.5470017	-41.6229198
34	N1500W	94244848	north	1500	-71.5441758	-41.6277530
35	N1400Ed	94244850	north	1399	-71.5456564	-41.6254469
36	N1300Ed	94244849	north	1309	-71.5469368	-41.6228665
37	N1300W	95145851	north	1328	-71.5452546	-41.6229617
38	baseline	95145852	flat	500	-71.5403972	-41.6043236
39	N1100C	94243676	north	1093	-71.7267465	-41.8007540
40	N1100E	94243675	north	1094	-71.7269887	-41.8009404

41	N1100W	94243674	north	1097	-71.7264609	-41.8011992
42	S1100C	94243686	south	1094	-71.7297139	-41.7758100
43	S1100E	94243685	south	1178	-71.7298962	-41.7759149
44	S1100W	94243684	south	1115	-71.7291658	-41.7759902
45	N1400C	94243679	north	1400	-71.7220378	-41.8051567
46	N1400E	94243678	north	1396	-71.7218853	-41.8049390
47	N1400W	94243677	north	1401	-71.7224535	-41.8055570
48	S1400C	94243689	south	1395	-71.7376018	-41.7675115
49	S1400W	94243688	south	1388	-71.7379255	-41.7676528
50	S1400E	94243687	south	1389	-71.7372070	-41.7673577
51	N1500M	94243680	north	1504	-71.7206217	-41.8057944
52	S1500M	94243690	south	1515	-71.7397869	-41.7663704
53	N900C	94243672	north	883	-71.7237938	-41.7968918
54	N900E	94243671	north	906	-71.7235864	-41.7970647
55	N900W	94243673	north	875	-71.7236710	-41.7965338
56	S900C	94243683	south	892	-71.7227444	-41.7910726
57	S900W	94243682	south	890	-71.7233255	-41.7909900
58	S900R	94243681	south	889	-71.7225268	-41.7910381

Table A.2 *List of all iButton loggers used in Study 2 of this thesis, with their respective serial numbers, aspects, elevations, and coordinates.*

No.	Serial No.	Aspect	Elevation	Longitude	Latitude
1	7F0000007A510241	north	500	-71.793194	-41.623551
2	000000007A484541	north	520	-71.792720	-41.623995
3	170000007A44C141	north	1200	-71.779598	-41.635436
4	640000007A45AD41	north	1300	-71.778296	-41.636311
5	000000007A47C241	north	600	-71.546693	-41.607110
6	D80000007A497E41	north	600	-71.546535	-41.607211
7	230000007A477D41	north	770	-71.548284	-41.611750
8	F10000007A442B41	south	500	-71.781721	-41.589083
9	C80000007A4FB041	south	800	-71.789404	-41.588316
10	B30000007A49DF41	south	1200	-71.797969	-41.587383
11	190000007A4E4241	south	1600	-71.810197	-41.583569
12	1F0000007A46BF41	north	1300	-71.546347	-41.623137
13	E00000007A4BB141	north	1000	-71.548726	-41.616777
14	720000007A4EE341	north	700	-71.553370	-41.609086
15	2C0000007A4E5041	north	1500	-71.775997	-41.638035
16	A30000007A4F1141	south	600	-71.572147	-41.591416
17	1A0000007A461C41	south	700	-71.562438	-41.586217
18	640000007A4C7C41	south	750	-71.561205	-41.585641
19	510000007A44A641	south	1050	-71.555070	-41.582388
20	2B0000007A450341	south	1100	-71.554447	-41.581687
21	7B0000007A4D0141	south	900	-71.556350	-41.584287
22	0C0000007A46B141	south	1191	-71.213868	-41.679518
23	170000007A486D41	north	1425	-71.228244	-41.680371

24	880000007A4EFB41	north	1400	-71.228542	-41.680176
25	4B0000007A4AFF41	north	1402	-71.229493	-41.672846
26	560000007A462441	north	1407	-71.225128	-41.675444
27	890000007A4D5541	south	1499	-71.218158	-41.673645
30	B80000007A4E4A41	flat	1144	-71.235736	-41.666110
33	CC0000007A4BF241	north	1000	-71.414633	-41.588037
34	3E0000007A461341	north	1000	-71.415200	-41.587835
35	8D0000007A469041	south	1100	-71.377916	-41.623976
36	4B0000007A446141	south	1500	-71.373929	-41.602863
37	A90000007A4F4E41	south	1000	-71.379110	-41.628003
38	040000007A4F2C41	south	900	-71.374686	-41.629838
39	3D0000007A505A41	south	1600	-71.566753	-41.570141
40	B80000007A44B041	north	1400	-71.411252	-41.621890
41	FC0000007A4C0C41	north	945	-71.402399	-41.615782
42	BC0000007A46A441	north	1068	-71.404959	-41.618465
43	7B0000007A46E241	north	713	-71.508163	-41.618119
44	960000007A4D3141	north	1400	-71.544006	-41.627810